GAZİ ÜNİVERSİTESİ

1926

CONTROL AND DESIGN OF MICROCONTROLLER BASED CAPACITOR CHARGING POWER SUPPLY USING PEAK CURRENT CONTROL MANAGEMENT

Furkan DEMİRBAŞ

IN PARTIAL FULFILLMENT OF THE REQUIREMENTS FOR THE DEGREE OF MASTER OF SCIENCE IN ELECTRICAL ELECTRONIC ENGINEERING DEPARTMENT

GAZİ UNIVERSITY
GRADUATE SCHOOL OF NATURAL AND APPLIED SCIENCES

JANUARY 2025

ETHICAL STATEMENT

I at this moment declare that in this thesis study, I prepared the thesis writing rules of Gazi University Graduate School of Natural and Applied Sciences;

- All data, information, and documents presented in this thesis have been obtained within the scope of academic rules and ethical conduct,
- All information, documents, assessments, and results have been presented by scientific ethical conduct and moral rules,
- All material used in this thesis that is not original to this work has been exhaustively cited and referenced,
- No change has been made in the data used,
- The work presented in this thesis is original,

or else, I admit all loss of rights to be incurred against me.

Furkan DEMİRBAŞ

24/01/2025

CONTROL AND DESIGN OF MICROCONTROLLER BASED CAPACITOR CHARGING POWER SUPPLY USING PEAK CURRENT CONTROL MANAGEMENT

(M.Sc. Thesis)

Furkan DEMİRBAŞ

GAZİ UNIVERSITY
GRADUATE SCHOOL OF NATURAL AND APPLIED SCIENCES

January 2025

ABSTRACT

Laser systems, camera flashes and medical systems require rapid and precise mechanism to store and discharge the energy. Capacitor Charging Power Supplies (CCPS) are an important subsystem for pulsed power applications. This paper investigates the design methodologies, control methods, and optimizations of CCPS. The performances of the conventional (non-optimal), hysteresis current-mode, constant off-time, constant on-time are analyzed. The optimum working principles which is boundary conduction mode with variable frequency are mentioned. On the other hand, the advantage and drawbacks of the discontinues conduction mode and continues conduction mode are compared. Also, the effects of the input voltage, charging current and switching frequency on charging time are analyzed with on their reliability and efficiency.

Science Code	:	93419
Key Words:	:	Capacitor charging power supply, hysteresis control, DCM, feed forward control, peak current control
Page Number	:	95
Supervisor	:	Assoc. Prof. Dr. Korhan KAYIŞLI

MİKRODENETLEYİCİ TABANLI KONDANSATÖR ŞARJLI GÜÇ KAYNAĞININ TEPE AKIM KONTROL YÖNETİMİ KULLANILARAK KONTROLÜ VE TASARIMI

(Yüksek Lisans Tezi)

Furkan DEMİRBAŞ

GAZİ ÜNİVERSİTESİ

FEN BİLİMLERİ ENSTİTÜSÜ

Ocak 2025

ÖZET

Lazer sistemleri, kamera flaşları ve medikal sistemler, enerjiyi depolamak ve boşaltmak için hızlı ve hassas bir mekanizma gerektirir. Kondansatör Şarjlı Güç Kaynakları (CCPS) bu tip darbeli güç uygulamaları için önemli bir alt donanımdır. Bu makale, CCPS'in tasarım metodolojilerini, kontrol yöntemlerini ve optimizasyonlarını araştırmaktadır. Geleneksel (optimal olmayan), histerezis akım modu, sabit kapalı zaman, sabit açık zaman kontrol metotlarının performansları analiz edilmiştir. Değişken frekanslı sınır iletim modu olan optimum çalışma prensiplerinden bahsedilmiştir. Diğer yandan, süreksiz iletim modu ile sürekli iletim modunun avantaj ve dezavantajları karşılaştırılmıştır. Ayrıca, giriş voltajı, şarj akımı ve anahtarlama frekansının şarj süresi üzerindeki etkileri, güvenilirlik ve verimlilikleri ile analiz edilmiştir.

Bilim Kodu	:	93419
Anahtar Kelimeler	:	Kondansatör şarjlı güç kaynakları, histerezis kontrol, DCM, ileri besleme kontrolü, tepe akım kontrolü
Sayfa Adedi	:	95
Danışman	:	Doç. Dr. Korhan KAYIŞLI

ACKNOWLEDGEMENTS

I would like to express my gratitude to my advisor, Associate Professor Dr. Korhan KAYIŞLI, for his invaluable guidance, support and for placing his trust in me throughout the thesis journey. I am sincerely grateful to my family, Fatma, Aslı, Engin, Doğukan, and Esra, for their unwavering support. I would also like to acknowledge the Artı Endüstriyel Elektronik family, particularly Atila KOÇ and Volkan UTALAY, for their invaluable partnership in the production and material supply of my thesis study.

CONTENTS

Page

Page

LIST OF TABLES

LIST OF FIGURES

Figure **Page**

Figure **Page**

Figure **Page**

LIST OF IMAGES

SYMBOLS AND ABBREVIATIONS

The symbols and abbreviations used in this study are presented below, along with their explanations.

Symbols	Explanations
%	Percentage
$\sqrt{}$	Square Root
Hz	Hertz
J	Joule
kV	Kilovolt
α	Alpha
W	Watt
mW	Milliwatt
V	Volt
A	Ampere
s	Second
µs	Microsecond
ms	Millisecond
t	Time
V_{Cf}	Target Capacitor Voltage
k	Transformer Coupling Coefficient
L	Inductance
C	Capacitor
N	Turns Ratio
C_{gs}	Gate-to-source Capacitance
C_{gd}	Gate-to-drain Capacitance
C_{ds}	Drain-to-source Capacitance
R_{DS}	Drain-to-source Resistance
V_{DS}	Drain-to-source Voltage
I_{pri}	Primary Current
I_{sec}	Seconder Current
V_f	Forward Voltage

Symbols	Explanations
pF	Picofarad
I_d	Drain Current
C_{iss}	Input Capacitance
C_{oss}	Output Capacitance
C_{rss}	Feedback Capacitance
V_{gs}	Gate-to-source Voltage
Q_g	Total Gate Charge

Abbreviations	Explanations
ADC	Analog to Digital Converter
ARR	AutoReload Register
BCM	Boundary Conduction Mode
CCM	Continuous Conduction Mode
CCPS	Capacitor Charging Power Supply
CRT	Cathode Ray Tube
DC	Direct Current
DCM	Discontinuous Conduction Mode
DMA	Direct Memory Access
DSFC	Dual Switch Flyback Converter
EMC	Electromagnetic Compatibility
EMI	Electromagnetic Interference
ESR	Equivalent Series Resistance
GND	Ground
GPIO	General Purpose Input Output
HBSRC	Half-Bridge Series Resonant Converter
LCD	Inductance-Capacitor-Diode
LDO	Low-dropout Regulator
LED	Light Emitting Diode
MOSFET	Metal Oxide Semiconductor Field Effect Transistor
NPN	Negative-Positive-Negative Transistor
PCB	Printed Circuit Board

Abbreviations	**Explanations**
PI	Proportional Integral
PNP	Positive-Negative- Positive Transistor
PRR	Pulse-to-pulse Repeatability
PSFB	Phase-Shifted Full Bridge
PWM	Pulse Width Modulation
RCD	Resistor-Capacitor-Diode
RMS	Root Mean Squared
SiC	Silicon-carbide Diodes
SMPS	Switched Mode Power Supply
TMR	Timer
TVS	Transient Voltage Suppression

1. INTRODUCTION

The usage areas and number of electronic products are rapidly increasing in ever-evolving technological world. The operating voltages of electronic products vary with the different fields of application. This diversity emphasizes the necessity for effective and flexible power management more than ever. The devices in the system may require voltage levels that are either lower or higher than those present in the system. Power converters play a crucial role in meeting the demand for different voltage levels by converting the input voltage. Thus, power converters serve as the fundamental link between systems. The power converters facilitate voltage conversion to ensure compatibility, efficiency, and safety across applications. For this reason, power converters have become essential components in almost all systems.

In systems, especially designed to manage high voltages, it is crucial to not only convert the voltage level, but also to store the converted voltage. In electronic systems, low voltage levels are often needed continuously, while high voltage levels are more often needed momentarily or for a period of time. High-output voltage power converters can have an output voltage ranging from 1 kV to 100 kV and an output power ranging from a few watts to hundreds of watts. However, high voltage power supply applications that are widely used in medical, airborne, and space applications generally demand rapid but high-intensity of energy (Song, Shin and Choi, 2001).

In certain applications, a capacitive load needs to be charged to thousands of volts. Capacitors are frequently preferred for such applications due to the ease of obtaining high voltage capacitors and their ability to discharge rapidly when current is drawn from them (Crawford, 1995 October). These applications require a DC power supply to efficiently charge large capacitors to high voltages (Islas, 2009). After a designated time period, the capacitor is triggered to discharge. All stored energy in the capacitor is released to generate an application-specific voltage pulse. The capacitor charging power supply must charge the capacitor before each repetition of energy release to the load (Song, Shin and Choi, 2001). Capacitor charging power supplies are commonly classified as high voltage DC power supplies due to their high voltage outputs.

In CCPS topologies, the input energy is first stored and then the stored energy is transferred to the output capacitor. The energy transferred to the capacitor is directly proportional to the charging time (transistor on time). By increasing the charging current the amount of energy transferred to the capacitor can be increased. However, increasing the current also increases the losses on the components. This will result in decreased efficiency and increased heating of the CCPS. Therefore, the current level must be within limits that do not endanger the system's reliability. Accordingly, when modifying the duty cycle, it is imperative to guarantee that the MOSFET remains within the prescribed current limits. In order to guarantee reliability, it is a typical approach to derive the duty cycle by measuring the primary current in CCPS applications. The CCPS operating cycle commences with the transistor being turn on. Subsequently, the MOSFET is turned off when the input current attains the specified level. Turning on the MOSFET again is done with the start of the next switching period.

Nevertheless, the use of a fixed switching frequency may result in suboptimal efficiency. When the secondary current reaches zero in a period of time shorter than that of the switching period, the converter is forced to operate in discontinuous conduction mode. The DCM represents an idle state. In an idle state, which the current is zero in both the primary and secondary sides, some of the energy stored in the capacitor is dissipated in the parasitic and load components This results in energy loss and consequently prolongs the charging time. In order to circumvent this issue, it is imperative that CCPS be operated in boundary condition mode. As the capacitor voltage increases, the boundary conditions are shifted. A change in the boundary conditions results in a variable switching frequency.

Considering the usage areas of CCPS, it should provide the same charging performance at different input voltages. In order to increase the efficiency and reliability of CCPS, an effective control method must be used. However, existing controllers are customized for specific designs. For this reason, the control method to be used in CCPS design should be developed with microcontrollers instead of existing controllers.

The existing control methods are related to the determination of boundary conditions. The inputs of the control algorithms are the primary current, the secondary current, and the capacitor voltage. The operational state of the transistor depends on the magnitude of the primary and secondary currents. Sensing the both side’s current is the most primitive method. The first controller was developed by Albert Wu at Linear Technology. The LT3420 monitors the currents on both sides of the circuit with its integrated sensing resistors. However, the LT3420 has a hysteresis for current limits. In Hysteretic Current-Mode Control, the transistor is reactivated when the secondary current diminishes to a value of α, which is a fraction of its peak value.

Efficiency and reliability are cornerstones of power supply design. Therefore, designers aim to minimize energy losses during the charging process by implementing sophisticated control techniques to ensure effective transfer of energy to the capacitor. The first methodology is using the constant on-time control method instead of the sensing the primary current. Similarly, alternative control methodologies have been proposed instead of sensing the secondary current. It was recommended by Richard Hanley Smith and Peter Graham Laws that the voltage on the switching elements be monitored in order to ascertain whether the currents are present or not. In the patent of Linear Technology, the output voltage was employed instead of measuring the secondary current. The input voltage and the reflected capacitor voltage were compared to determine the discontinuity. While the constant on-time control can be used, constant off-time control method can be implemented. However, it can be observed that as the capacitor voltage increases, the rate of decrease of the secondary current also increases. Therefore, feed-forward-controlled off-time method was discovered. The off-time is calculated by measuring the capacitor voltage after the primary current reach its threshold level. Then, calculating the time needed for the secondary current to fall a specified value.

The objective of this study is to investigate the performance of the proposed control methods and to mention the optimizations for the CCPS. The simulations have been performed by using the LTspice simulator software with non-ideal switching components and ideal transformer. The control systems have been constructed using behavioral voltage sources. The controllers have been integrated into the flyback converter in order to facilitate the analysis process.

Chapter 2 of the thesis details the application areas, requirements and operational structure of CCPS. In Chapter 3, the proposed control methods for CCPS are compared. In Chapter 4, the operating structure and operating modes of the flyback converter topology are detailed. In Chapter 5, the experimental setup implemented in this study is explained in detail. In

Chapter 6, conclusions and recommendations are presented and an overall evaluation is made.

2. EXPLANATION OF THE CCPS

High voltage pulsed power engineering is one of the academic fields in the literature. This field focuses on researching capacitor charging circuits and pulsed power applications (matsusada, 2021). This type of power supplies is also known as a capacitor charging power supplies (CCPS). The purpose of capacitor charging power supplies is to charge a capacitor to a specific voltage level with control algorithms.

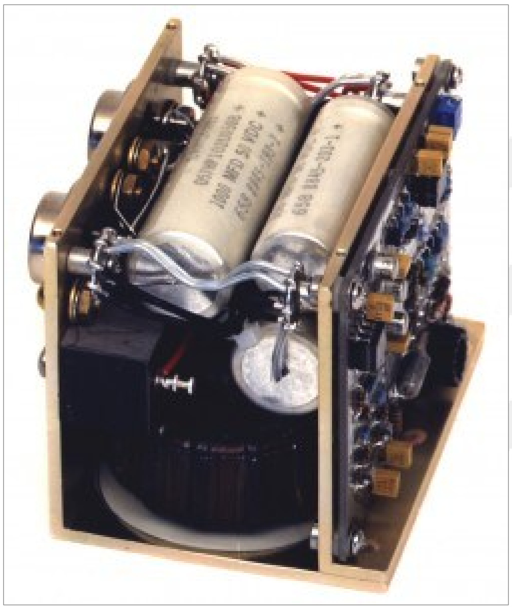

Figure 2.1. Example of CCPS

2.1. Usage Areas of the CCPS

Some applications require a capacitor to be charged to high voltages and then rapidly discharged by an external device. Some of the notable applications where CCPS is in use are:

<u>Flash photography</u>

Camera flashes require high electrical energy to operate. They use CCPS to generate and store this energy. When triggered by user, the energy stored in the capacitor is rapidly discharged. This produces a high-intensity flash of light used in photography.

Pulse power applications

CCPS may use in applications that require high power in a short duration. Medical equipment, laser systems, and experimental setups are among the applications that require precise and powerful energy pulses.

Voltage multipliers

Capacitor charging circuits are often integrated into voltage multiplier configurations. These arrangements are used in applications such as cathode ray tube (CRT) displays, x-ray machines and other devices requiring high DC voltages.

Power backup systems

Certain electronic devices and systems may incorporate capacitor charging circuits as part of a power backup system. There may be a short-term energy need during power outages or when there is a high energy demand from the load. In such cases, capacitors can serve as energy stores by providing power to the line they are connected to.

High-energy physics experiments

CCPS are used in high-energy physics laboratories and research facilities. Some specific experimental conditions required precise and intense bursts of energy. CCPS can deliver that energy for experimental setups.

Electrostatic precipitators

In industrial applications, CCPS are used in electrostatic precipitators. These devices use charged plates to remove particles from gas. Capacitor charging helps to charge the plates to the required high voltages.

Electronic warfare systems

Certain military applications, particularly in electronic warfare, may use CCPS to deliver powerful and fast electronic pulses for various purposes.

Electric fence energizers

In agricultural and security applications, CCPS is used in electric fence energizers. These devices periodically provide high voltage pulses to keep animals or intruders away from the area that needs to be protected.

These examples highlight the versatility of the CCPS. They also show that they can be used in a variety of applications where rapid discharge of stored energy is required.

2.2. Requirements of the CCPS

To ensure proper efficiency, functionality, and reliability, it is important to consider several fundamental requirements when designing capacitor-charged power supplies. It's important to find a balance between cost and efficiency. This often requires careful component selection and design optimization. Smaller sizes are important in power electronics. Smaller sizes require compact designs. So, careful integration of components is critical. Given the usage areas of CCPS, it is crucial that the design should be compact.

Efficiency

Efficiency is a cornerstone of power supply design. In CCPS, achieving higher efficiency requires minimizing energy losses during the charging process. The goal of designers is to reduce losses during the charging process. Consequently, it is recommended that designers optimize the transformer design, select components with low power dissipation, and implement sophisticated control techniques to ensure effective transfer energy to the capacitor.

Functionality

Each system has its own specific requirements. Ensuring functionality requires customizing the power supply to meet the specific requirements of the intended application. In most capacitor charging applications, there is a limited amount of time to charge the capacitor to specified voltage levels. The CCPS must reach the desired target voltage within this time. To ensure the effective integration of a CCPS within a targeted system, it is essential to consider the power requirements, voltage levels, and timing constraints. Nevertheless, it is challenging to satisfy all the requirements. Therefore, it is advisable to prioritize the requirements.

Reliability

The charging time is related with the transferred energy to the capacitor in each pulse. Additionally, the transferred energy is directly proportional to the charging current. By increasing the charging current, the amount of delivered energy to the capacitor can be increased. However, increasing the current also increases the conduction losses on the components. This will result in decreased efficiency and increased heating of the CCPS. Reliability is a non-negotiable criterion that demands meticulous component selection, effective cooling mechanisms to manage heat dissipation, and the incorporation of safety features to prevent component failures or system malfunctions. Therefore, the current level must be within limits that do not endanger the system's reliability.

Pulse-to-pulse repeatability

Pulse-to-pulse repeatability is essential for capacitor charging power supplies, particularly in applications where precision and consistency of energy delivery are critical (Pokryvailo, Carp and Scapellati, 2010 October). Pulse-to-pulse repeatability ensures uniform delivery of energy to the capacitor. The concept of pulse-to-pulse repeatability refers to the ability of a power supply to produce stable output voltage. Since the output voltage represents the target voltage level in CCPS, the feedback circuits of the control logic must work perfectly to determine the target voltage. "With many charging topologies, the output voltage exhibits an overshoot due to the inherent remanent energy stored in the power converter elements" (Cravero, Maestri, Retegui, Benedetti, and Uicich, 2014 December). These overshoots can cause a deterioration in Pulse-to-pulse repeatability.

Size

When the usage areas of CCPS are examined, it is understood that the size of the design is an important factor. Since space is limited in such systems, the power supply must be as small and light as possible. Especially in medical or laser applications, the lightness and small size of the design are advantages.

2.3. Suitable Topologies of the CCPS

There are several suitable topologies that meet the requirements of capacitor charging systems, each with its own advantages and disadvantages.

2.3.1. Resonant converter

In recent years, the resonant converter has become one of the preferred topologies for CCPS design. Resonant converters are a type of switched mode power supply (SMPS) that use resonant circuitry. The advantages of the resonant converter are achieving soft switching, reducing switching losses and improving overall efficiency. These types of converters operate by creating a resonance between the inductive and capacitive elements in the circuit. This resonant circuitry allows for zero voltage or zero current switching during the switching cycle.

One of the main advantages of resonant converters is their ability to achieve high efficiency. Overall efficiency is improved by reducing switching losses with soft switching methods. Efficiency improvements help conserve energy. Also, the soft switching of resonant converters helps to reduce electromagnetic interference. This makes the resonant converter suitable for radio frequency-sensitive environments. Furthermore, resonant converters offer the advantage of reduced stress on components. The soft-switching helps extend the life of these components like semiconductor devices, capacitors and inductors. Despite these advantages, resonant converters have certain drawbacks. The design of the resonant converter is complex and often requires advanced control algorithms. Achieving and maintaining resonance requires precise control. The control circuitry can be more complex compared to simpler converter topologies. One of these control structures is variable frequency control.

> "In variable frequency resonant converters there is a tradeoff between high voltage/current stresses and wide frequency range. Either extreme can result in high radiated and conducted EMI respectively. Proper filter design becomes a very important factor in noise performance for variable frequency topologies." (Caldeira, Liu, Dalal, and Gu, 1993).

Additionally, resonant converter has certain limitations. Since there is a dependence on the load, it is not comfortable with a wide range of input voltage and load variation. Even when no load is connected to the circuit, a significant amount of current can circulate through the tank element, resulting in poor efficiency at lighter loads. These considerations increase the conduction losses of the switching element.

Moreover, the cost of resonant converters tends to be higher than simpler converter topologies. This increased cost is due to the need for specialized components such as resonant inductors and capacitors. The availability of these specialized components may be limited. Therefore, providing these components may increase the overall cost and potentially affect the feasibility of using resonant converters, especially in cost-sensitive applications.

There are two main types of resonant converters (series and parallel) commonly used in CCPS. In (Pehlivan, 2019) and (Rotman and Ben-Yaakov, 2013), a comparison was made between the charging characteristics of the series and parallel resonant converters. The comparison mentions that the series resonant topology is typified by a decreasing average load current while the output voltage increases. Accordingly, in order to maintain the required average output power and efficiency, a higher output current is required in the first charge stage. Thus, it is evident that the Series Resonant topology has limitations and cannot be charged to a voltage higher than its design. Furthermore, in applications that necessitate charging with low voltage using this topology, efficiency is compromised due to the requirement of high input currents.

In contrast, the comparison states that the power transferred to the output capacitor in the capacitor charger based on parallel resonant topology, increases linearly. Therefore, there is no upper limit for the target voltage, except for power loss. Thus, the parallel resonant topology is capable of efficiently charging in a wide range of output voltage.

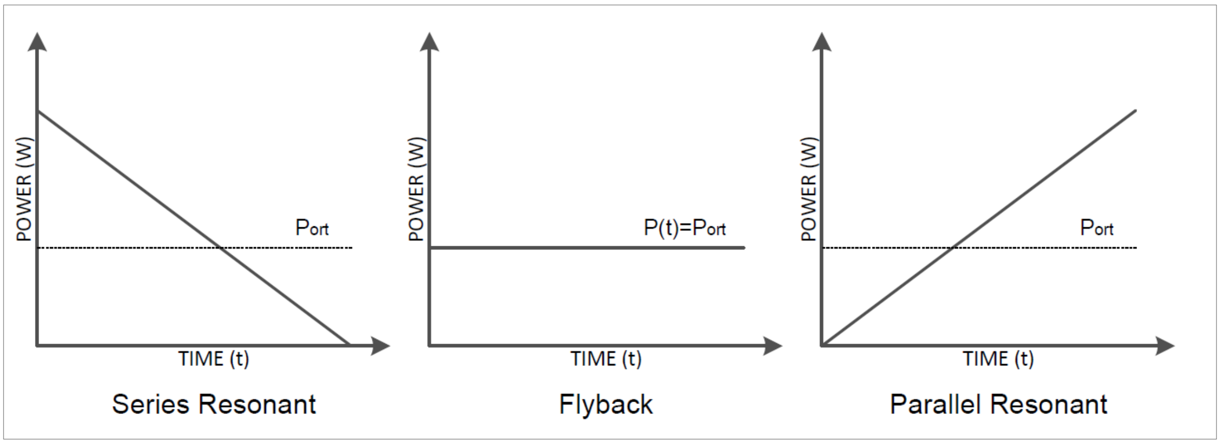

Figure 2.2. Charging profiles of three possible topologies (Pehlivan, 2019) (Rotman and Ben-Yaakov, 2013)

In (Rotman and Ben-Yaakov, 2013), the parallel and series resonant converter topologies have been studied with respect to their gain and high current requirements. It is mentioned that the resonant converter has two gains, the resonant tank gain and the transformer winding ratio. It is emphasized that the resonance gain of the series resonance topology is less than one, so obtaining a high output voltage in the series resonance topology depends only on the transformer winding ratio. Since the parallel topology has a resonance gain greater than unity, transformer dimensions can be further reduced (Sheng, et al., 2007 May). Also,

> "High power chargers, fed from low input voltage, have relatively high input current. Series and series-parallel resonant topologies have difficulty handling the high currents drawn from the low input voltage source due to the very low ESR needed at the series capacitor. However, drifting of magnetization current is blocked. Common phenomenon at resonant parallel topology is an uncontrolled magnetization current, which could lead to transformer saturation, due to the lack of series capacitor." (Rotman and Ben-Yaakov, 2013).

2.3.2. The phase-shifted full-bridge converter

The phase-shifted full-bridge converter is another type of topology that used for CCPS designs. The full-bridge configuration of the phase-shifted full-bridge typically consists of four switches. It employs a phase-shifting control strategy to regulate the power flow. The converter's structure of four switches distributes stresses and increases efficiency. Additionally, phase shift control between the switches behaves like resonant mode operation. This soft switching behavior minimizes power dissipation during transitions. This allows for increasing the overall efficiency. However, precise control algorithms are needed to achieve and maintain the desired phase shift operation. As with resonant converters, this complexity can make system design and integration difficult.

According to (Kavak, Candan and Aydemir, 2020), the primary disadvantages of the PSFB converter are the high voltage ringing and the reverse recovery losses in the secondary rectifier diodes. In references (Candan, Kavak and Ankaralı, 2019), (Kavak, Candan and Aydemir, 2020), and (Kavak, 2020), output inductor-less PSFB topologies were proposed as a solution to the aforementioned problems. It is mentioned in the references that, output inductor-less PSFB eliminates the need for dissipative snubber circuits. This approach reduces the number of components in the PSFB topology. However, it is still more costly and complex than other topologies. Therefore, PSFB converters are often used in medium to high-power applications where the benefits of resonant operation and precise control outweigh the challenges of increased complexity and cost. Additionally, the selection of the secondary rectifier diode has become more important.

2.3.3. Flyback converter

Flyback converter is another common topology used in CCPS design due to its simple operating principle. The flyback converter stores energy in the primer side of the transformer during the switch on time and transfer the stored energy to the secondary side during the switch off time. The flyback converter which is a popular type of power supply topology that provides isolation between the input and output side. This isolation is achieved by having both windings on the same transformer. The transformer makes it possible to get different output voltages from one input.

The electrical isolation of the flyback converter makes it suitable for applications where safety and isolation are a requirement. For this reason, it is preferable in places where size of the converter is a significant factor, such as CCPS. This design of this converter is simpler compared to other isolated converters. This simplicity can result in reduced costs and time of the manufacturing processes, particularly in applications with medium power requirements (Elmes, Jourdan and Abdel-Rahman, 2009). In today's marketplace, the most alternative topology that can be used instead of a flyback converter is considered to be a resonant converter. In contrast to the resonant converter, flyback converter provides constant power to the charged capacitor when working at a constant switching frequency. (Rotman and Ben-Yaakov, 2013). This provides a simpler and more applicable control structure. Flyback converter topology contains a single switching element. Thus, using of the variable frequency is easy with the flyback controller.

However, the flyback converter has some limitations. Flyback converters can present challenges in transformer design and cause potential efficiency issues at high power levels. Therefore, the flyback converter is suitable for relatively lower power applications compared to other isolated topologies. The flyback converter may cause voltage spikes when the switch is closed. Voltage spikes can stress components. Therefore, it may require additional protection circuits. This can result in higher levels of electromagnetic interference (EMI) and require consideration of electromagnetic compatibility (EMC) in the design.

In reference (Cravero, Maestri, Retegui, Benedetti and Uicich, 2014 December), a comparison was presented for suitable topologies (half-bridge series resonant converter, dual switch flyback converter and full-bridge phase-shifted converter). These three topologies were compared based on their charging time, average output current, and output voltage precision.

> "It can be noted that the charging time is approximately the same for the three chargers. The HBSRC performs a linear charging process, while with the other topologies the charging voltage slope is variable. The slope variation is most significant for the DSFC. Moreover, for target voltages lower than V_{MAX}, the DSFC has the maximum voltage slope, which implies that this topology has the higher charging power.
>
> The HBSRC produces a constant average current, while the other ones present a variable average current. It should be noted that the average current behaviour is related to the linearity of the charging process. Moreover, DSFC and FBPSC have maximum average current at the beginning of the charge and then it decreases when the output voltage increases. This feature implies that these topologies have a charging power higher than the HBSRC for low voltages.
>
> It can be noted that in the three topologies the precision is increased when the output voltage is higher. For the presented designs, the HBSRC presents better precision when the charging voltage is low, while for higher voltages the FBPSC presents a superior precision." (Cravero, Maestri, Retegui, Benedetti and Uicich, 2014 December).

The choice of topology depends on the specific requirements of the application, including factors such as efficiency, voltage regulation, and cost. The choice of topology depends on the specific requirements of the capacitor charging power supply, such as input voltage range, output voltage, power level, and efficiency targets. Each topology has its advantages and disadvantages, and the selection should be based on a thorough understanding of the application's needs.

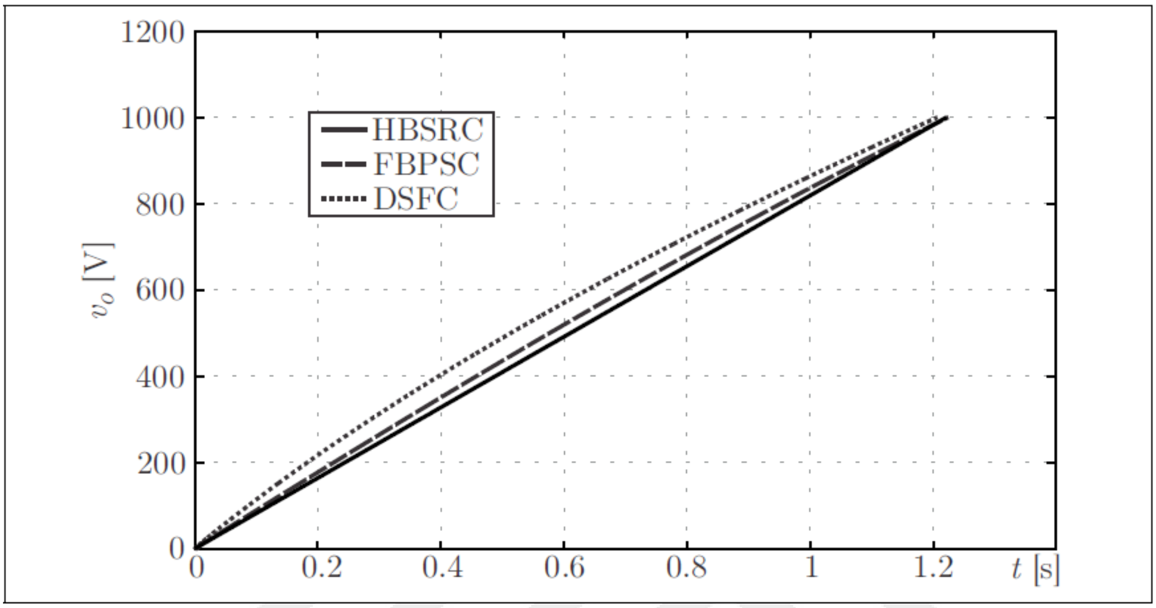

Figure 2.3. Output voltage of comparison (Cravero, Maestri, Retegui, Benedetti and Uicich, 2014 December)

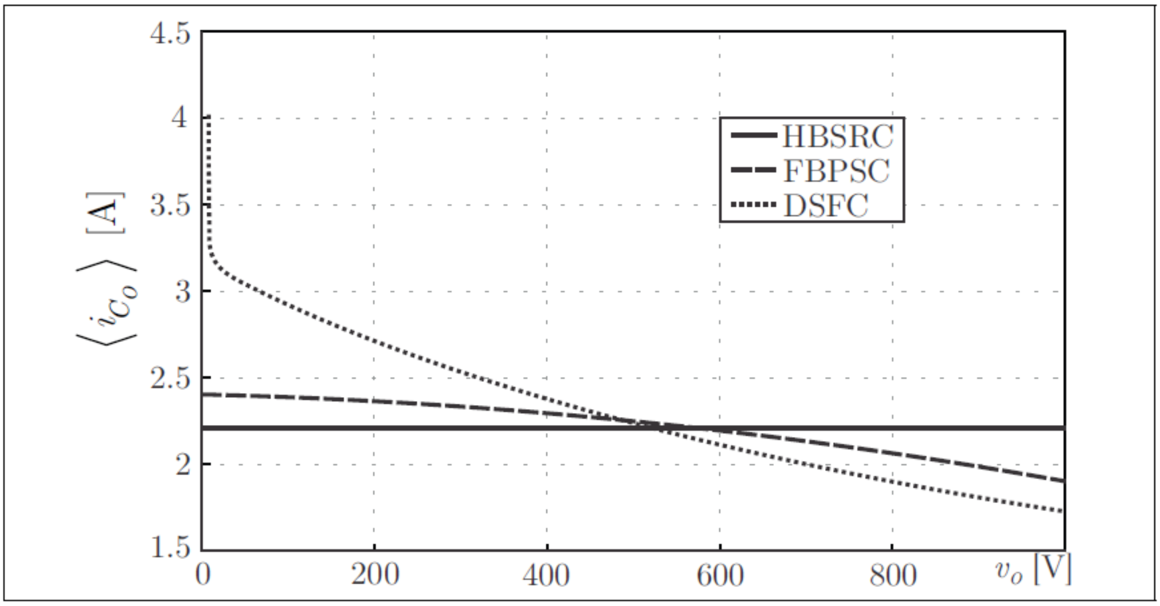

Figure 2.4. Average output current of comparison (Cravero, Maestri, Retegui, Benedetti and Uicich, 2014 December)

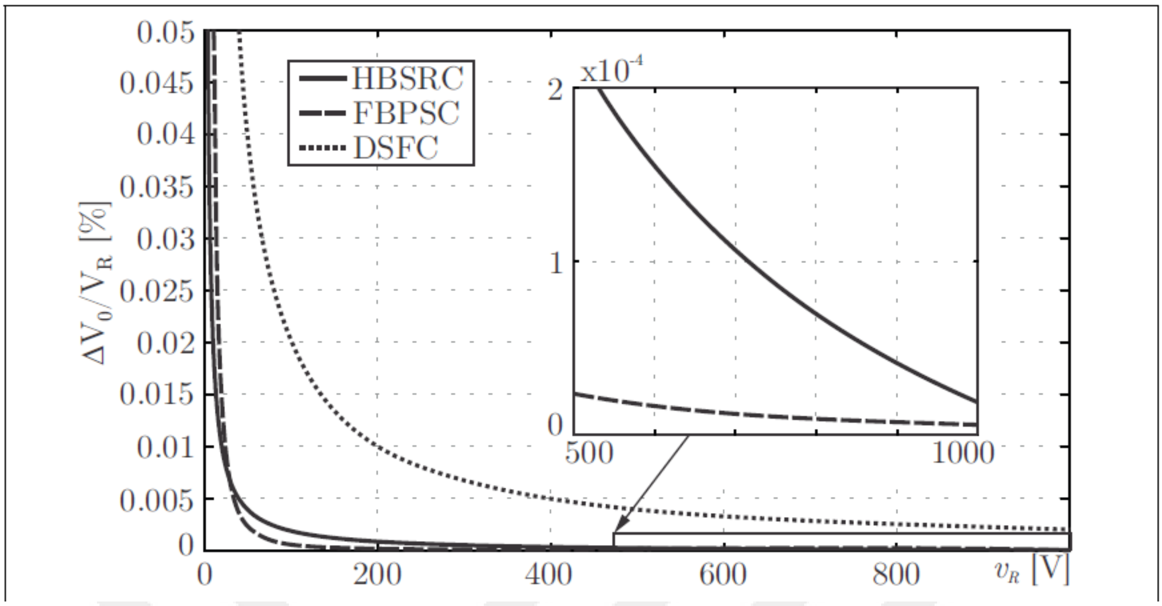

Figure 2.5. Output voltage precision of comparison (Cravero, Maestri, Retegui, Benedetti, and Uicich, 2014 December)

2.4. Mods of the CCPS

A standard charge cycle for a CCPS is shown in figure 2.6. When the charge cycle starts, the capacitor is initially discharged state. In the charge mode, CCPS continues to charge the capacitor until the capacitor voltage reaches the target voltage level. The charge mode is a high-power mode. The CCPS is operated to its full capacity to charge the capacitor. Once the target voltage level is detected, the CCPS stops the charging process and the capacitor is ready to discharge. However, due to the operating structure of the system, the capacitor may not discharge immediately. When the charging process is stopped, the capacitor will lose its energy due to some parasitic resistances and the leakage of the capacitor. These losses result in low energy when the capacitor is discharged. To compensate for these losses when the target voltage is reached, the CCPS switches to regulation mode, where the charge on the capacitor is retained by energy pulses. In contrast to charge mode, regulation mode is a low power mode in which the CCPS waits for the capacitor to discharge (Song, Shin and Choi, 2001).

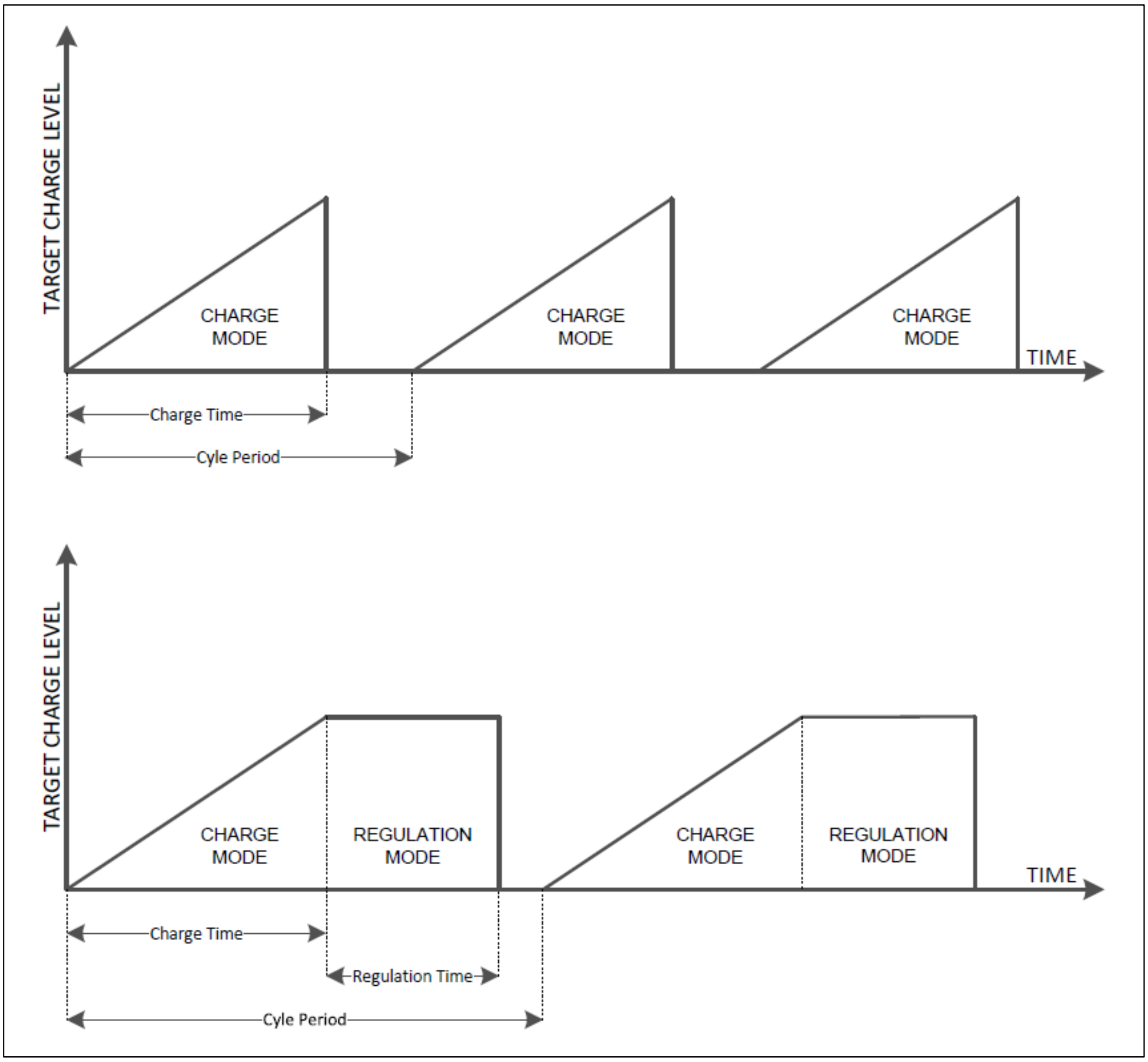

Figure 2.6. Charge cycle for a CCPS

3. CONTROL METHODS

This section classifies the existing control methods mentioned in the literature and presents the results of simulations of these methods. It also outlines the key points of controlling the CCPS.

3.1. Nonoptimal Charging Method

The transistor's on and off times are determined by detecting primary and secondary currents. The transistor is turned off when the primary current reach the specified level. When the secondary current reaches zero, the transistor is turned on again. This prevents CCPS from entering the discontinuous conduction mode. To terminate the charging process, the voltage of the output capacitor is measured (United States of America Patent No. US4489369A, 1983)

3.2. Hysteretic Current-Mode Control

Similarly, in hysteretic current-mode control, the transistor is deactivated when the primary current reaches the current limit. In contrast with the conventional approach, the transistor is reactivated when the secondary current diminishes to a value of α, which is a fraction of its peak value. The charge of the capacitor is proportional to the average value, and the power dissipations are proportional to the root-mean-square (rms) value of the current. Accordingly, Sokal posits that the optimal strategy is to generate a flat-topped current pulse by turning on the transistor as early as possible. An increase in the α value has the effect of increasing the average of the secondary current and bringing the secondary current closer to a flat-topped profile. This results in a reduction of the charging time and I^2R losses. Nevertheless, the activation of the transistor during the conduction of the secondary diode results in the generation of reverse recovery current in the diode. Accordingly, an increase in the value of α results in an enhancement of the turn-off losses in the diode (United States of America Patent No. US4070699A, 1975)

3.3. Measuring the Switching Voltages Instead of the Currents

In case a transistor is used as the primary switching element, the primary current may be approximated through the observation of the collector-emitter saturation voltage or the base-emitter voltage of the transistor. The same concept can be applied to the secondary side if the secondary switching component is selected to be a P.N.P or N.P.N. transistor. However, the crucial aspect of the secondary current is not the precise value of the current itself. It is sufficient to ascertain whether the secondary current is existing or not. Accordingly, it is reasonable to determine the secondary current by measuring the presence of a reverse voltage across the diode (United States of America Patent No. US4104714A, 1977)

3.4. Constant On-Time Control with Feed-Forward-Controlled

In order to detect the primary current, the transistor is maintained in a conducting state for a predetermined duration with Eq. 3.1. In the constant on-time control method, the variability of the input voltage is a significant factor. When a battery pack is utilized as a source of supply voltage for the CCPS, the battery voltage will experience a decline over time. In the event of a reduction in the input voltage, the previously calculated on-time may fail to provide the requisite primary current. This results in an increase in the charging time. Similarly, an increase in input voltage may result in a rise in primary current that exceeds the specified limit value for a predetermined on-time period, potentially leading to damage to the transistor.

$$t_{on} = \frac{I_{Pri_{(pk)}} (1 - \alpha)\, L_{Pri}}{VCC} \tag{3.1}$$

3.5. DCM Comparator Without Sensing Capacitor Voltage

In the developed controller, LT3468, the output voltage was employed instead of measuring the secondary current. In instances where the transistor is turned off, the voltage present on the secondary side is reflected back to the primary in direct proportion to the transformer winding ratio. When the ‘SW’ pin voltage declines to a level below ‘VIN’, the output of the DCM comparator is triggered. Subsequently, the next switching cycle begins. Additionally, the reflected voltage is compared with the output voltage reference point to stop the charging process. The target voltage can be established by modifying the turn ratio. In contrast, the LT3750 was designed to rapidly charge large capacitors to a user-adjustable target voltage. Furthermore, this control method provides isolation of the controller and the secondary side.

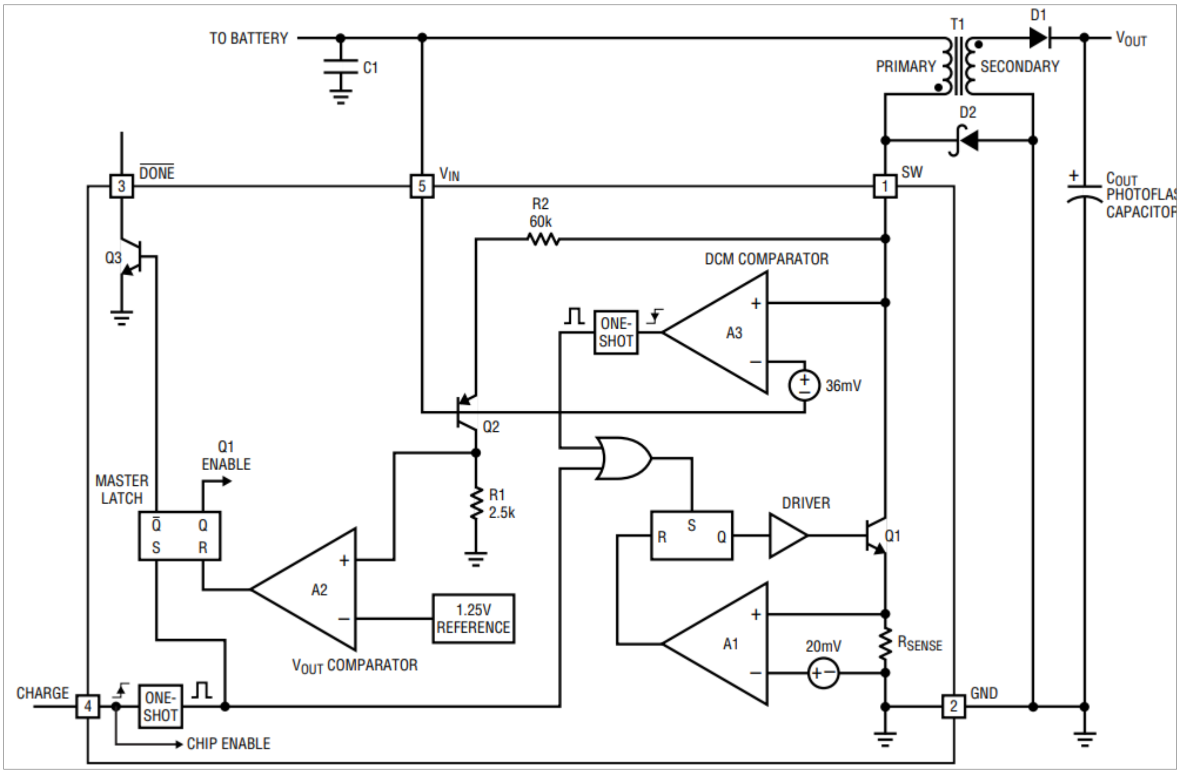

Figure 3.1. Block diagram of LT3420 (Linear Technology, 2022)

3.6. Peak Current Mode Control with Feed-Forward-Controlled Off Time

This is a form of constant-off-time current-mode control. However, it can be observed that as the capacitor voltage increases, the rate of decrease of the secondary current also increases. The use of a constant off-time may result in the converter operating in DCM. Therefore, the off-time should not be constant. Similarly, the transistor is turned off according the primary current limit. The capacitor voltage is measured each time when the transistor is turned off. Then, the off-time is calculated with Eq. 3.2. Furthermore, hysteretic current mode control can be applied to the calculation (United States of America Patent No. US5485361A, 1995)

$$t_{off} = \frac{I_{Pri_{(pk)}}(1-\alpha)kL_{Pri}}{\frac{V_C}{N}} \tag{3.2}$$

3.7. Simulations Studies

In order to analysis the performances of the proposed control techniques, the entire system presented in figure 3.2 has been modeled and simulated using the LTspice simulation tool. The flyback converter was selected due to its simplicity. In the present era, the application of control methodologies to microcontrollers has become a prevalent practice. In order to utilize microcontrollers, gate drivers are needed that permit a low-voltage digital signal to drive the power MOSFETs. Thus, the LTC7004 was used to apply the control signal directly. The control signal was generated through the implementation of behavioral voltage sources to execute the simulation in microcontroller manner.

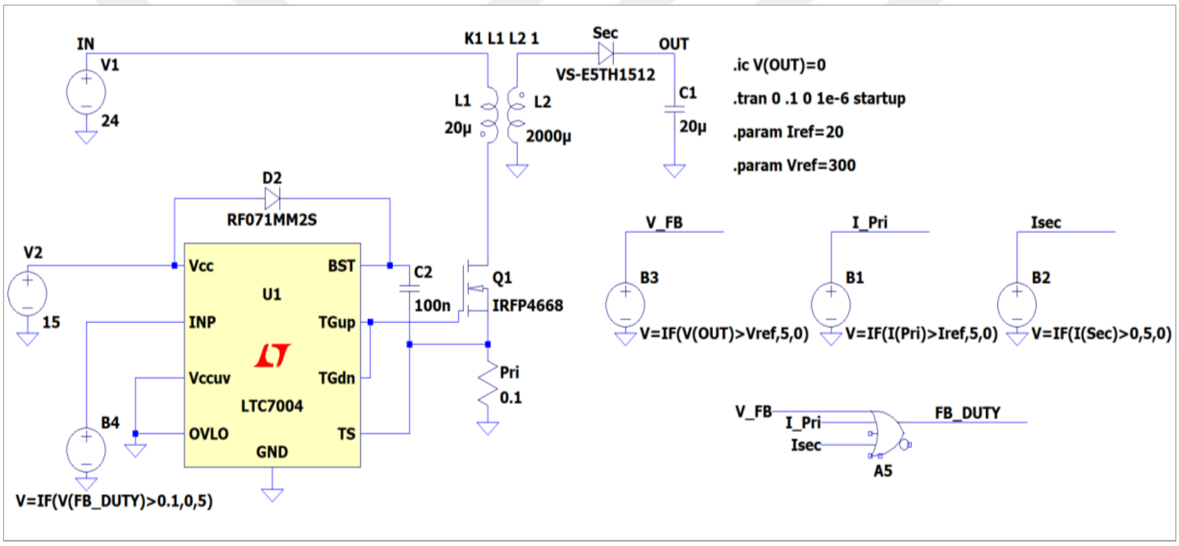

Figure 3.2. Schematic of LTspice

<u>Constant and variable frequency</u>

Figure 3.3 and 3.4 depicts the effects of the using of the constant and variable frequency. In the case of discontinuous conduction, a period of time exists during which the currents on both sides are at zero. This results in the dissipation of some of the energy stored in the capacitor in the parasitic and load components. In boundary conduction mode, the sequence of the energy pulses (switching frequency) is increased. In consequence, the charging time of the BCM is less than DCM as shown in figure 3.5. The discrepancy in charging time can be attributed to the lower switching frequency of the DCM. An increase in the switching frequency will result in a reduction in the charging time. As previously stated, the off time

is dependent on the capacitor voltage. The fall time of the initial pulses is significantly longer. If a high frequency is selected, it will result in the transistor turning on while the secondary current is above the acceptable threshold. This will subsequently lead to an increase in the primary current at the outset. Consequently, there is a limit to the switching frequency when operating in the DCM.

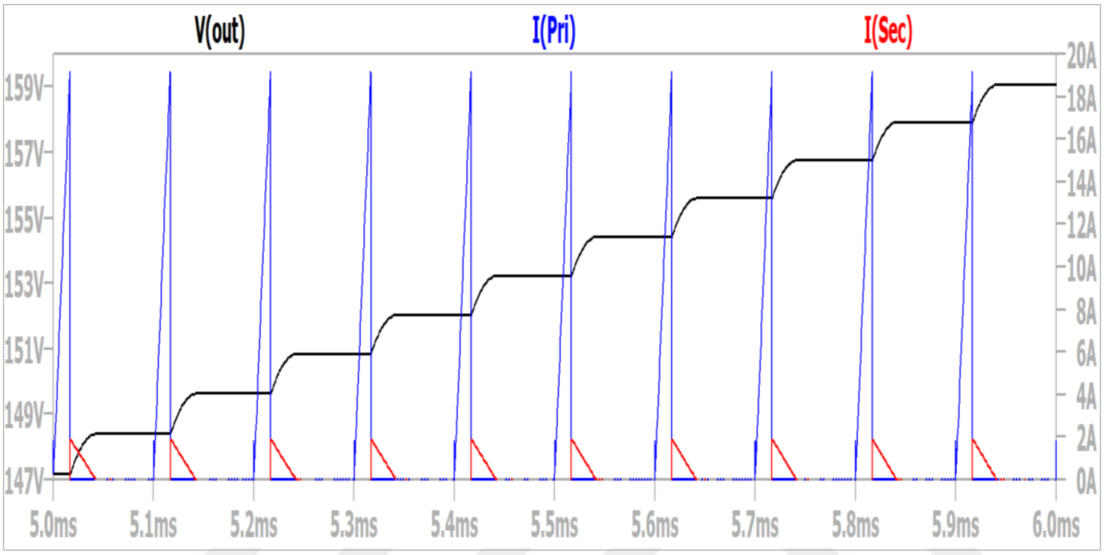

Figure 3.3. Constant frequency graphs

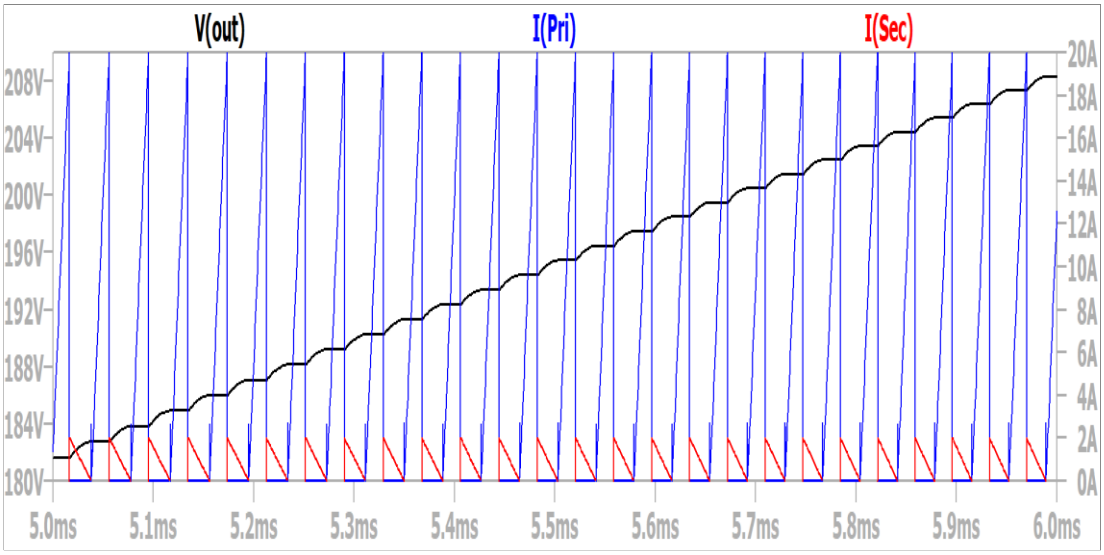

Figure 3.4. Variable frequency graphs

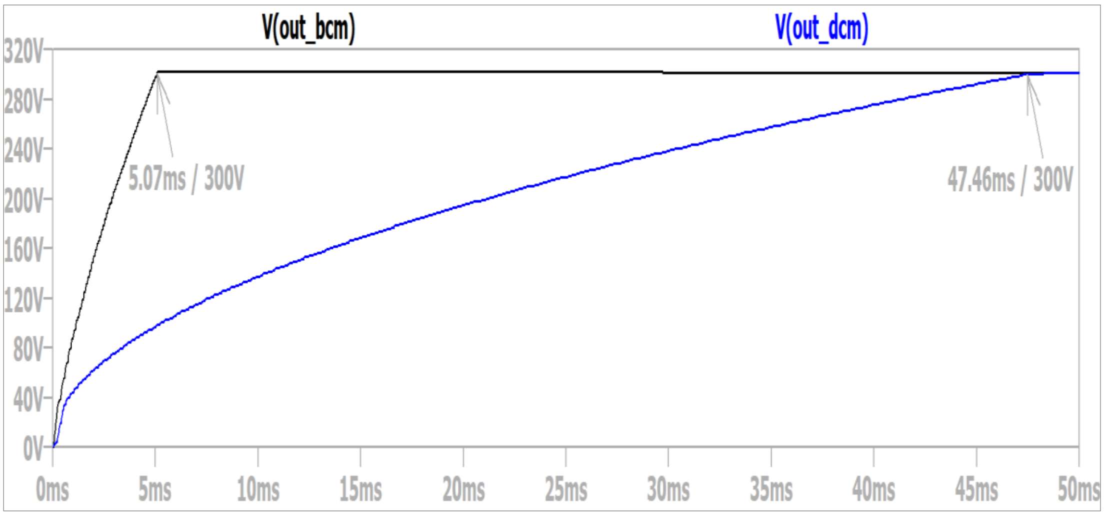

Figure 3.5. Charging time of variable and constant frequency

<u>Relationship between peak current and charging time</u>

The energy transferred to the capacitor is directly proportional to the charging time (transistor on time) as shown in figure 3.6. By increasing the charging current the amount of energy transferred to the capacitor can be increased. However, increasing the current also increases the losses on the components. This will result in decreased efficiency and increased heating of the CCPS. Therefore, the current level must be within limits that do not endanger the system's reliability.

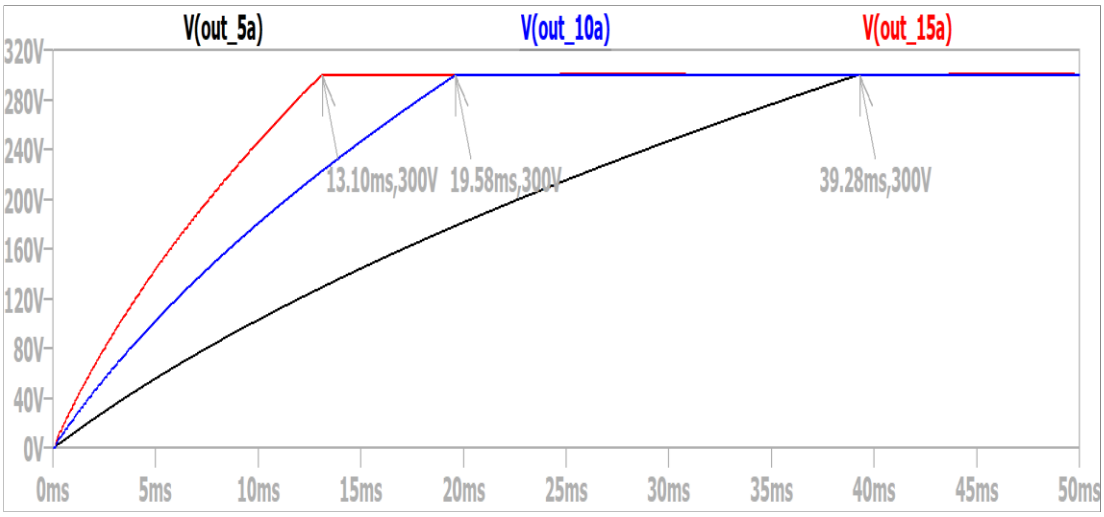

Figure 3.6. Charging times with different primary currents

Table 3.1. Effects of primary current

Primer Peak Current	Charging Time	Transistor's Losses (avg)	Diode's Losses (avg)	Measured Transistor On-Time	Calculated Transistor On-Time
5A	39.40ms	312.17mW	415.15mW	4.27μs	4.16μs
10A	19.62ms	336.48mW	475.05mW	8.45μs	8.33μs
15A	13.05ms	455.91mW	593.19mW	12.63μs	12.5μs

Relationship between VCC, peak current and charging time

The charging time and the peak current are related to the supply voltage. Alterations in input voltage over a fixed time interval result in changes in peak current. The outcomes of the primer current and the charging time graphs with varying input voltages are illustrated below.

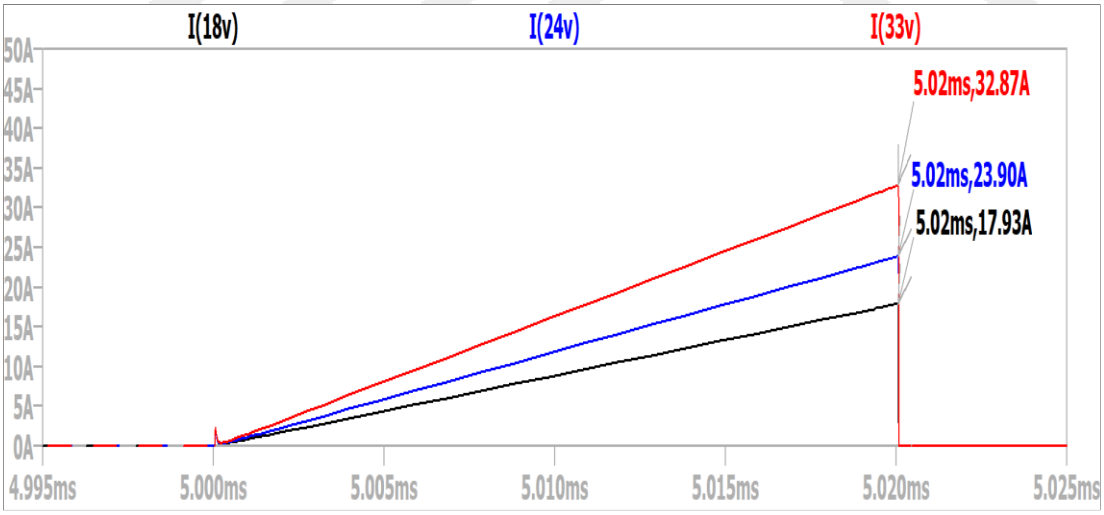

Figure 3.7. Primary currents with constant on-time and different input voltages

The Constant On-Time Control without Feed-Forward-Controlled was simulated. The on-time was selected as 20 μs. Increasing the supply voltage reduces the charging time as shown in figure 3.8. To implement the Feed-Forward-Control, the current values depending on the input voltage are calculated according to Eq. 3.3. The measured and the calculated primer peak currents were compared in table 3.2. As can be seen in figure 3.10, the feeding of the input voltage to the peak primary current control method could equalize the charging time.

$$I_{Pri_{(pk)}} = \frac{t_{on}\, VCC}{(1-\alpha)\, L_{Pri}} \tag{3.3}$$

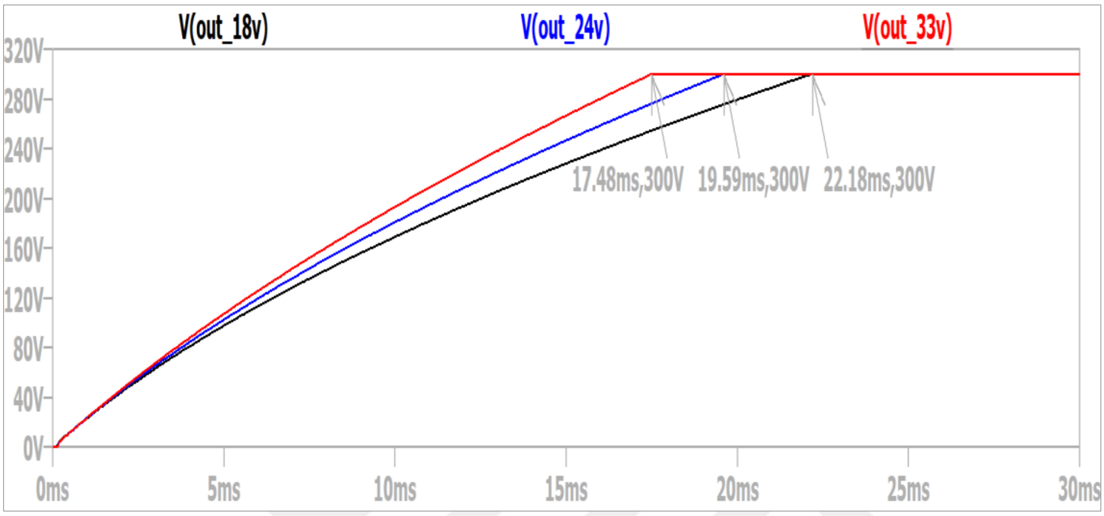

Figure 3.8. Charging time with different input voltages

Table 3.2. Primary currents with different input voltages

Input Voltage	Measured Primer Peak Current	Calculated Primer Peak Current
18V	11.23A	11.19A
24V	9.98A	9.92A
33V	8.97A	8.88A

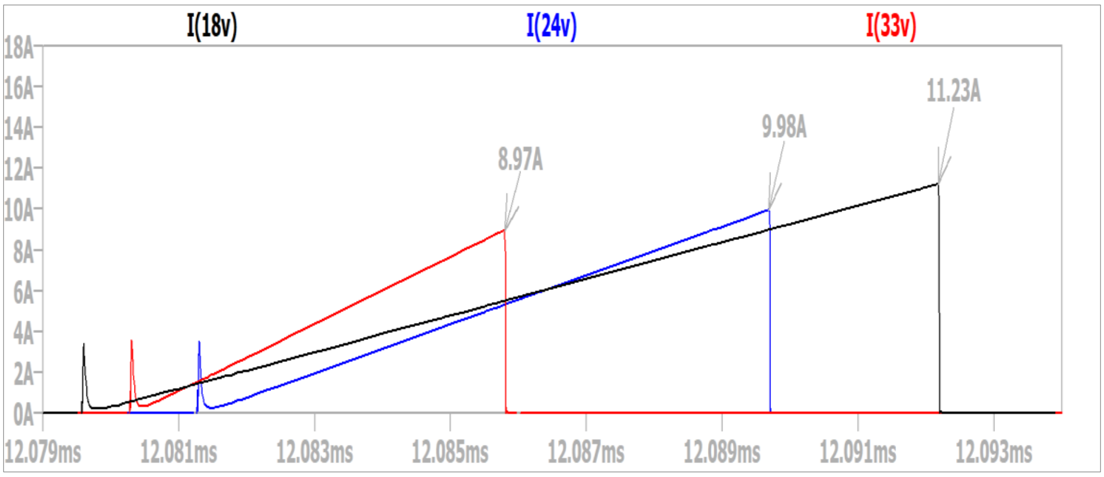

Figure 3.9. Primary currents with different input voltages

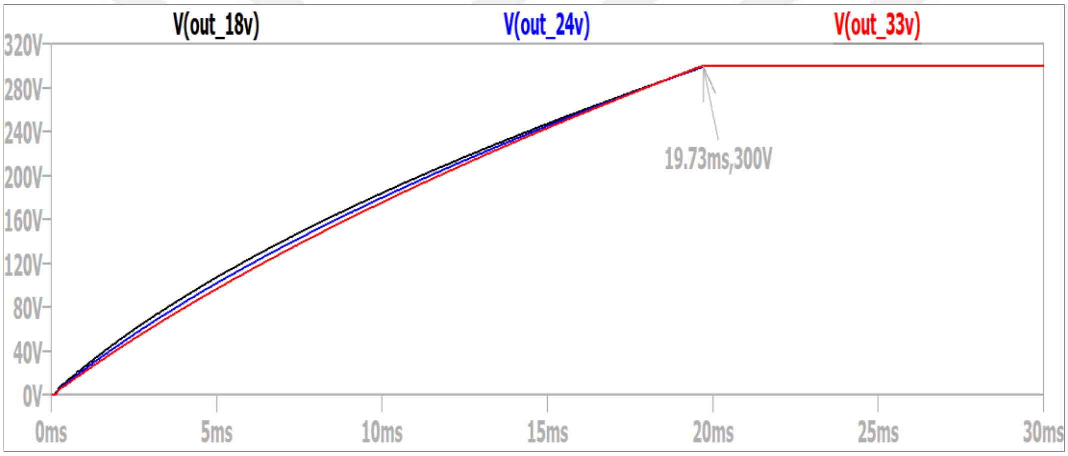

Figure 3.10. Charging time with feed-forward of input voltage

<u>Relationship between alfa, average current and charging time</u>

In a diode, the reverse recovery current is dependent upon the forward current of the diode. The high alfa value means a high current during the secondary diode conduction. The reverse recovery current is analyzed with different α values. An increase in the value of α results in an enhancement of the turn-off losses in the diode. However, this also increased the average output current, which shortened the charge time. In the simulation the peak value of the secondary current was 5A. Accordingly, the α values was calculated using the Eq. 3.4.

$$\alpha = \frac{I_{Sec_{(off)}}}{I_{Sec_{(pk)}}} \tag{3.4}$$

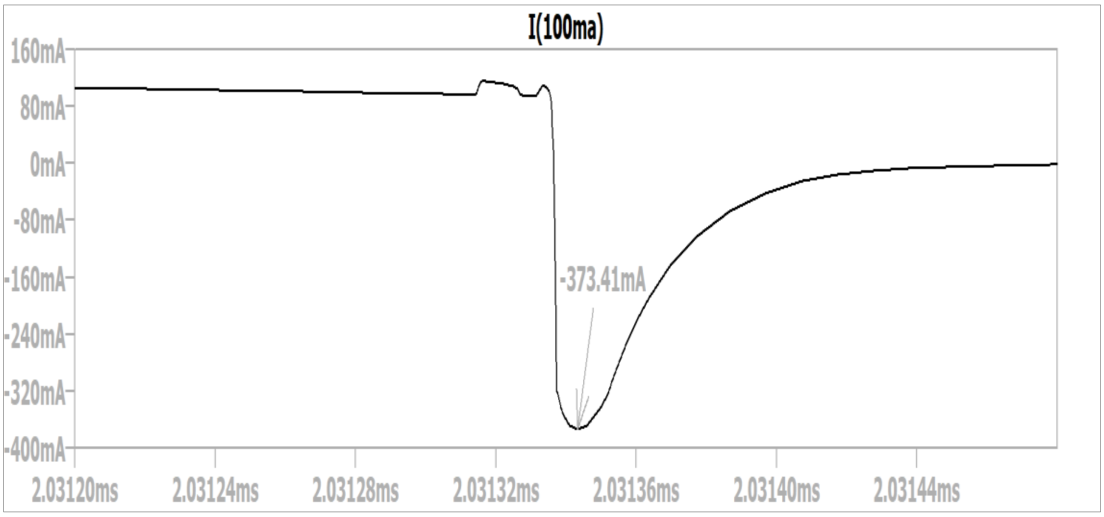

Figure 3.11. Reverse recovery current (α=0.02)

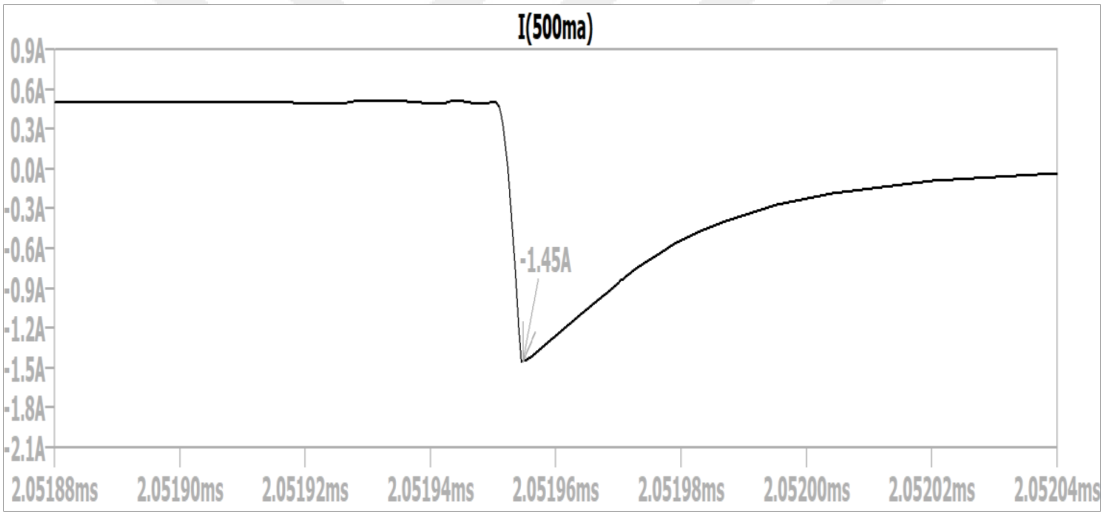

Figure 3.12. Reverse recovery current (α=0.1)

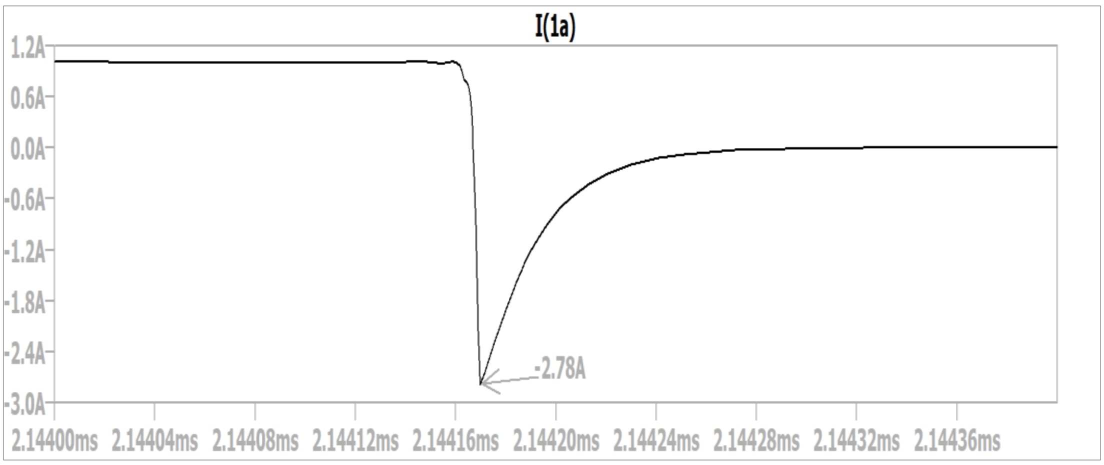

Figure 3.13. Reverse recovery current (α=0.2)

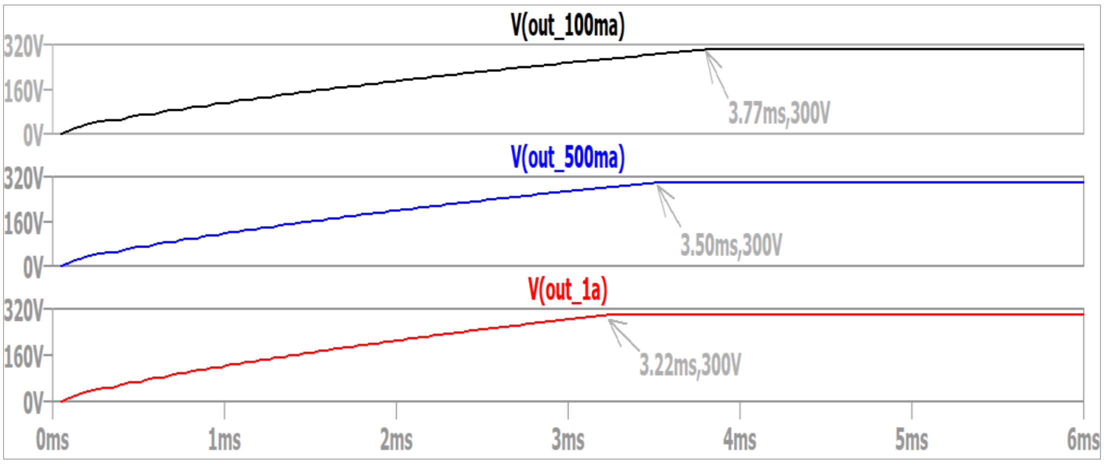

Figure 3.14. Charging times with different α values

Table 3.3. Effects of α values

Hysteresis	Charging Time	Measured Seconder Avg. Current	Measured Seconder RMS Current
100mA (α=0.02)	3.77ms	1.58A	2.34A
500mA (α=0.1)	3.50ms	1.71A	2.44A
1A (α=0.2)	3.22ms	1.86A	2.57A
3A (α=0.6)	2.48ms	2.41A	3.16A

<u>Regulation mode controls</u>

The charging process is terminated when the capacitor voltage reaches the desired level. When the charging process is stopped, the capacitor will lose its energy due to some parasitic resistances and the leakage of the capacitor. To compensate for these losses small energy pulses should transfer to the capacitor. However, a high primary current limit causes more energy to be transferred than necessary. This results in overshoot in the output voltage. Charging is completed when the capacitor voltage reaches the desired value. However, the last packet of energy delivered to the capacitor may result in an output voltage above the target voltage. For this reason, the ability to work in regulation mode should be added to the control algorithm. The LT3420 has an automatic refreshing feature which allows the capacitor to remain charged. However, this refreshing occurs at a predetermined rate and is not dependent on the change in output voltage and output load. Unlike the LT3420, the LT3751 directly senses the output voltage and enters low noise regulation mode. The LT3751 has constant thresholds for changing modes. The LT3751 will operate in regulation mode for approximately the last 10% of the charge. This increases the charge time.

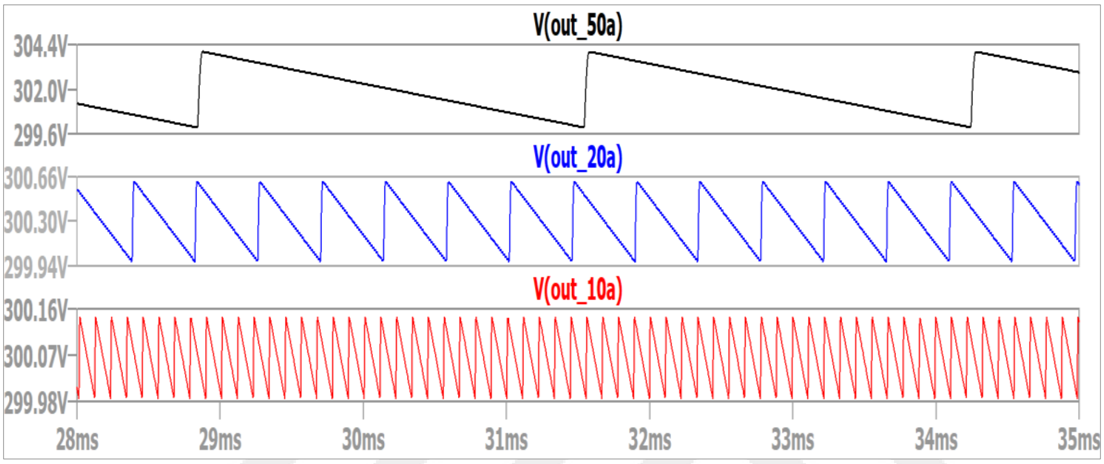

Figure 3.15. Output voltage ripple graphs with different primary currents

A low peak current limit results in low ripple and high frequency in the regulation mode.

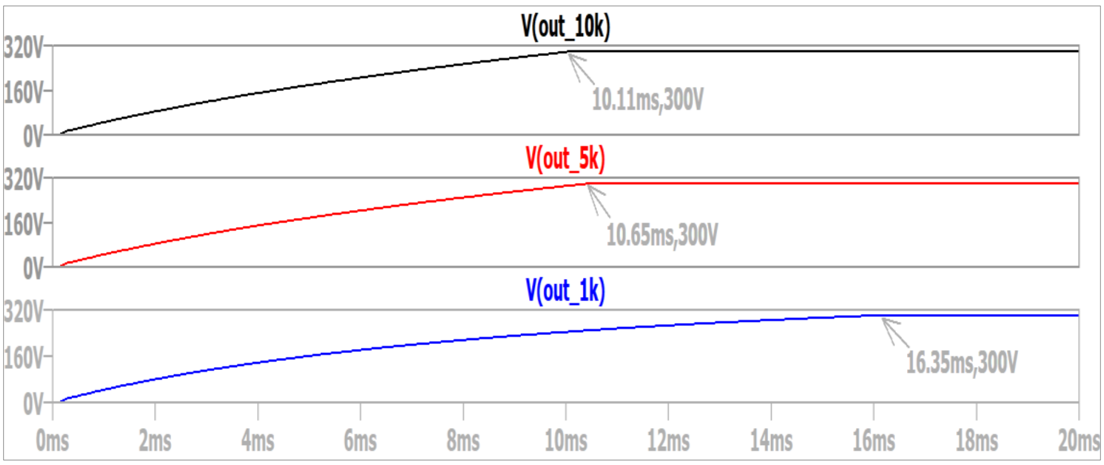

Figure 3.16. Charging times with different output loads

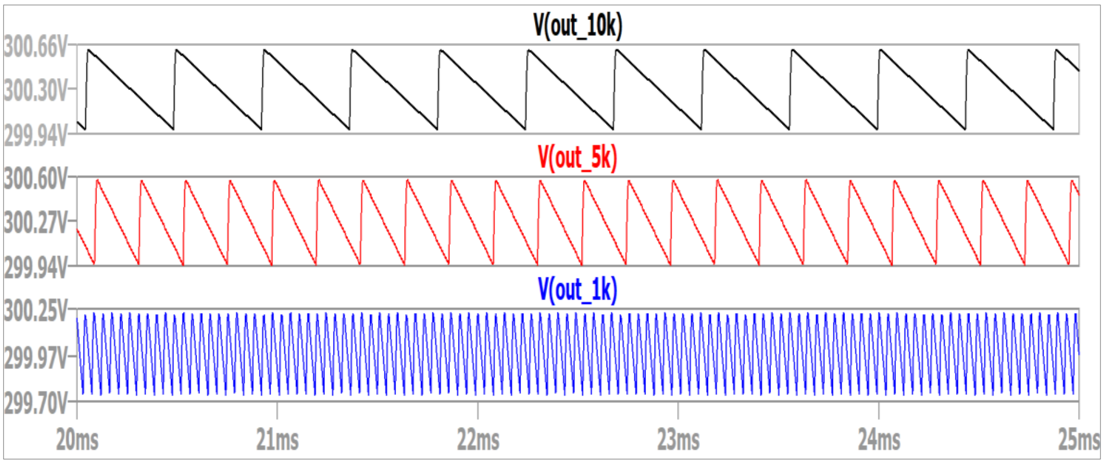

Figure 3.17. Output voltage ripple graphs with different output loads

A low output load results in high ripple and high frequency in the regulation mode.

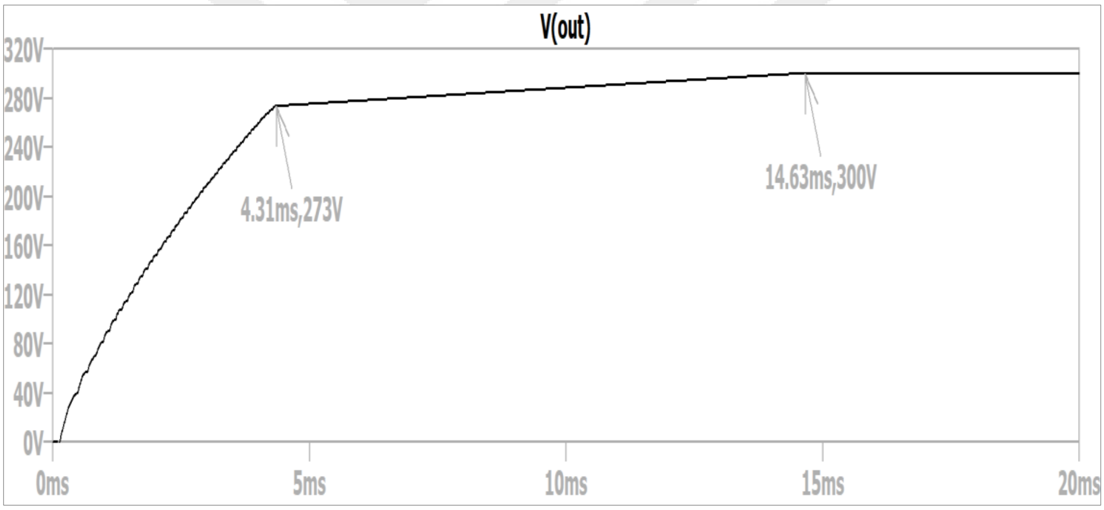

Figure 3.18. Charging time graph of LT3751

4. FLYBACK CONVERTER

A flyback converter is a topology which is used in switched-mode power supplies (SMPS). This isolated topology is especially well-suited for low to medium power levels because of some drawbacks. Nevertheless, the flyback converter also possesses certain advantages. The simplicity of its design and its ability to provide multiple output voltages are two of the most commonly cited advantages of this topology.

4.1. Structure and Operations Principle

Figure 4.1 shows the structure of the topology. The flyback converter consists of an active switch, a transformer, a rectifier diode and a filter capacitor. The flyback converter requires less component to operate. Thus, it is cost-effective and efficient. There are various topologies in the literature that are similar to each other. The operational principles of the flyback converter and the buck-boost converter are analogous. The buck-boost converter uses an inductor to store energy. In contrast to the buck-boost converter, the flyback converter uses a transformer to store energy. The transformer also provides isolation between the primary and secondary sides. Indeed, the transformer of the flyback converter serves a similar function to that of a coupled inductor. In contrast to transformers used in other topologies, it has an air gap. In contrast to alternative converter types, the flyback converter does not have an output inductance filter. Consequently, the design and effective cost of the converter are reduced. The working principle consists of three main phases.

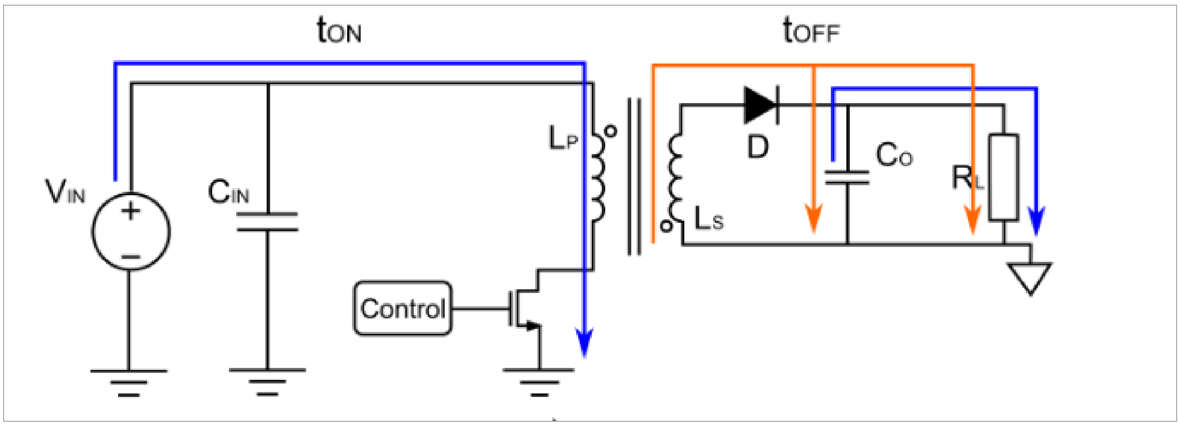

Figure 4.1. t_{ON} and t_{OFF} (monolithicpower)

Stage 1 (t0 – t1)

Upon the activation of the switch, the primary side of the transformer will begin to function as an inductor, thereby initiating the storage of energy from the input. In this phase, all energy is accumulated within the transformer core in the form of a magnetic field. During this phase of energy storage, the output side will exhibit no voltage. The diode in the secondary winding is unable to conduct at this time due to the presence of reverse polarity (reverse biased). Consequently, no energy flows through the secondary circuit.

Stage 2 (t1 – t2)

When the switch is deactivated, the polarity of the primary side of the transformer is reversed. This results in the induction of voltage in the secondary side due to electromagnetic induction. This induces a forward bias in the diode, and the magnitude of the induced voltage is proportional to the turn ratio. When the diode is in a conducting state, the energy that has been stored is transferred from the secondary winding to the output (load and output capacitor).

Stage 3 (t2 – t0)

This state can be described as idle state. The term "idle state" is typically employed to describe a situation in which the device is not transferring energy. In other words, it is not supplying power from input to output. The current is not present on either side. Therefore, the output voltage is typically maintained by the energy stored within the output capacitor. It is important to note that the current stage is only accessible in the discontinuous conduction mode (DCM). These switching phases are repeated until the desired output voltage is achieved.

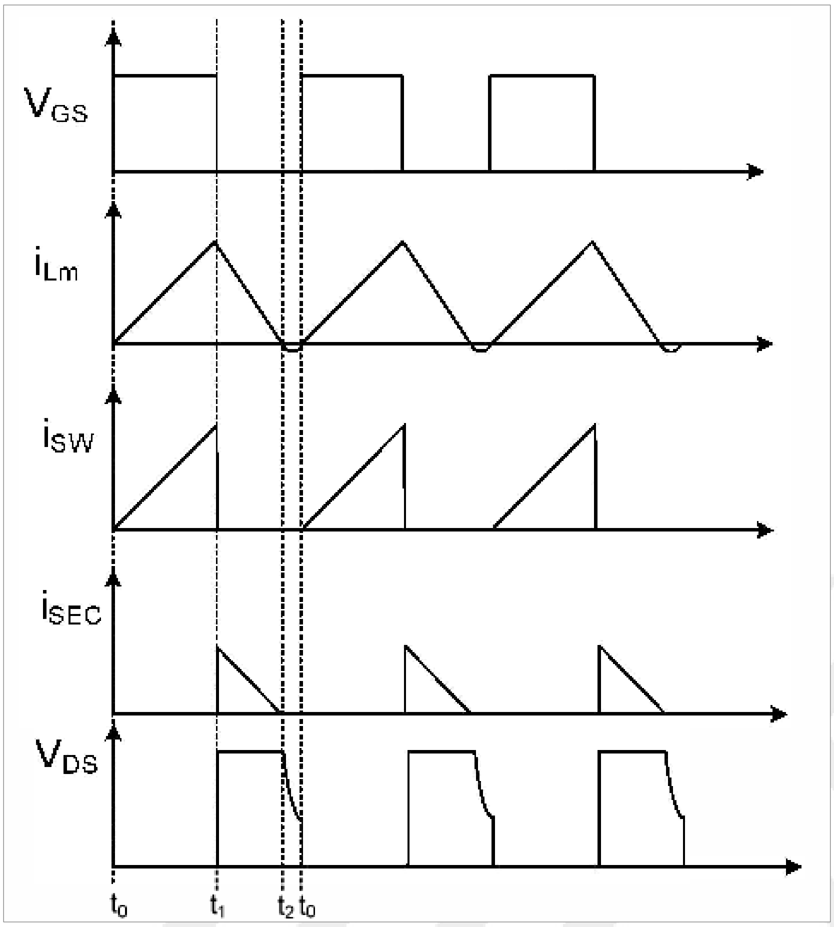

Figure 4.2. Waveforms of flyback converter (Chen and Liang, 2014)

4.2. Operations Modes (CCM-DCM-BCM)

In power electronics, operating modes are classified according to the state of current in a switching cycle.

4.2.1. Continuous conduction mode (CCM)

In CCM, the current in the primary winding does not fall to zero at the end of the switching cycle. Instead, it maintains a positive value over the course of the cycle. Therefore, it is evident that the energy stored within the magnetic core of a transformer will never reach zero. Consequently, the core is always possessed of a certain degree of magnetic energy. The process of energy storage and transfer is continuous.

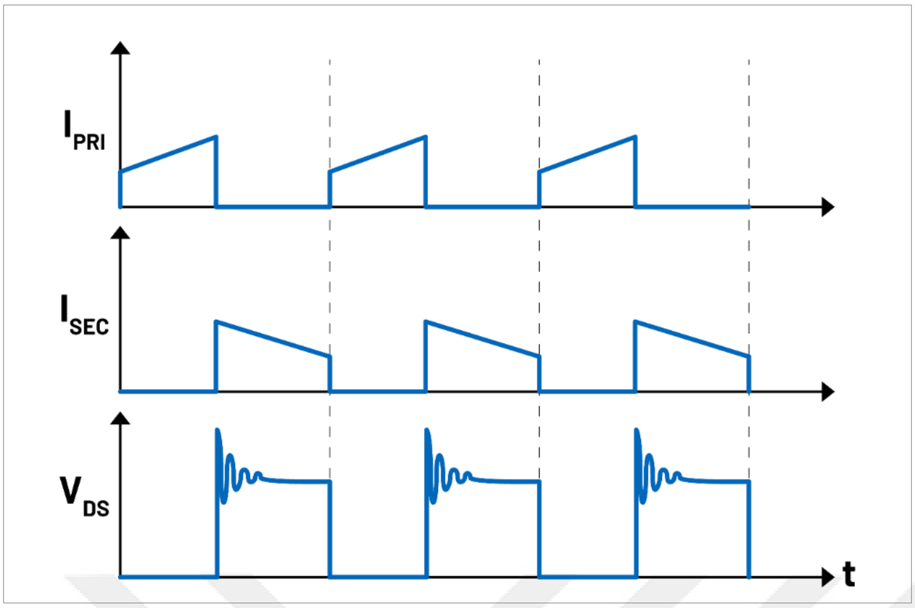

Figure 4.3. Waveforms of CCM (Redhair)

4.2.2. Discontinuous conduction mode (DCM)

When the switch being deactivated for a relatively extended period of time, the energy stored in the secondary winding is fully transferred to the output. In contrast to the CCM, the current flowing through the primary and secondary windings is reduced to zero. The transfer of energy occurs through the discharge of all stored energy into the load and output capacitor.

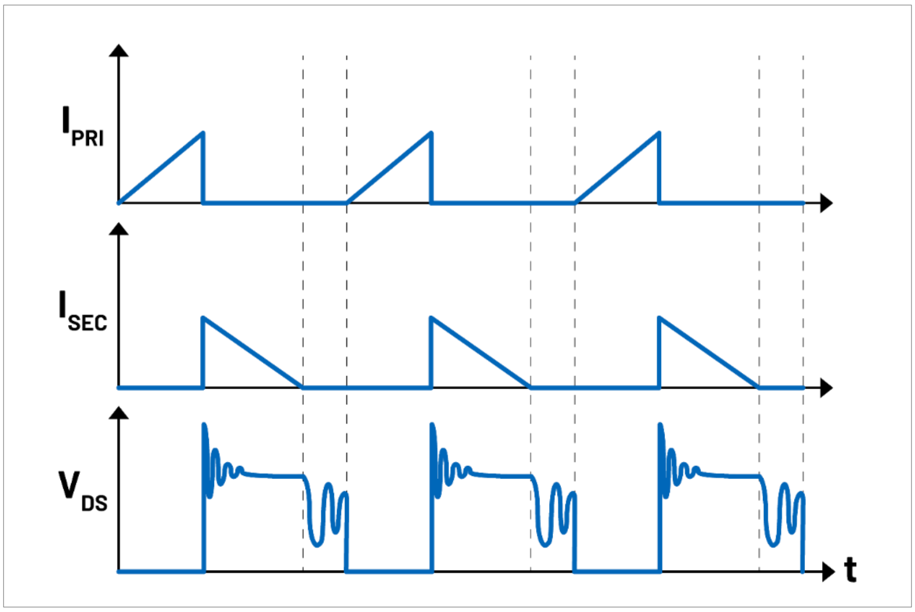

Figure 4.4. Waveforms of DCM (Redhair)

4.2.3. Boundary conduction mode (BCM)

The energy stored in the transformer core is reduced to zero with each switching cycle, yet the subsequent cycle commences without delay. In other words, as soon as the current reaches zero, the switch is activated once more. In each switching cycle, the core is fully discharged, and this occurs without interruption.

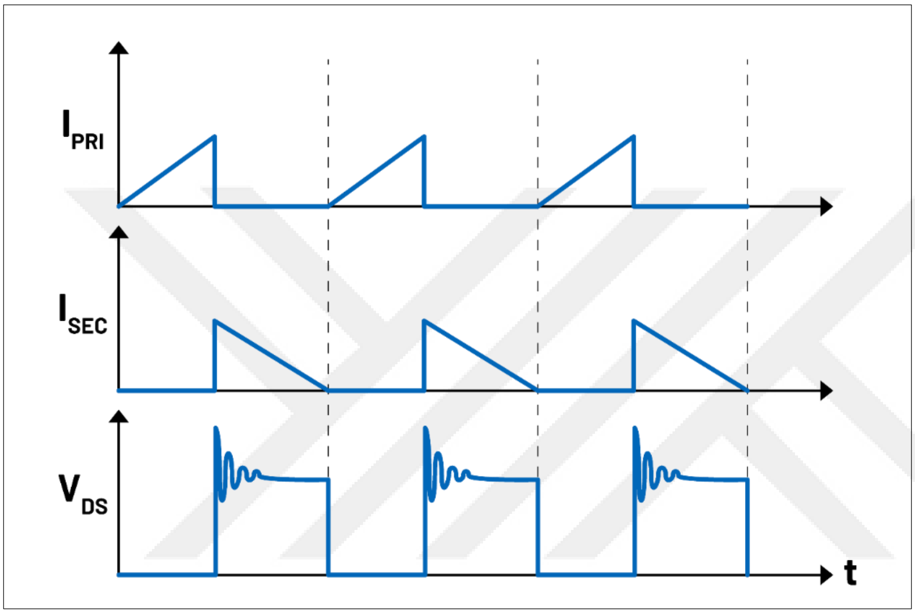

Figure 4.5. Waveforms of BCM (Redhair)

4.2.4. Compare of mods

In switching power supplies such as flyback converters, the CCM, DCM, and BCM represent optimized energy transfer methods for different operating conditions. The selection of these modes is dependent upon the manner in which the energy stored within the transformer core is managed and the load requirements. The advantages and disadvantages of each mode are relative to the power level, dynamic response requirements, and cost objectives of the application.

CCM is a mode of operation that provides stability in energy transfer. The energy stored in the transformer never reaches zero, which allows the output voltage and current to fluctuate less. CCM is generally favored in high power applications and offers a lower level of electromagnetic interference (EMI). However, due to the large size of the transformer and filter elements, it occupies more space in the design and can increase cost. Additionally, efficiency at low loads is lower than DCM.

DCM is a mode of operation in which the energy stored in the transformer is fully discharged with each switching cycle. In this mode, the design can be accomplished with smaller components and the control system is more straightforward, which results in a reduction in cost. However, the fluctuations in output voltage and current are more pronounced. DCM is typically preferred in devices such as LED drivers and low-power adapters due to its high efficiency in light load applications. It may be necessary to take additional precautions during the design phase due to the potential for a high EMI level.

BCM represents a synthesis of CCM and DCM. Upon reaching zero, the transformer current initiates the subsequent switching cycle, so that the energy transfer is uninterrupted by resetting each cycle. This operational mode ensures efficient performance at light loads while maintaining control of the electromagnetic interference (EMI) level. However, the control circuitry is complex, and the efficiency may not be as optimal as CCM in high-power applications. BCM is typically the preferred mode in adapters where energy efficiency is of paramount importance and in applications where light load transients are a common occurrence.

In selecting between these three modes, it is essential to consider the specific requirements of the intended application, including power level, stability, cost, size, and electromagnetic interference (EMI). CCM provides stability at high power levels, while DCM is optimal for low-cost and light-load applications. BCM is appropriate for applications of moderate complexity that necessitate the management of electromagnetic interference and the optimization of energy efficiency.

Table 4.1. Comparison of CCM, DCM and BCM

Parameters	CCM	DCM	BCM
Current Status	Continuous (never zero)	Discontinuous (decreases to zero)	Continuous (decreases to zero)
Stability	High	Low	Medium
Efficiency	High at high power	High at light load	Medium (efficient at light load)
Transformer Size	Large	Small	Medium
EMI Level	Low	High	Medium
Control Complexity	Medium	Simple	Complex
Output Diode Reverse Recovery Loss	High	Low	Low
MOSFET Switching Loss	Highest	Low	Lowest
Conduction and Windings Losses	Low	Highest	High
Operating Frequency	Fixed	Fixed	Variable
Applications	High power applications	Low power applications	Low power applications

4.3. Snubber

In flyback converters, due to the leakage inductance of the transformer and the rapid switching, sudden and high voltage spikes occur. This may cause damage to the circuit elements.

The snubber is a protection circuit used to damp unwanted voltage spikes and noise during switching especially during the discharge of the accumulated energy in the transformer. Snubber prevents circuit elements to damage and reduces electromagnetic interference (EMI). Snubber circuits are helpful to ensure the safety of the converter and increase the stability of the converter. A properly designed snubber circuit extends the life of the components, reduces EMI and improves the overall reliability of the system.

The effect of leakage inductance

In flyback transformers, an ideal magnetic coupling between the primary and secondary windings cannot be achieved. Therefore, some magnetic energy is stored as leakage inductance. The leakage inductance cannot transfer the energy to the secondary side. This energy is released to the primary side when the MOSFET turns off. When the MOSFET turns off, the current flowing in the primary winding is rapidly terminated. However, according to Lenz's law, the change of the direction of the current within the coil induces a voltage. The leakage inductance wants to counteract this current change and sends the energy back as voltage. This rapid energy conversion causes sudden voltage spikes. These voltage spikes can damage switching elements or cause electromagnetic interference (EMI) in the circuit.

High frequency operation and resonance

Flyback converters usually operate at high frequencies. At high frequency, stray inductance and parasitic capacitances in the circuit can create a resonance effect. This resonance causes an unwanted voltage ripple in the circuit. This can make it difficult for the device to meet electromagnetic compatibility requirements.

4.3.1. Passive snubber

The passive snubber is a type of snubber technique that the energy within the snubber circuit is dissipated through heat transfer. It contains a capacitor and a resistor to store voltage spikes and then dissipate the stored energy as heat. It is straightforward and cost-effective. However, due to the loss of energy through heat, its efficiency may be limited. Therefore, it is more preferred in low power applications. If higher voltage protection is needed, a diode can be added to the circuit. The diode directs energy in a certain direction, allowing it to be stored in the capacitor. Similarly, the energy stored in the capacitor is later discharged through the resistor. In order to increase efficiency, it is important to control energy without converting it into heat. A Zener or TVS (Transient Voltage Suppressor) diode can be added to the circuit. These diodes limit voltage spikes when they exceed a certain threshold. They offer faster response time. For this reason, they are preferred in applications where the high-speed protection is requiring. However, it only works effectively within a certain voltage range.

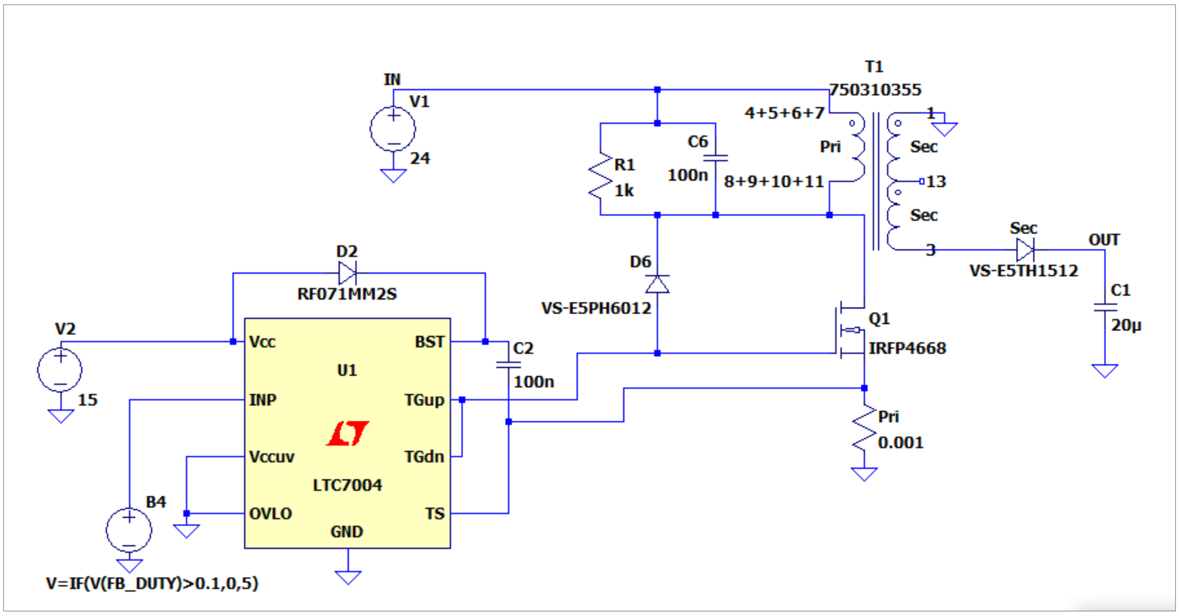

Figure 4.6. Schematic of passive snubber

4.3.2. Active snubber

Efficiency is of great importance in new generation circuits. Therefore, recovering energy lost through heat is important to increase efficiency. Unlike passive snubber circuits, active snubber circuits contain active elements (e.g. transistors). These circuits recover the energy while controlling voltage spikes caused by leakage inductance. As a result, active snubber helps increase overall efficiency.

Generally, leakage inductance energy is transferred to the clamp capacitor for storage. Stored energy is then used again. Active snubbers are more complex compared to passive snubbers. Since it contains a switching element, it requires extra control circuit elements. However, there are also versions that do not need to be controlled by an external controller. LCD snubber is a type of regenerative snubber that contains only passive elements (inductor, capacitor and diode). The Inductor in the circuit stores the sudden energy increases and transfers this energy to the capacitor. Diodes in the circuit limit voltage increases by directing the energy flow similarly the passive snubbers. The energy accumulated in the capacitor is returned to the circuit in the next switching cycle. Thus, system efficiency increases.

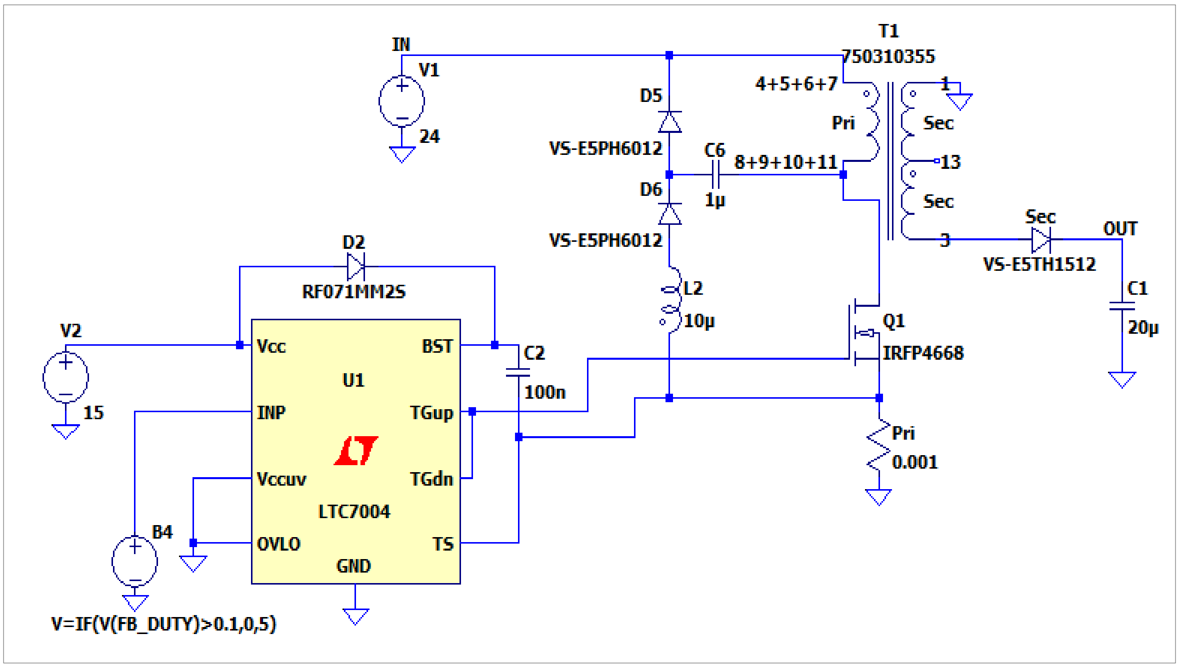

Figure 4.7. Schematic of active snubber

Table 4.2. Comparison of snubber circuits

Parameters	Passive Snubber	Active Snubber
Energy Status	Heating	Regenerative
Efficiency	Low	High
Complexity	Low	High
EMI Level	Medium	Low
Cost	Low	High

4.3.3. Simulations of snubber circuits

Simulations were conducted using the Flyback circuit prepared in the LTspice environment, without the snubber circuit, with the passive snubber circuit, and with the active snubber circuit. The RCD topology was selected for implementation in the passive snubber circuit. The LCD topology was selected for the active snubber circuit. In the simulation studies, measurements were taken with varying capacitor and resistor values. According to the simulation results, the capacitor value in the snubber circuit has a direct impact on spike voltage suppression. In the active snubber circuit, an increase in capacitor value results of increase in the current passing through the diode. However, the change to the capacitor had minimal effect on efficiency and charging time. The need for high-current diodes will increase the cost. Since the energy is directed back to the switch in the active snubber circuit, the efficiency is higher than the passive snubber circuit. While the higher resistance in the passive snubber circuit provides a reduction in charging time, it created resonance within the circuit. A lower resistance value can be used in order to get more stable operating structure. However, as the resistance value decreases, the limited current value also increases. This necessitating the use of resistors with higher power values. Since size is important criterion in CCPS applications, it's important to pay attention to the resistor size. Tests were carried out by charging the 20μF capacity with 60 amps to 300V.

Table 4.3. Simulation results of snubber circuits

Topology	Charging Time	Resistor Power	Diode Current	Efficiency	Input Energy	Output Energy	V_{SPIKE} (Max)
Without Snubber	3,35ms	-	-	93%	0,96J	0,90J	190V
RCD (100nF 1 Ω)	15ms	387W	-	9,5%	9,35J	0,89J	57V
RCD (100nF 10 Ω)	4,14ms	37W	-	63%	1,41J	0,89J	91V
RCD (100nF 100 Ω)	3,03ms	4,6W	-	68%	1,31J	0,89J	96V
RCD (100nF 1K Ω)	2,88ms	0,4W	-	65%	1,36J	0,89J	97V
RCD (10nF 10 Ω)	4,12ms	36W	-	64%	1,39J	0,89J	140V
RCD (1µF 10 Ω)	3,67ms	29W	-	44%	2,03J	0,88J	65V
LCD (10nF)	3,33ms	-	35A	95%	0,94J	0,9J	174V
LCD (100nF)	3,45ms	-	58A	95%	0,94J	0,9J	100V
LCD (1µF)	3,73ms	-	69A	92%	0,97J	0,9J	67V

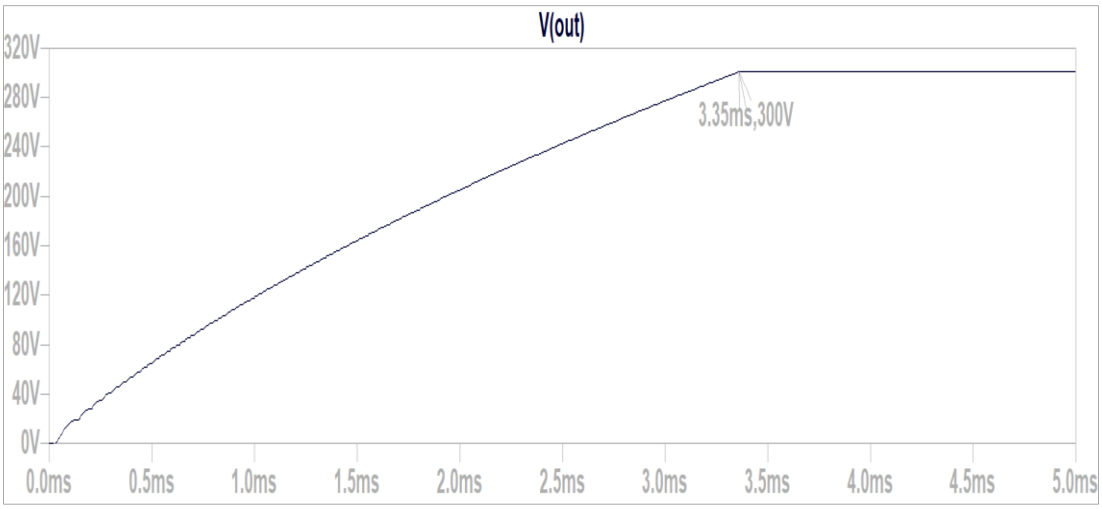

Figure 4.8. Charging time graph without snubber

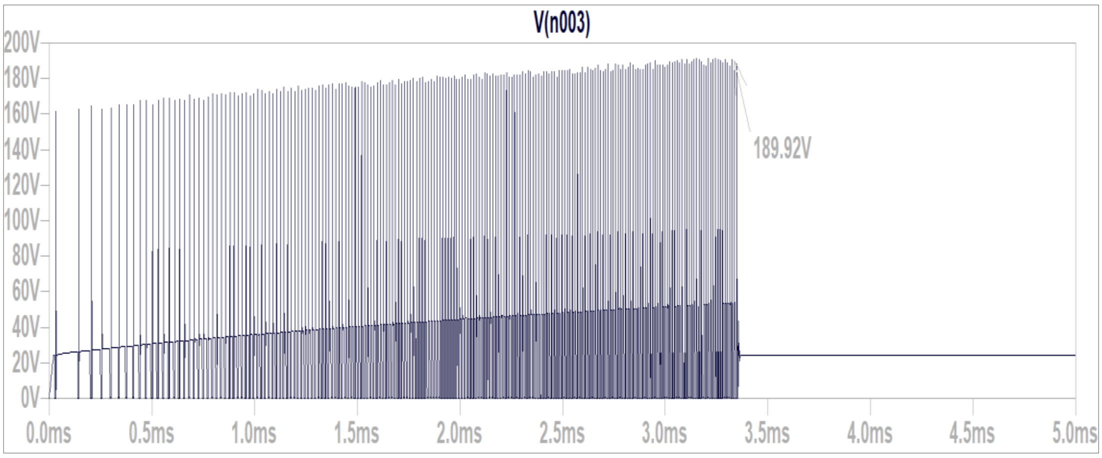

Figure 4.9. Voltage spikes graph without snubber

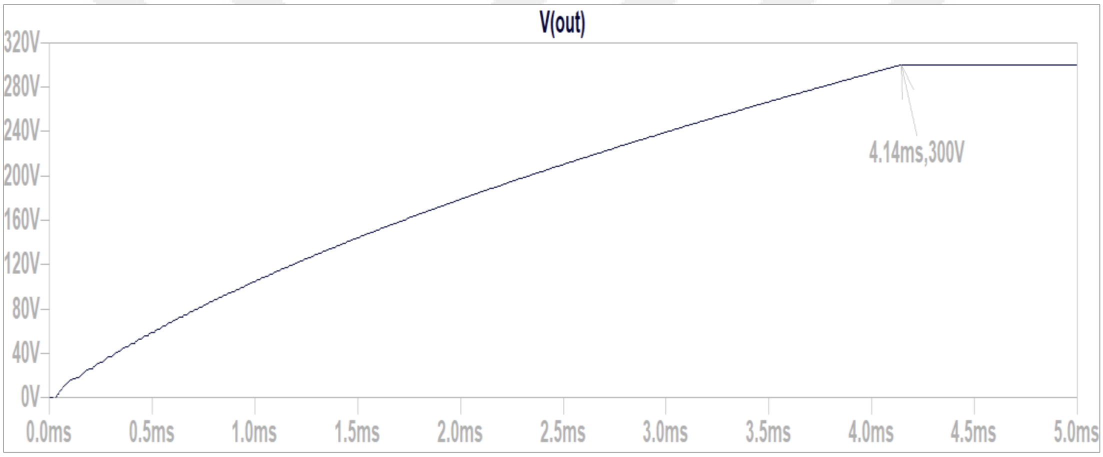

Figure 4.10. Charging time graph with RCD (100nF 10 Ω)

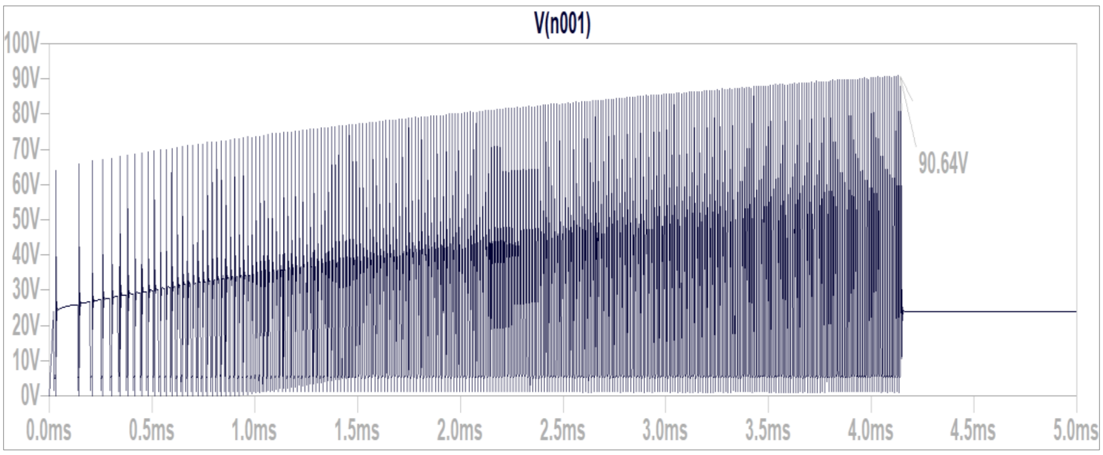

Figure 4.11. Voltage spikes graph with RCD (100nF 10 Ω)

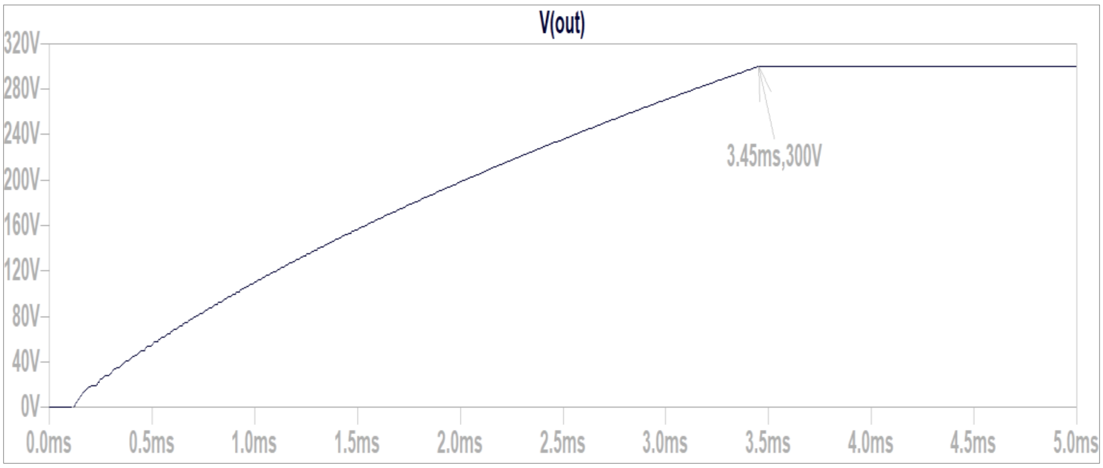

Figure 4.12. Charging time graph with LCD (100nF)

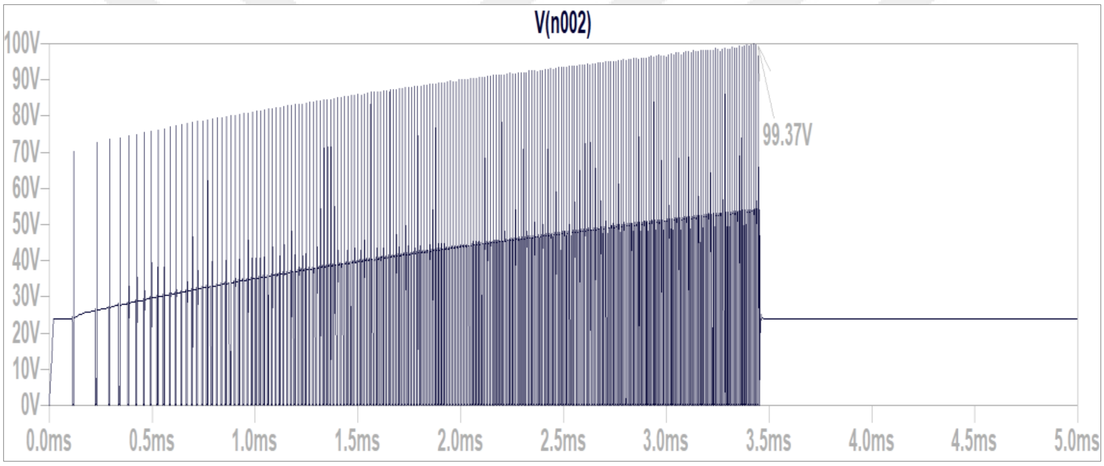

Figure 4.13. Voltage spikes graph with LCD (100nF)

5. EXPERIMENTAL STUDIES

In this section the schematic, software and PCB design was detailed. The oscilloscope graphs of the experimental studies were mentioned.

5.1. Schematic Design

The thesis study focused on control algorithms developed for CCPS. For this reason, the flyback converter topology, in which control algorithms can be analyzed most easily, was preferred.

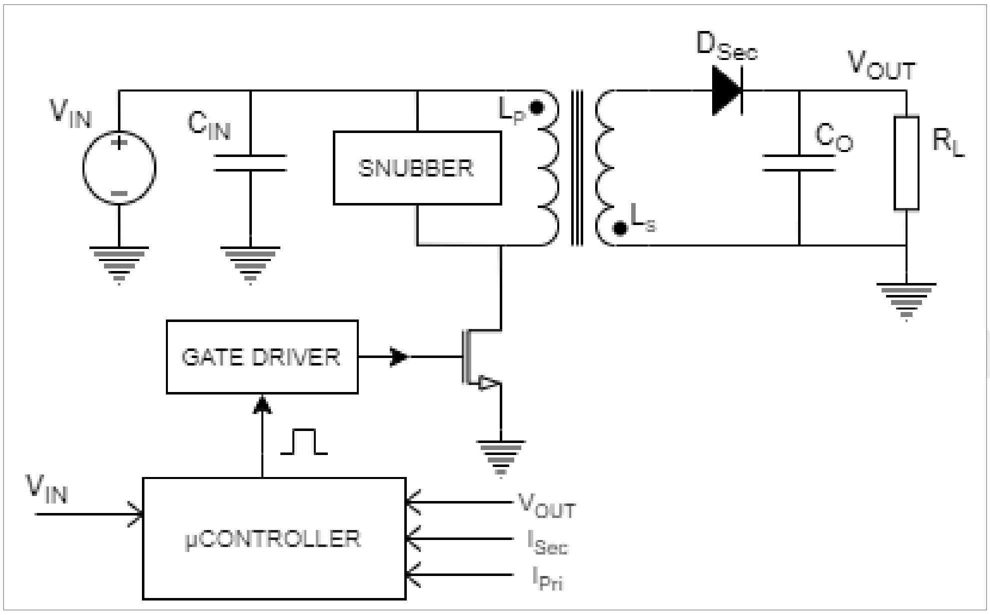

Figure 5.1. Topology of CCPS

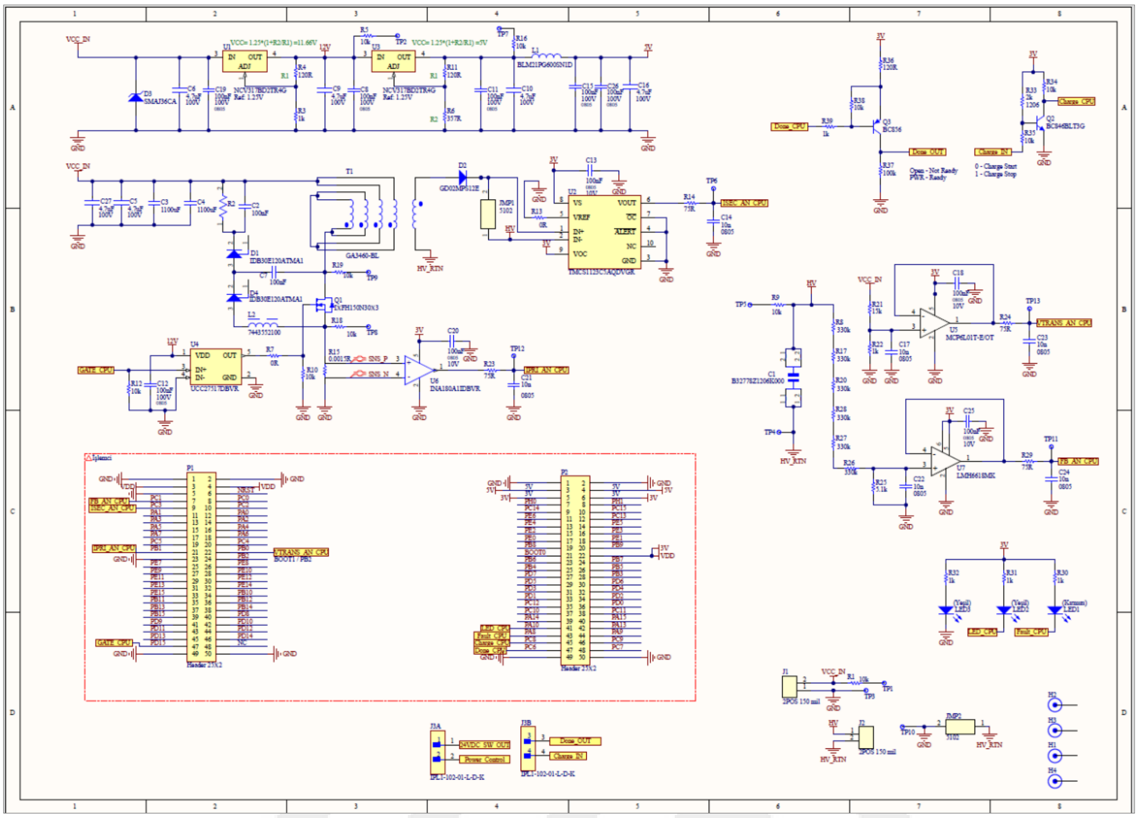

Figure 5.2. Schematic of design

5.1.1. Regulator circuits

A typical input voltage of the CCPS to operate is between 18-33VDC. However, the subcircuits used in the design may require supply voltages lower than the input voltage. In the designed circuit, the input voltage is reduced to 11,66V voltage level in order to drive the switch. Similarly, a 5V converter circuit was added for other subcircuits. Voltage conversions were carried out with Linear and low-dropout (LDO) regulators. Linear regulator is a voltage regulator that reduces the output voltage to a constant value by dissipating the excess of the input voltage as heat. Linear regulators are preferred due to their simple design and lower costs for applications that do not require high efficiency. In this study, LDO preferred to use for voltage regulations because LDO requires fewer external components. The 'NCV317BD2TR4G' was preferred due to its high input voltage range and output current. The output voltages are calculated according to the Eq. 5.1.

$$V_{OUT} = 1{,}25V\left(1 + \frac{R_2}{R_1}\right) \tag{5.1}$$

$$V_{OUT_{U1}} = 1{,}25V\left(1 + \frac{1000}{120}\right) = 11{,}66V \tag{5.2}$$

$$V_{OUT_{U3}} = 1{,}25V\left(1 + \frac{357}{120}\right) = 4{,}96V \tag{5.3}$$

Table 5.1. Parameters of ‘NCV317BD2TR4G’

Parameters	Value
Input Voltage (max)	40V
Output Voltage Range	1.2 - 37V
Output Current	1.5A

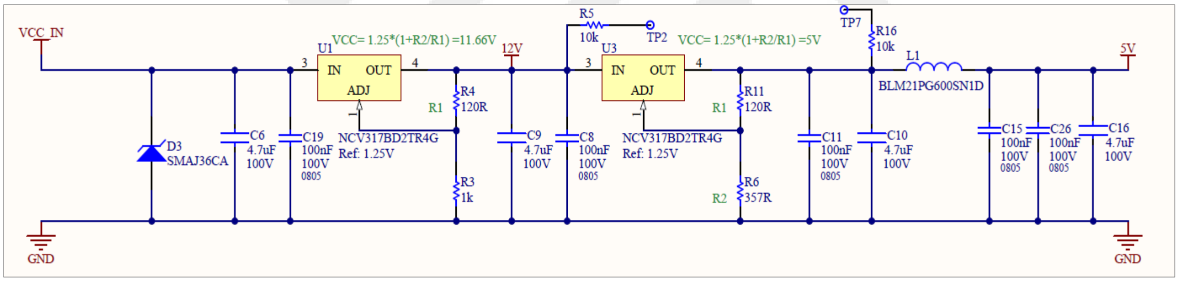

Figure 5.3. Schematic of regulator circuit

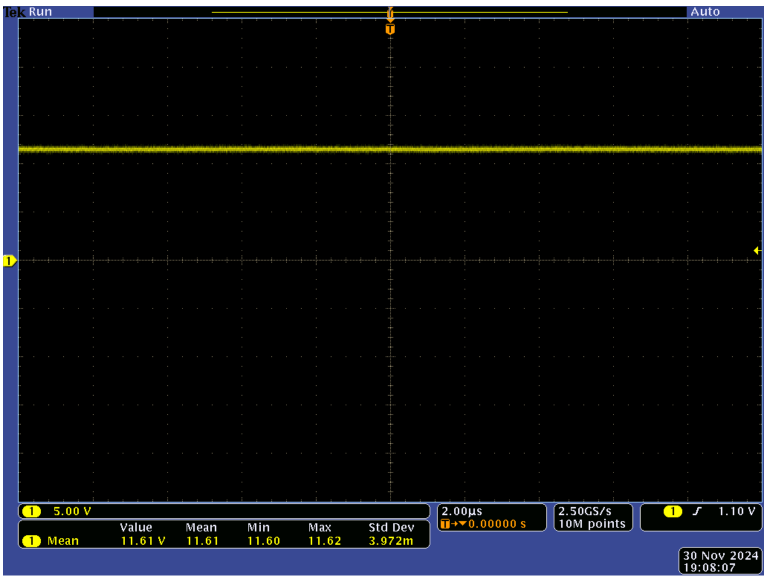

Image 5.1. Output voltage of U1

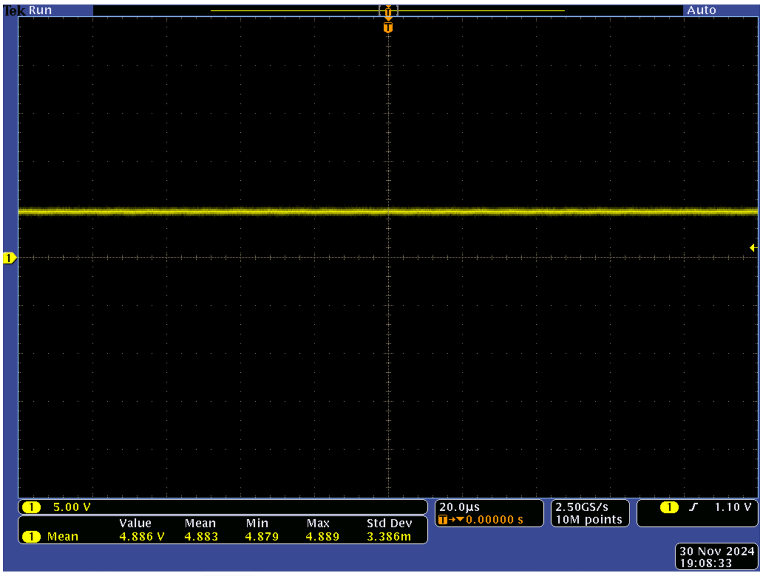

Image 5.2. Output voltage of U3

5.1.2. Selecting of the MOSFET

When the operating modes of the flyback converter are examined, it is seen that there are sudden voltage increases (spikes) on the MOSFET during switching. While selecting the switch, the maximum voltage level to which the MOSFET can be exposed was taken into consideration. When the MOSFET is deactivated, it is exposed to a voltage level which equal to the sum of the output voltage reflected by the transformer ratio and the input voltage. A margin must be left for voltage spikes that may occur above the calculated voltage level.

$$V_{Drain\,(max)} = \frac{V_{OUT}}{N} + V_{IN} \tag{5.4}$$

The current flowing through the primary side directly affects the charging time. For this reason, the peak current value that will meet the required charging time must be calculated according to Eq. 5.5. The primary peak current flows through the MOSFET. Therefore, the switching element that can provide this current must be selected.

$$I_{P(pk)(single\,pulse)} = V_{Cf}\sqrt{\frac{C}{kL}} \tag{5.5}$$

Input capacitance (C_{gs} and C_{gd}) affects the switching speed of the MOSFET. Lower capacitance allows faster switching. The parasitic capacitances on the MOSFET are inversely proportional to the $V_{DS\ (max)}$ voltage. Higher $V_{DS\ (max)}$ voltage may allow lower parasitic capacitances. However, there are also disadvantages brought by high $V_{DS\ (max)}$. Moffet's, which generally have high $V_{DS\ (max)}$ voltage, also have higher $R_{DS\ (on)}$ internal resistance. $R_{DS\ (on)}$ resistance has a great impact on the conduction losses that occur when the MOSFET is in conduction. High $R_{DS\ (on)}$ value causes increased MOSFET losses and heating of the MOSFET. Considering these parameters, 'IXFH150N30X3' was preferred. The selection of a 'TO247' case for the preferred switching element facilities heat dissipation.

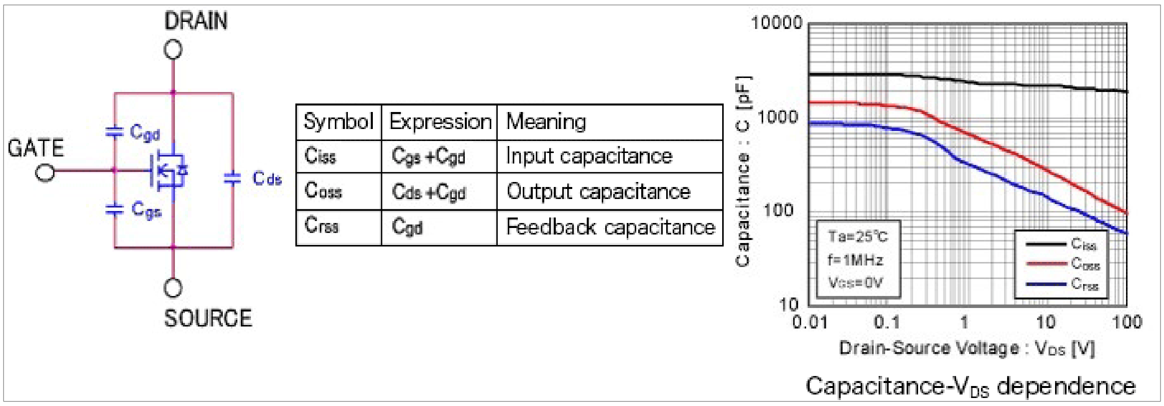

Figure 5.4. Parasitic capacitances of MOSFET (techweb, 2017)

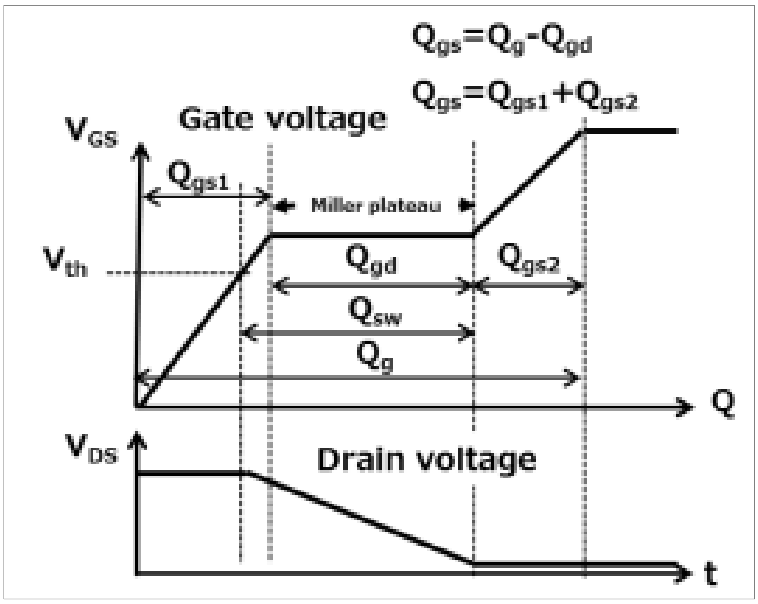

Figure 5.5. Voltage graphs of MOSFET (TOSHIBA, 2023)

Table 5.2. Parameters of 'IXFH150N30X3'

Parameters	Value
FET Type	N-Channel
Drain to Source Voltage (V_{ds})	300V
Current – Continuous Drain (I_d)	1.5A
$R_{ds\ (on)}$	8.3mΩ
Gate Charge (Q_g)	177nC
$V_{gs\ (th)}$	4,5V
Input Capacitance (C_{iss})	13100pF

5.1.3. Gate driver

V_{GS} (Gate-Source Voltage) of the MOSFET is a critical parameter that controls the switching of the MOSFET. The voltage applied to the gate terminal must be at a sufficient level compared to the source terminal to conduct the MOSFET. This level is called threshold voltage (V_{th}). Enhancement mode MOSFET was preferred in the design for easy management. This type of MOSFETs do not let to flow any current through when the gate-source voltage is not applied. Positive V_{GS} voltage allows current flow through the MOSFET. The threshold voltage (V_{th}) for most N-type MOSFETs is typically between 1-4V, although a higher V_{GS} voltage may need to be applied for the MOSFET to fully conduct. (e.g, 10-12V). Digital outputs of microcontrollers (e.g. 3,3V or 5V) can be used to trigger low-power MOSFETs. However, high voltage MOSFETs a usually require higher V_{GS}. On the other hand, MOSFETs do not switch into conduction only by applying sufficient V_{GS} voltage. In order to conduct the MOSFETs, the gate charge (Q_g) capacity must be filled. The charging time of the capacities is directly proportional to the current applied. However, the current levels that microcontrollers can provide are not sufficient to fill these capacities in a short time. This situation should not be ignored when using a microcontroller to trigger the MOSFET. Special MOSFET drivers are used to drive higher speed and powerful MOSFETs. These drivers can increase the gate voltage to 10-12V or more when necessary.

Another advantage of the flyback converter is that the switching element is on the low-side. Low-side switching refers to placing the switch between the load and the ground point (GND) of the circuit. In Low-Side driver circuits, it is easier to provide (V_{th}) voltage since the source terminal of the switch is GND. For this reason, the 'UCC27517DBVR' was used for the gate driver IC.

A series resistor (10Ω-100Ω) connected to the gate terminal is used to limit the gate current and reduce voltage spikes in the circuit. Additionally, adding a pull-down resistor (e.g. 10kΩ) between the gate and source prevents the MOSFET from unwanted triggering. Initially, a gate resistor was not used in the design study. However, it has been observed that the MOSFET produces oscillation when it starts conducting. For this reason, a series resistor was added to the gate terminal in the later parts of the study. The point to be considered here is that the series resistor does not dampen the applied gate signal.

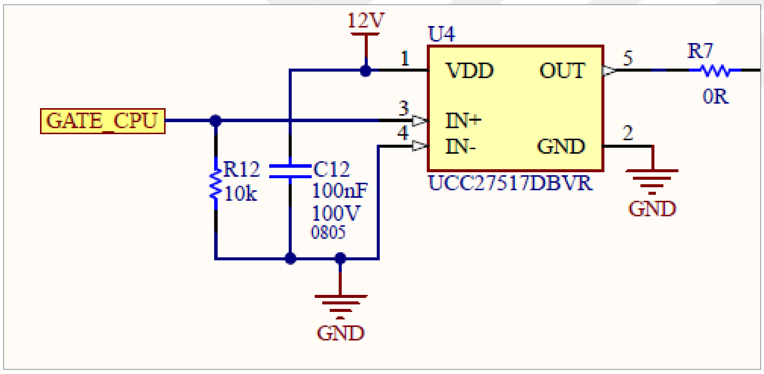

Figure 5.6. Schematic of gate driver circuit

5.1.4. Selecting of the transformer

The turn ratio of the transformer directly affects the transferred energy rate to the secondary side. Higher energy transferred means shorter charging time. Nevertheless, as the transformer's winding ratio is reduced, the voltage applied to the switching element will increase. Since the current value on the secondary side will increase, the cost and losses of the selected diode will increase. The most important factor for transformers in flyback converters is leakage inductance. High leakage inductance causes voltage spikes, loss of efficiency and high EMI levels. For this reason, special transformers with low leakage inductance can be used in CCPS applications. Another important criterion of CCPS designs is small dimensions. Therefore, the size of the CCPS should also be taken into consideration when choosing the transformer.

MANUFACTURER	PART NUMBER	SIZE L × W × H (mm)	MAXIMUM I_{PRI} (A)	L_{PRI} (μH)	TURNS RATIO (PRI:SEC)
Coilcraft	DA2033-AL	17.4 × 24.1 × 10.2	5	10	1:10
www.coilcraft.com	DA2034-AL	20.6 × 30 × 11.3	10	10	1:10
	GA3459-BL	32.65 × 26.75 × 14	20	5	1:10
	GA3460-BL	32.65 × 26.75 × 14	50	2.5	1:10
	HA4060-AL	34.29 × 26.75 × 14	2	300	1:3
	HA3994-AL	34.29 × 28.75 × 14	5	7.5	2:1:3:3*
Würth Elektronik/Midcom	750032051	28.7 × 22 × 11.4	5	10	1:10
www.we-online.com	750032052	28.7 × 22 × 11.4	10	10	1:10
	750310349	36.5 × 42 × 23	20	5	1:10
	750310355	36.5 × 42 × 23	50	2.5	1:10
Sumida	C8117	23 × 18.6 × 10.8	5	10	1:10
www.sumida.com	C8119	32.2 × 27 × 14	10	10	1:10
	PS07-299	32.5 × 26.5 × 13.5	20	5	1:10
	PS07-300	32.5 × 26.5 × 13.5	50	2.5	1:10
TDK	DCT15EFD-U44S003	22.5 × 16.5 × 8.5	5	10	1:10
www.tdk.com	DCT20EFD-U32S003	30 × 22 × 12	10	10	1:10
	DCT25EFD-U27S005	27.5 × 33 × 15.5	20	5	1:10

*Transformer has three secondaries where the ratio is designated as PRI:SEC1:SEC2:SEC3

Figure 5.7. Suggested transformers for CCPS (Linear Technology, 2017)

The special transformers produced for CCPS were examined. 'GA3460-BL' was preferred due to its small size, high current and low leakage inductance value. In addition, the low primary inductance of this product allows faster switching. However, low primary inductance also increases the rate of rise of the primary current. In such a case, it is an important criterion that the microcontroller must have enough processing power to sample the primary current.

5.1.5. Current sensing

Primer current sensing

A shunt resistor was used to detect the value of the primary current. Since the gate driver does not get any reference from the source terminal of the MOSFET, the voltage of the source terminal should not increase too much. For this reason, 1,5mΩ resistor value was preferred. Thus, the $V_{GS\ (th)}$ value was achieved under all operating conditions. However, 1,5mΩ value produces a voltage of 1,5mV for 1 ampere. Such low voltage levels are difficult to detect even with high-resolution microcontrollers. For this reason, the voltage read from the shunt resistor was amplified with a differential amplifier and then transmitted to the microcontroller. Common-mode range, bandwidth, rail to rail, slew rate and gain error values were taken into consideration when selecting the differential amplifier. Common mode range voltage of the differential amplifier determines the maximum operating input voltage of the design. After necessary reviews, 'INA180A1IDBVR' was preferred.

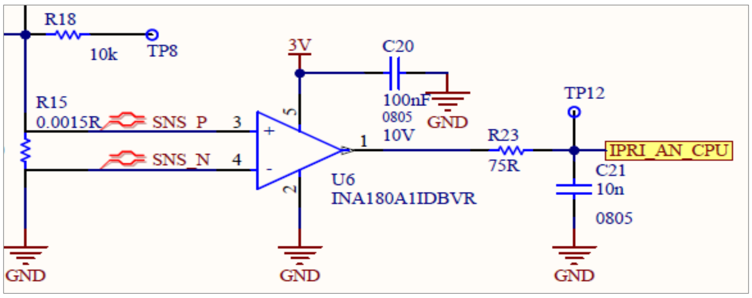

Figure 5.8. Schematic of primer current sensing circuit

<u>Seconder current sensing</u>

The amplifier is exposed to a higher voltage on the secondary side than on the primary side. The amplifier is only exposed to input voltage on the primary side. However, the amplifier is exposed to capacitor voltage on the secondary side. Due to the high capacitor voltage, an amplifier was not preferred for the secondary current sensing circuit. Instead of, hall-effect sensor, one of the most used current sensing circuits, was used. The hall-effect sensor is usually made of a semiconductor material. When the magnetic field passes over the sensor, a voltage is generated at the sensor output. This voltage is directly proportional to the strength of the magnetic field. This output voltage was used to measure the intensity of the magnetic field (secondary current). As with differential amplifiers, the operating voltages of the hall-effect sensor's input pins are also important. 'TMCS1123C5AQDVGR' was preferred due to its high insulation voltage value. In both reading circuits, gain ratios should be selected depending on the resolution and durability of the microcontroller to be used.

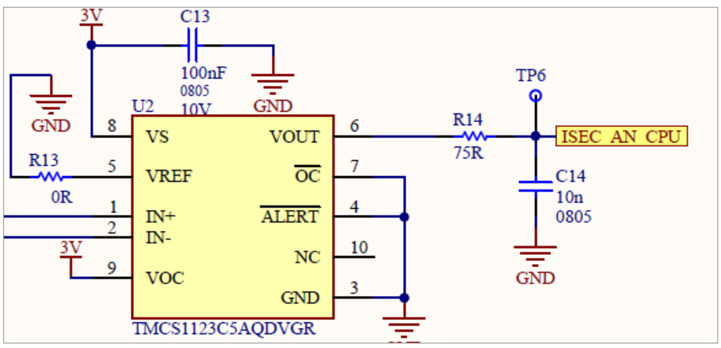

Figure 5.9. Schematic of seconder current sensing circuit

5.1.6. Voltage sensing

Resistor divider circuit was preferred to read input and output voltages. The outputs of Op-Amps cannot be higher than the supply voltages. Therefore, a voltage follower was added after the resistor divider to protect the microcontroller pins. However, the selected Op-Amp must follow the rate of change in the input voltage. Therefore, a faster Op-Amp (LMH6618MK) was preferred in the output voltage reading circuit.

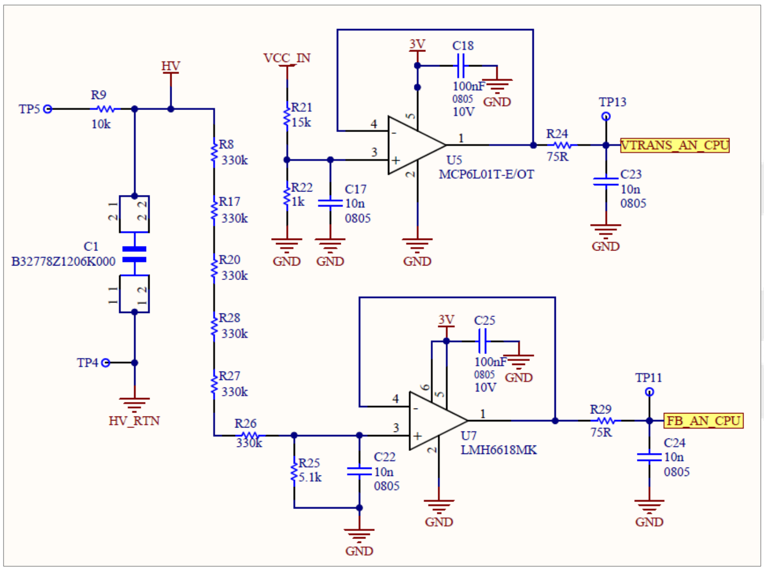

Figure 5.10. Schematic of voltage sensing circuits

5.1.7. Discrete signals

Almost all CCPS have two basic discrete signals. The first signal is 'charge_inhibit', which is used to command to start charging. The ‘charge_inhibit’ signal is transmitted to the CCPS as an external command. Another discrete signal is the 'done' signal, which means that the charging is completed. The 'done' signal is transmitted to the user by CCPS. These signals are generally used with the Open/GND structure. For this reason, N.P.N or P.N.P transistors can be used to build the circuits depending on whether the signals are input or output.

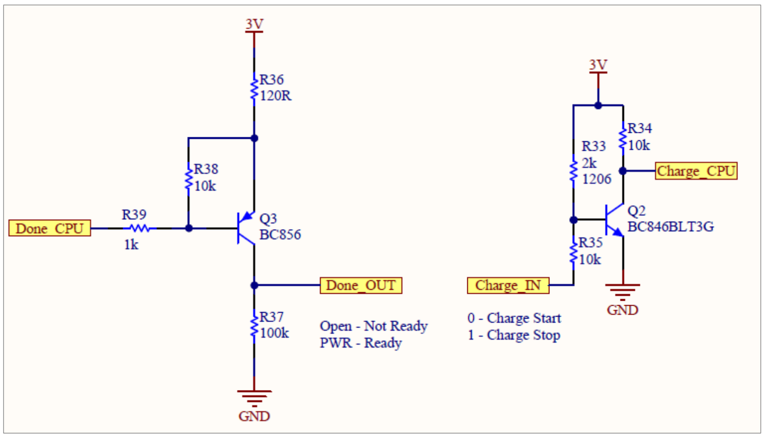

Figure 5.11. Schematic of discrete signal circuits

5.1.8. Snubber circuit

Within the scope of the thesis study, the comparative analysis of the active and passive snubber structures was aimed. For this reason, RCD and LCD snubber topologies were added to the design together. However, the two topologies were not used at the same time.

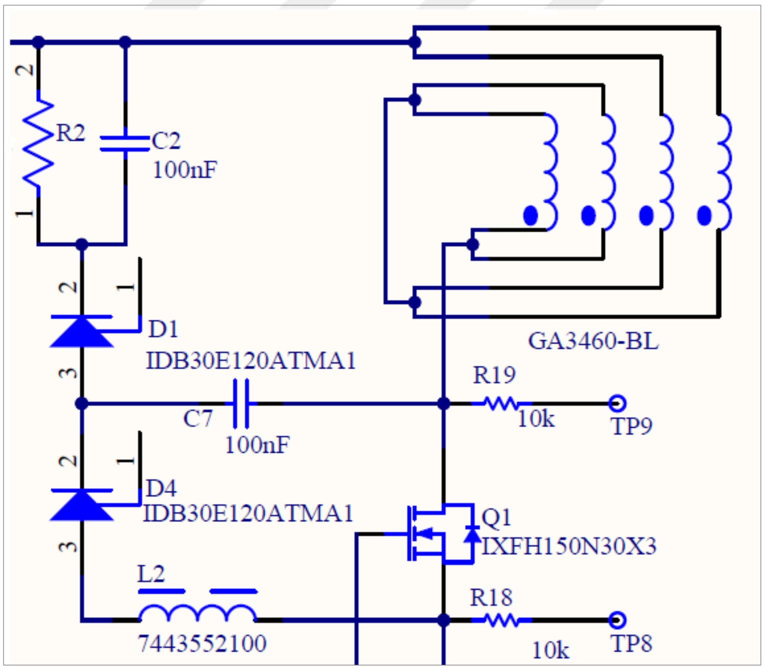

Figure 5.12. Schematic of snubber circuit

5.1.9. Importance of diode in CCPS

Regardless of the chosen topology, the secondary rectifying diode is a critical component. During the conduction of the secondary output diode, energy is transferred from the primary side of the transformer to the secondary side. The transformer induces a voltage in the secondary winding and the diode allows current to flow through the energy storage capacitors to charge the capacitors.

Conduction losses are directly proportional to charging current. High conduction losses lead to longer charging times. The relationship between diode losses and charging time is crucial for optimizing the overall efficiency of the CCPS. The losses in the diode during conduction are mainly due to its forward voltage drop (V_f). Additionally, the reverse recovery time of the diode can also affect the losses. Diodes with lower forward voltage drop and faster recovery times can help reduce conduction and switching losses, particularly in high-frequency applications. Therefore, diode characteristics are important in achieving the desired charging time to meet the application's requirements.

The silicon-carbide diodes have negligible recovery times. Therefore, the SiC diodes should be preferred for the CCPS designs. The ‘GD02MPS12E’ was selected because of its high voltage and current ratings.

5.1.10. Selecting of the microcontrollers

While selecting the microcontroller in the thesis study, many parameters were taken into consideration; processing power, supply, maintenance and sample software numbers. Since there may be any change of the microcontroller, the balcony card design method was used in the microcontroller circuits. For the added balcony card, the 'STM32F407 Discovery' development card, which is thought to be suitable for the thesis study in terms of its availability and features, was chosen. 'STM32F4DISCOVERY' contains an ‘Arm Cortex-M4 Core’ based microcontroller (STM32F407VG).

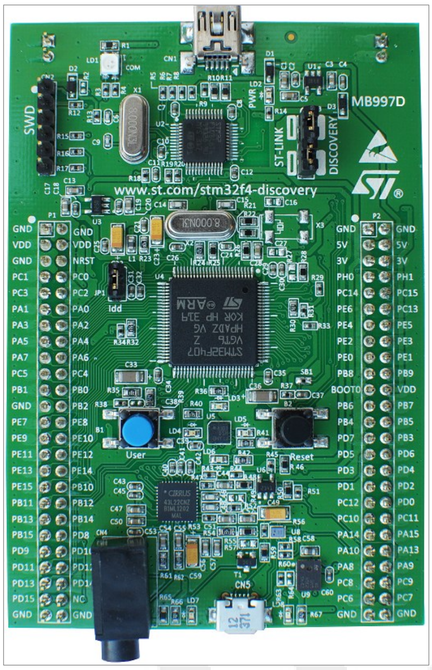

Figure 5.13. The STM32F4DISCOVERY (st, 2020)

5.2. PCB Design

The printed circuit board (PCB) was created using the Altium Designer. The high current paths were routed with the appropriate routing widths. The routing of high-current lines is designed with short paths and minimal turns to minimize the potential EMI. The regulator circuits are placed far away from the sensing circuits to ensure that high temperatures will not affect the analog reading. In the design of analog reading circuits, differential lines were used to ensure signal integrity. In addition, layouts were made at sufficient distances to prevent crosstalk from affecting the analog readings. Test points were placed on critical signals. The locations of the test points were chosen close to the reference point of the signals.

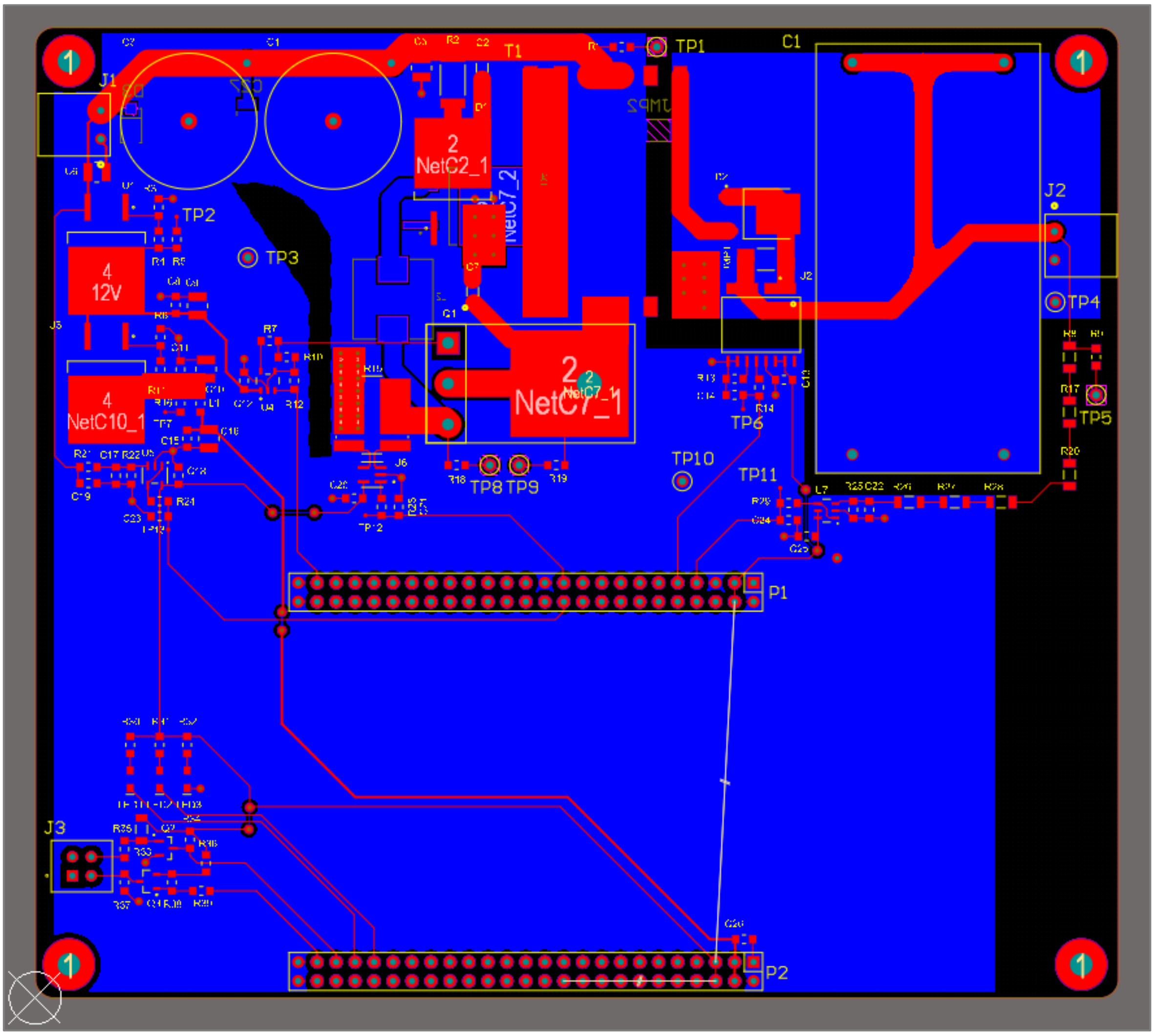

Figure 5.14. PCB in Altium Desginer

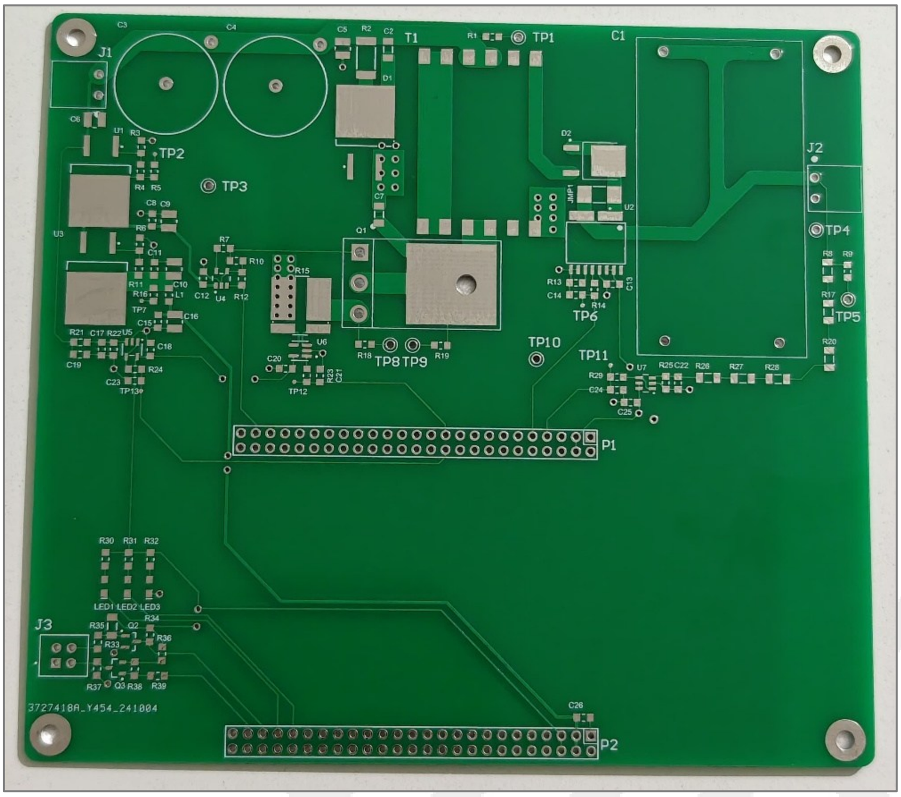

Figure 5.15. PCB without assembly

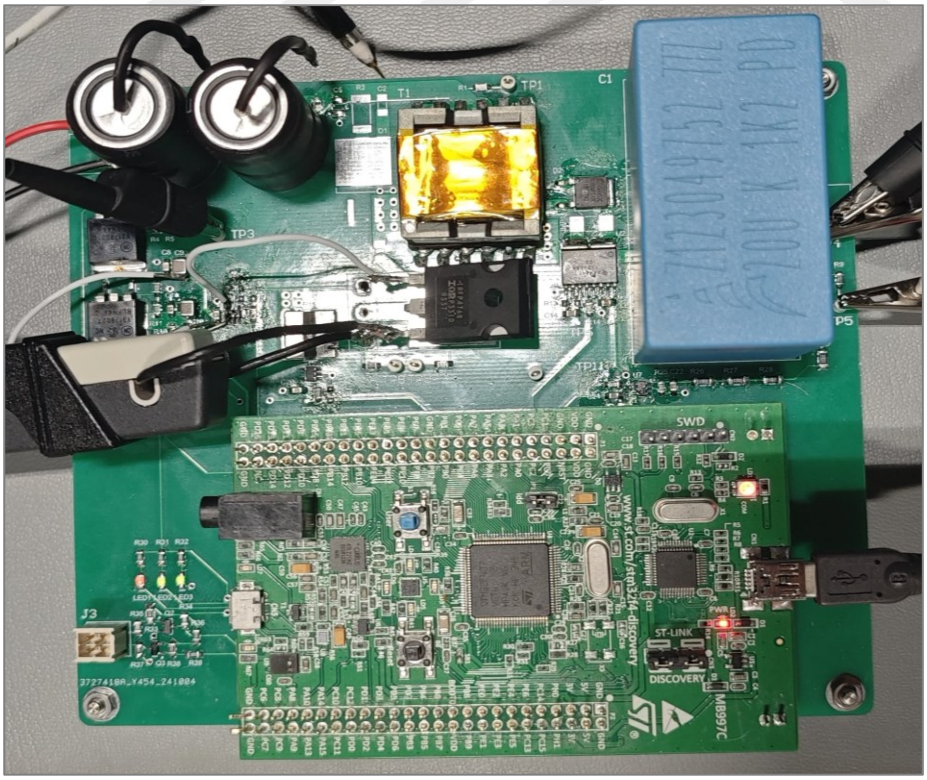

Figure 5.16. PCB with assembly

5.3. Software Design

The initializations of software were carried out with the STM32CubeMX initialization code generator. STM32CubeMX was used to make the relevant pin assignments and peripheral settings. Timer and ADC peripherals were used. STM32CubeIDE integrated development environment was used for coding.

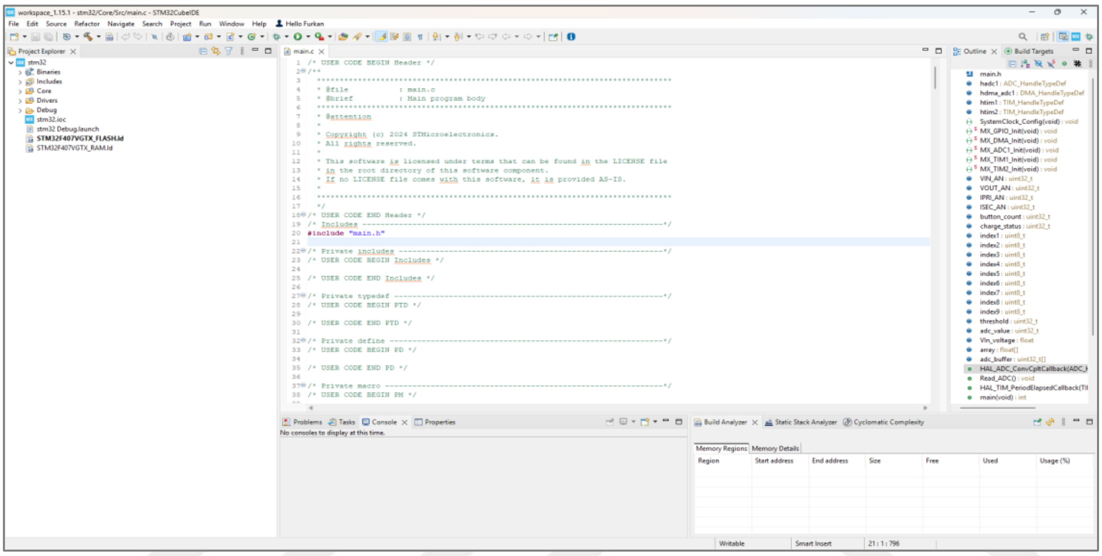

Figure 5.17. The STM32CubeIDE

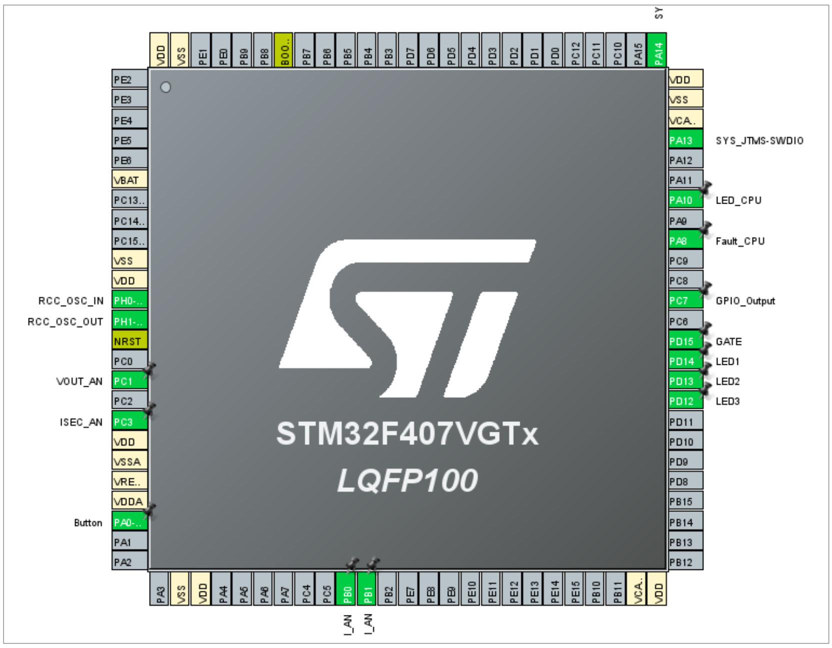

Figure 5.18. The STM32CubeMX

5.3.1. ADC peripherals

There are different methods for ADC (Analog-to-Digital Converter) for STM32 microcontrollers. The conversion method can be selected according to the speed, precision and power consumption requirements of the application.

Polling method

Polling method is a method in which a single conversion is performed. The application is simple. However, it blocks the microcontroller until the conversion is completed.

```
HAL_ADC_Start(&hadc1); // Start ADC conversion
if (HAL_ADC_PollForConversion(&hadc1, 1000) == HAL_OK) {
    uint32_t adcValue = HAL_ADC_GetValue(&hadc1); // Get the ADC conversion result
}
HAL_ADC_Stop(&hadc1); // Stop ADC
```

Figure 5.19. Example code for polling method

Interrupt method

In computing, an interrupt is a microcontroller event that causes to stop executing the current task and switch to another task. After an interrupt occurs, the previous operation is not completed until the operation within the interrupt is completed. After the interrupt is completed, the previous operation is continued. Thus, the Microcontroller can do other instructions during the ADC conversion. Interrupt operations are specified in a special subroutine. When an interrupt occurs, the operations in this subroutine are performed.

```
void HAL_ADC_ConvCpltCallback(ADC_HandleTypeDef *hadc) {
    if (hadc->Instance == ADC1) {
        uint32_t adcValue = HAL_ADC_GetValue(hadc); // Get the ADC conversion result
    }
}

// Main code
HAL_ADC_Start_IT(&hadc1); // Start ADC conversion in interrupt mode
```

Figure 5.20. Example code for interrupt method

DMA method

DMA (Direct Access Memory) is a structure used for data transferring between memory and peripherals. The aim of DMA is to speed up the data flow with a shorter path. By using the DMA method in the ADC application, the conversion result can be saved directly to the specified address in the memory. By interconnecting ADC and DMA peripherals, DMA operation can be triggered by the termination of the ADC conversion. Thus, other instructions can be performed until the conversion is completed. When the conversion is completed, the ADC result is transferred to the specified variable using the DMA method. This method is often used in applications that require a constant flow of data. Thus, it provides continuous data reading at high speed.

```
uint32_t adcBuffer[10]; // Buffer to store ADC results

// Start ADC conversion with DMA
HAL_ADC_Start_DMA(&hadc1, (uint32_t*)adcBuffer, 10);

// The data is automatically transferred to adcBuffer.
```

Figure 5.21. Example code for DMA method

Comparison of sampling rate

In order to measure the speed of DMA and interrupt method, GPIO operations were carried out in the relevant functions. Measurements were taken at the driven GPIO pin via the oscilloscope. The pin driving process is defined by first making the relevant pin logic high and then logic low. However, revisions were made in the test setup to ensure that the time taken for pin driving functions does not affect the measurement results. The blinking operation, which was performed with two instructions, was reduced to a single instruction with the toggle function. However, the toggle function uses ‘HAL’ libraries developed for STM32. Thus, this improvement still has a delay. Therefore, the relevant operations were carried out directly with register-based operations without using a library.

```
//GPIO Write Instructions
HAL_GPIO_WritePin(GPIOC, GPIO_PIN_7, GPIO_PIN_SET);
asm("NOP");
HAL_GPIO_WritePin(GPIOC, GPIO_PIN_7, GPIO_PIN_RESET);

//Toggle Function
HAL_GPIO_TogglePin(GPIOC, GPIO_PIN_7);

//Register-based Instructions
GPIOC->BSRR = GPIO_PIN_7;
asm("NOP");
GPIOC->BSRR = (uint32_t)GPIO_PIN_7 << 16U;
```

Figure 5.22. Codes of test

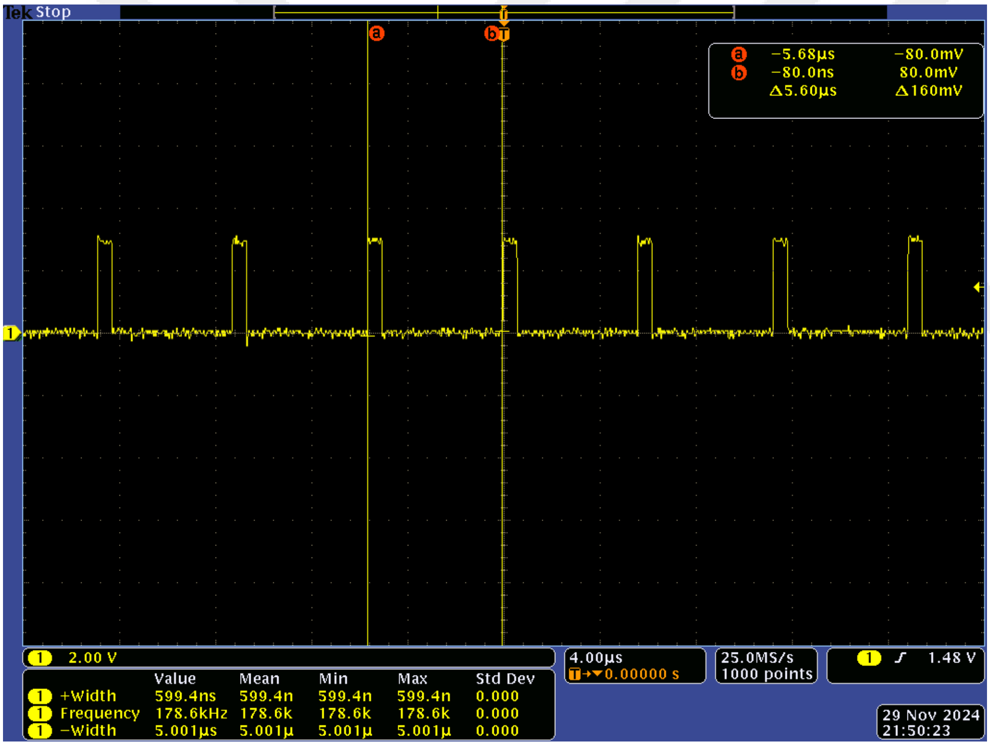

Image 5.3. Graphs of DMA method with GPIO instructions

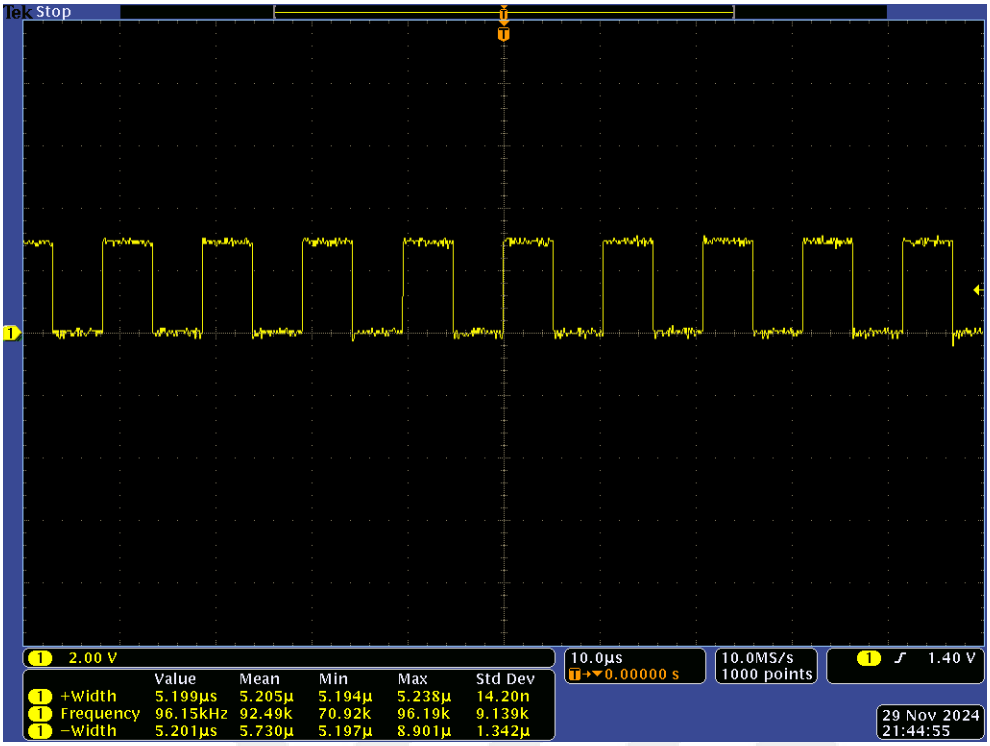

Image 5.4. Graphs of DMA method with toggle function

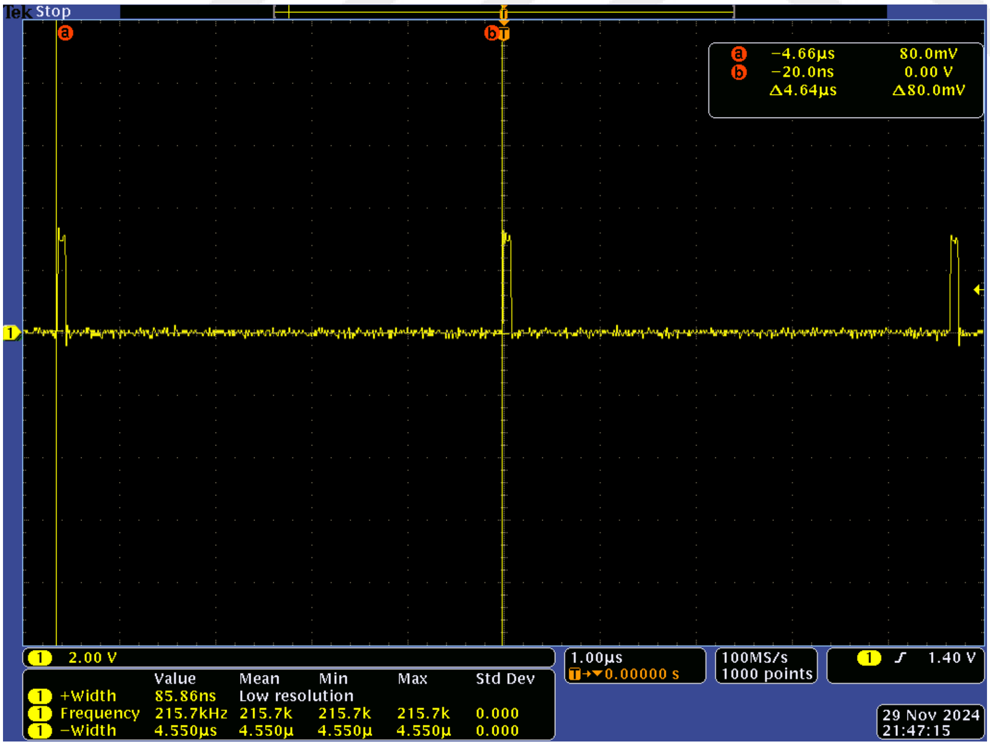

Image 5.5. Graphs of DMA method with register-based instructions

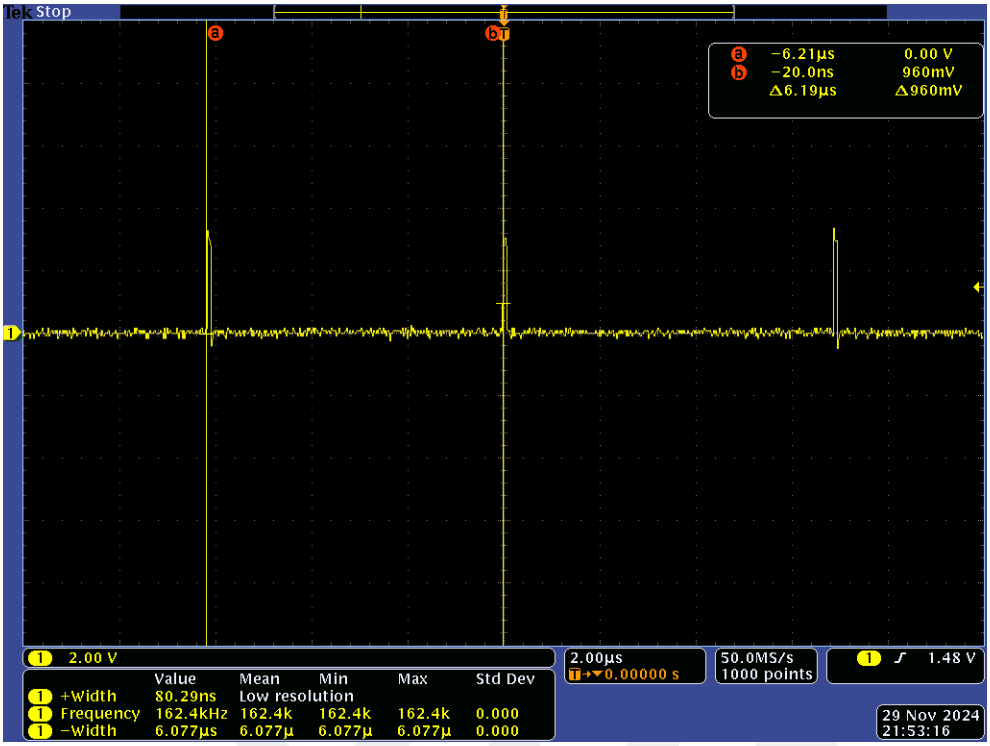

Image 5.6. Graphs of interrupt method with register-based instructions

Despite the improvements made, the sampling times obtained in DMA and interrupt methods are high for CCPS applications. For this reason, the polling method was preferred. However, the polling method was not performed with the functions in the HAL library, as shown in figure 5.19. Polling method was carried out with register coding. Although the polling method blocks the microcontroller throughout the conversion, it works faster than other methods even at lower operating frequencies. Performing register-based processing is an advantage for increasing the sampling rate. By decreasing the resolution, the sampling rate can be increased further. Conversion speed is dependent to the resolution. Lower resolution allows for faster conversion times. However, the parameter that most affects the sampling rate is the operating frequency of the processor.

Resolution	$t_{Conversion}$
12 bits	12.5 Cycles
10 bits	10.5 Cycles
8 bits	8.5 Cycles
6 bits	6.5 Cycles

Figure 5.23. Resolution vs conversion time (st)

Table 5.3. Comparison of conversion times

ADC Clock Frequency	Resolution	Conversion Time
36MHz	12 bits	862ns
36MHz	6 bits	709ns
18MHz	12 bits	1321ns
9MHz	12 bits	2083ns

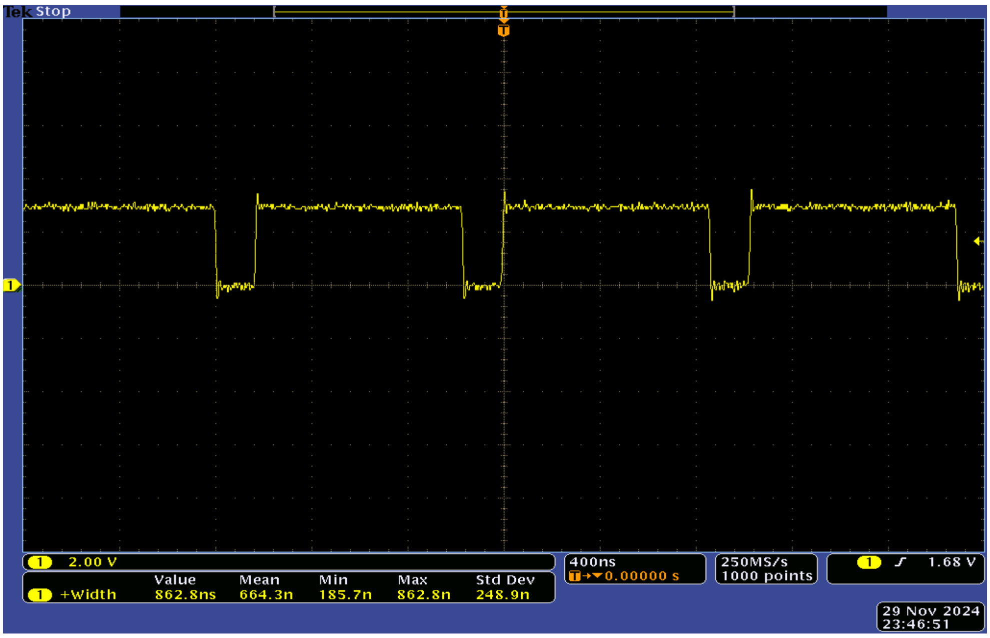

Image 5.7. Conversion time graphs with 36MHz and 12bits

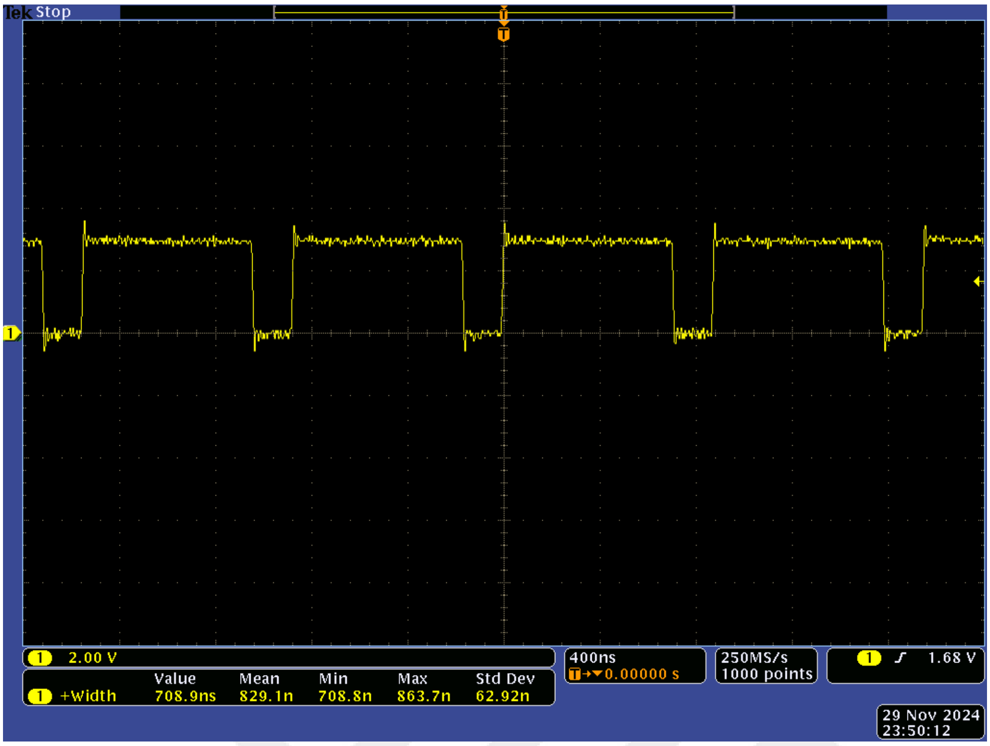

Image 5.8. Conversion time graphs with 36MHz and 6bits

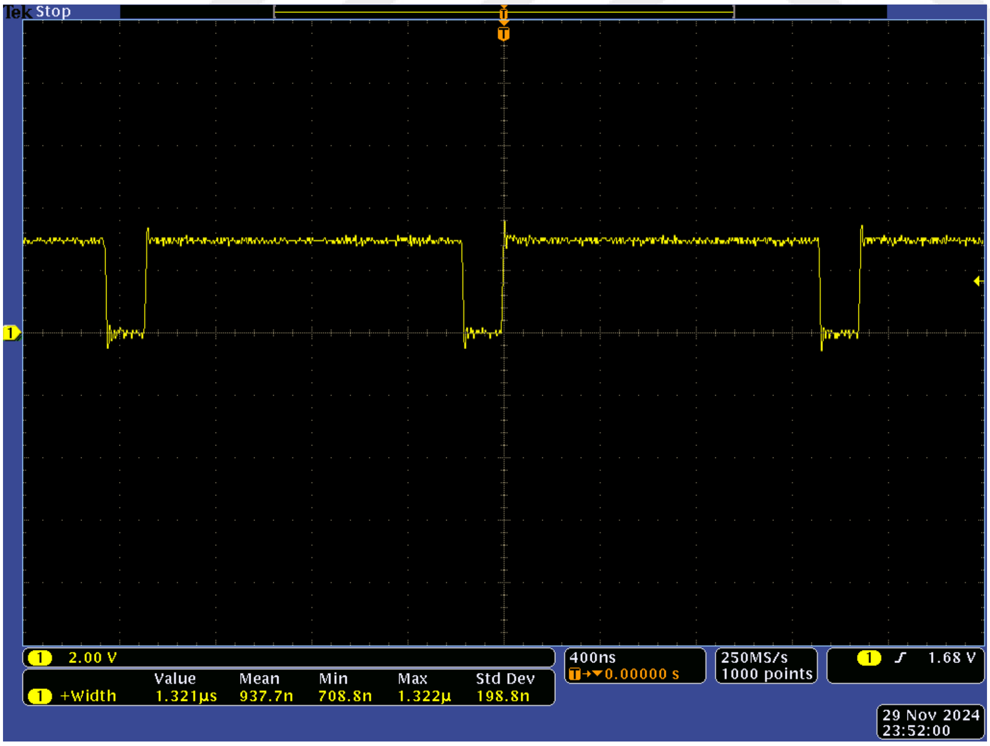

Image 5.9. Conversion time graphs with 18MHz and 12bits

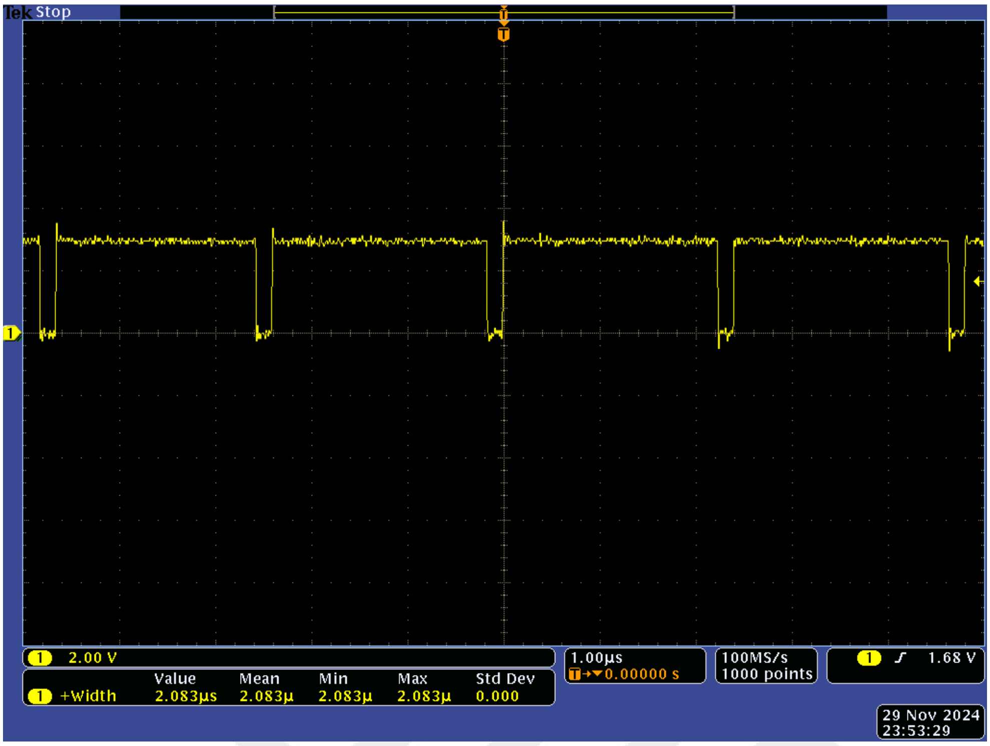

Image 5.10. Conversion time graphs with 9MHz and 12bits

5.3.2. TMR and PWM peripherals

Timer interrupt is used to run a process at certain intervals. When interrupt is enabled, pulse counting starts at the selected clock frequency. An interrupt occurs when the count value reaches a specified value. This called as overflow. Clock settings must be done before using the timer peripheral. Timer's counting speed can be determined by the system clock. However, when the system clock is high, the prescaler value is increased to obtain a lower counting speed. The counter period of the timer is set with the ARR (AutoReload Register) Value. Timer period can be determined according to Eq. 5.6 and 5.7.

$$Timer_{CLK} = \frac{System_{CLK}}{Prescaler} = \frac{72MHz}{48} = 1{,}5MHz \tag{5.6}$$

$$Timer_{Freq} = \frac{Timer_{CLK}}{ARR} = \frac{1{,}5MHz}{50} = 30kHz \tag{5.7}$$

In order to drive the switch, a trigger signal must be generated. PWM (Pulse Width Modulation) peripheral is used for square wave generation to trigger the MOSFET.

Triggering the PWM interrupt is connected to the timer counter. When the timer reaches its maximum value, a new switching period begins. The duty cycle of the PWM signal is determined by the value of the pulse register. The ratio of the pulse value to the ARR value determines the duty cycle.

$$Duty\ Cycle = \frac{Pulse\ Register}{ARR} \tag{5.8}$$

5.4. Analyzing of Charging Time

The charging time depends on input voltage, peak current and switching frequency. Analyzes of parameters affecting charging time were examined on the designed card.

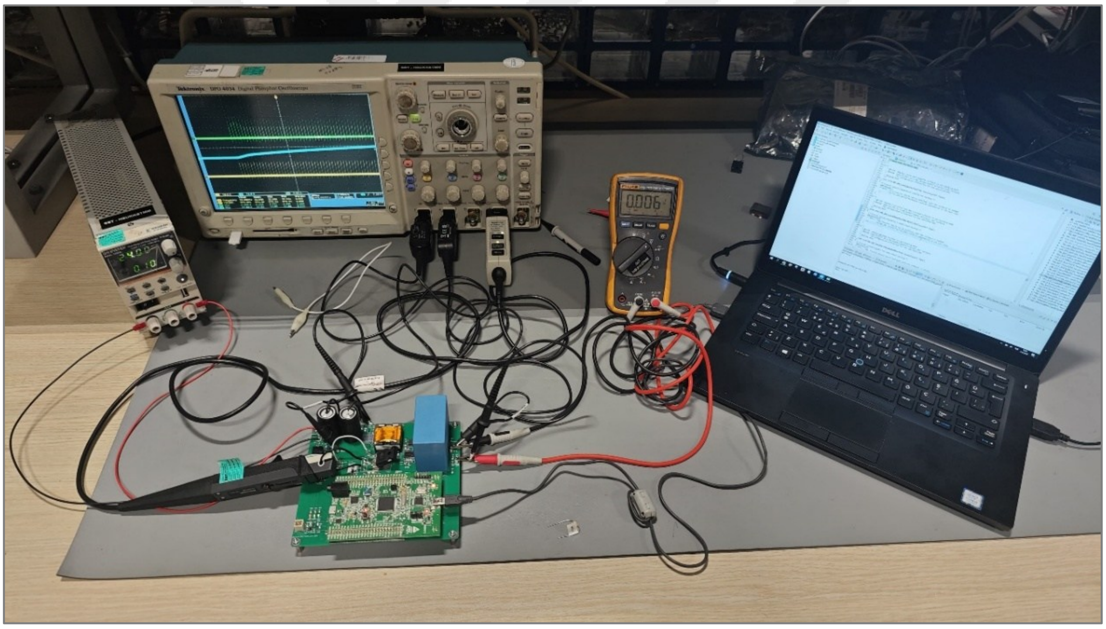

Image 5.11. Test setup

5.4.1. Effects of input voltage

Ohm's Law indicates that as the input voltage increases, the current in the circuit also increases. Consequently, increasing the peak current also shortens the charging time. The design was operated with four different input voltages under the same conditions.

Image 5.12. Charging graphs with 18V input

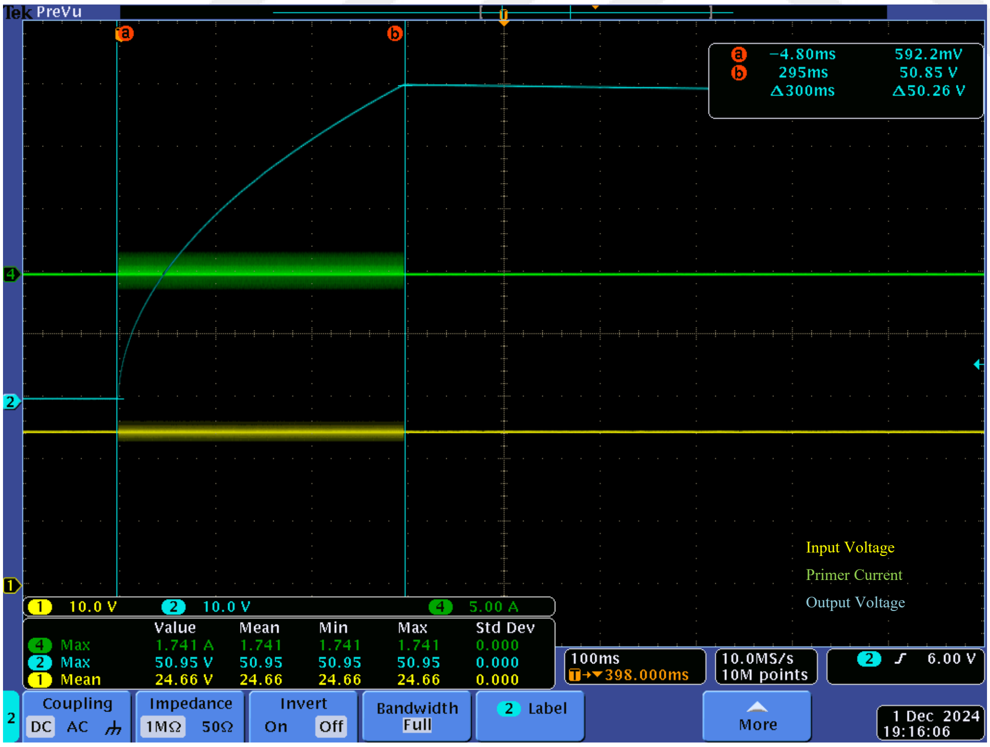

Image 5.13. Charging graphs with 24V input

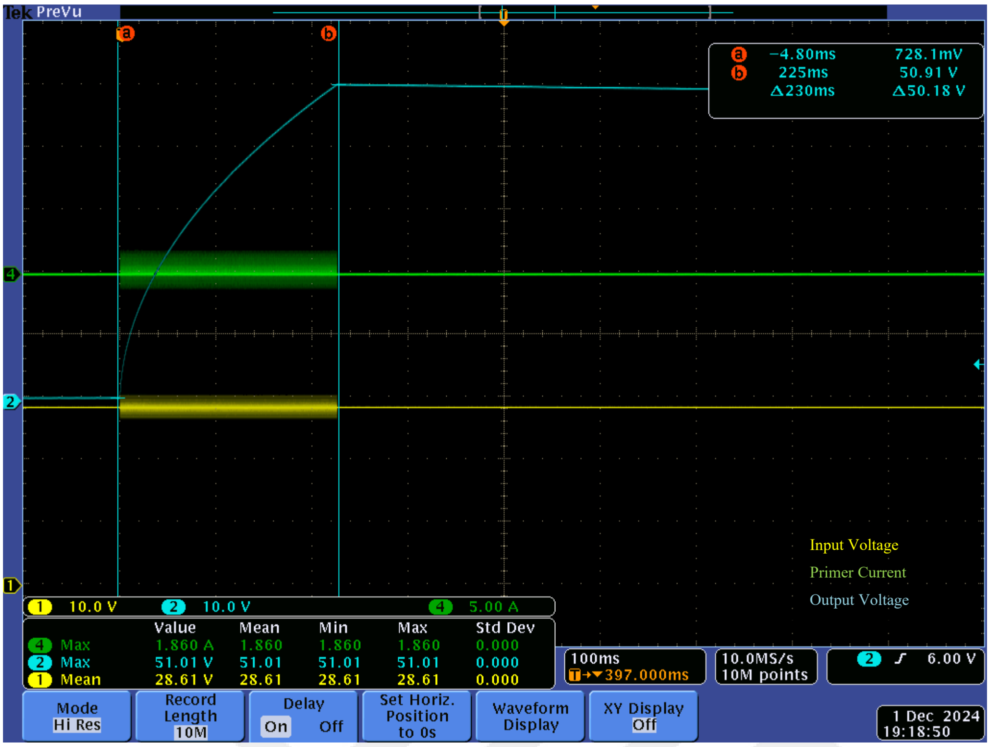

Image 5.14. Charging graphs with 28V input

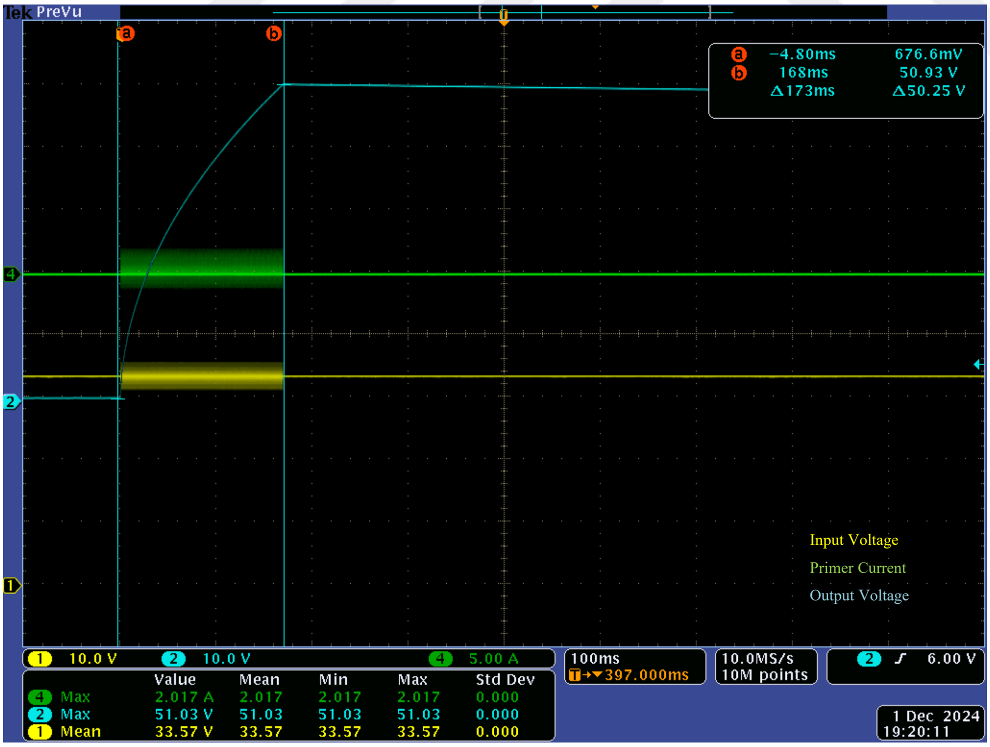

Image 5.15. Charging graphs with 33V input

5.4.2. Effects of peak primary current

Primary current is an important parameter that determines the amount of energy stored in the transformer. The high amount of energy stored in the transformer means that the amount of energy transferred to the capacitor is also high. Increasing the primary current can be realized by increasing the conduction time of the MOSFET. The conduction time of the MOSFET is adjusted by the PWM peripheral. Firstly, the duty cycle of the PWM signal was set to 2%, 4% and 6% respectively. With duty cycle, the primary current is increased and charging time is shortened. Then, the duty cycle was brought to 10%. Increasing of the duty cycle so high was led to spikes at the primary current at the beginning of the charging process. The reason for the increases in current is due to the converter operating in CCM mode. In CCM mode, the MOSFET is re-conducted before the secondary current drops to zero. When the MOSFET starts to conduct, the energy in the secondary side is reflected to the primary side. This causes the primary current to rise and causes spikes in the drain voltage. Therefore, the frequency measurements of the oscilloscope were incorrect. Finally, the duty cycle was brought to 20%. However, the gate driver failed due to voltage spikes.

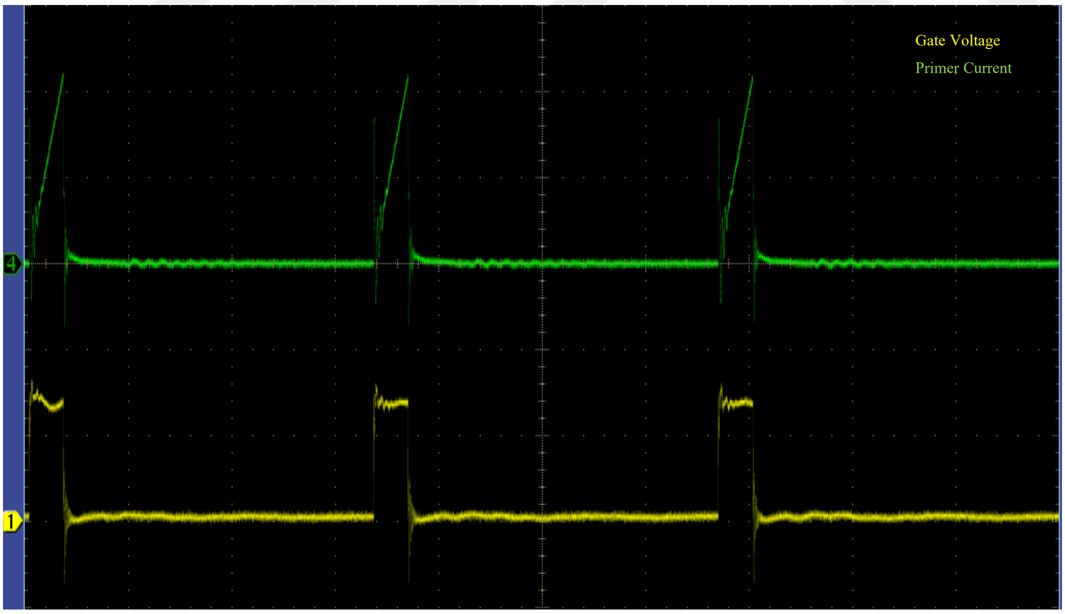

Image 5.16. Primer current spike

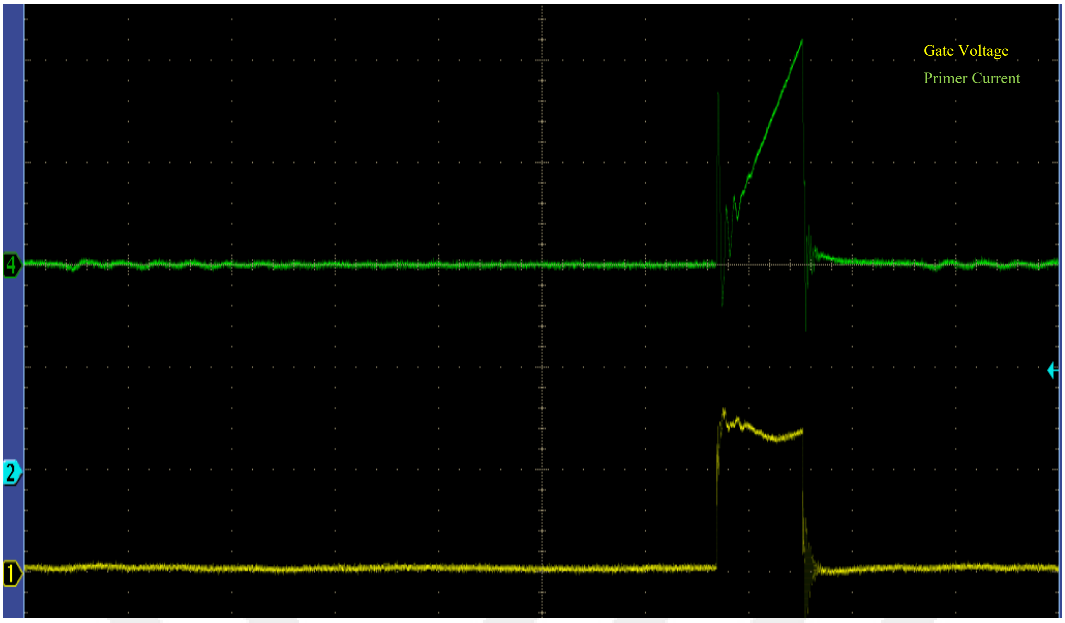

Image 5.17. Primer current spike zoom

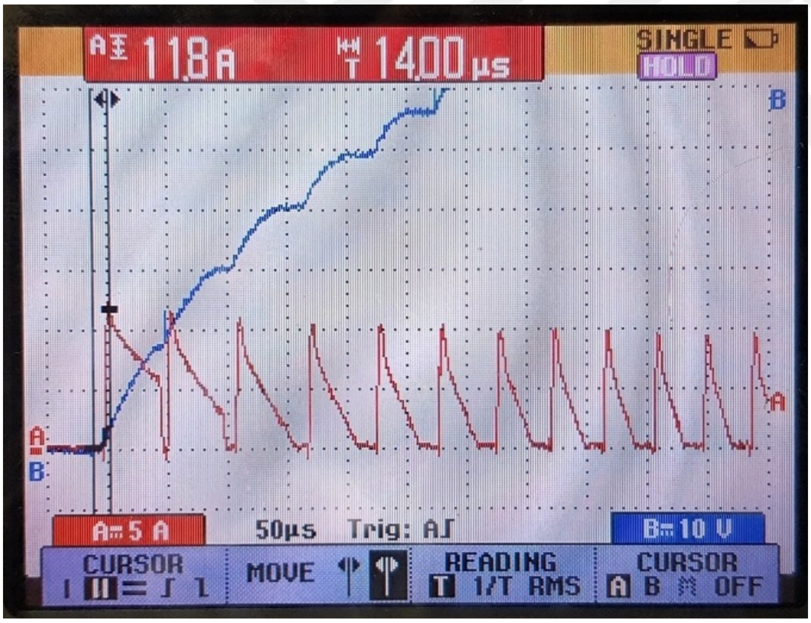

Image 5.18. Example of seconder current

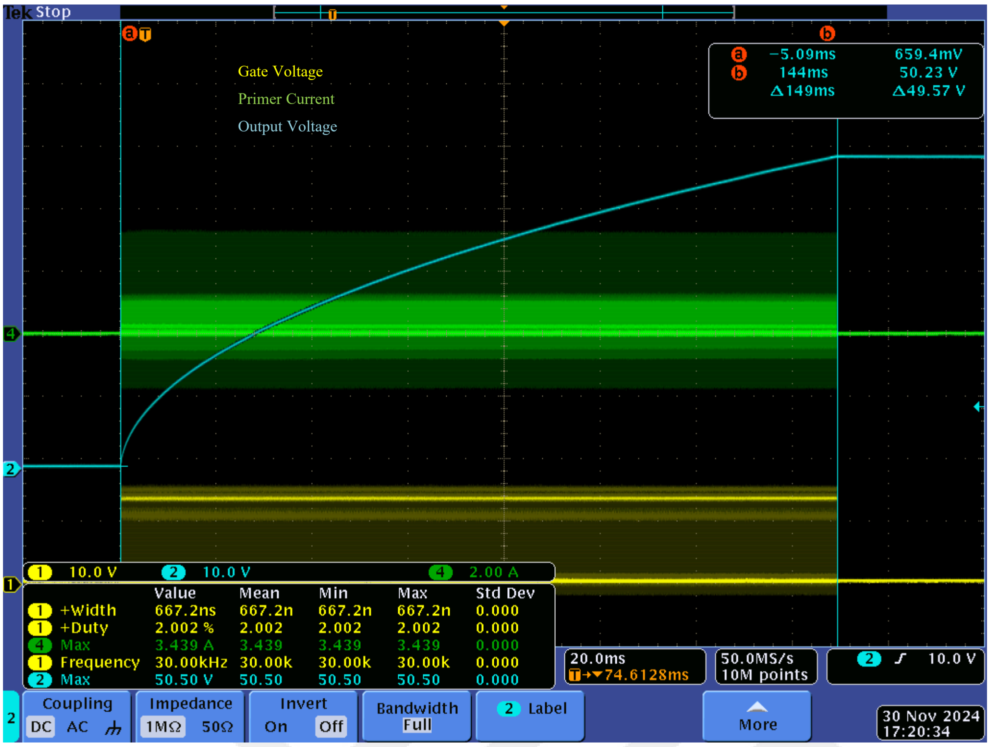

Image 5.19. Charging graphs with 2% duty cycle

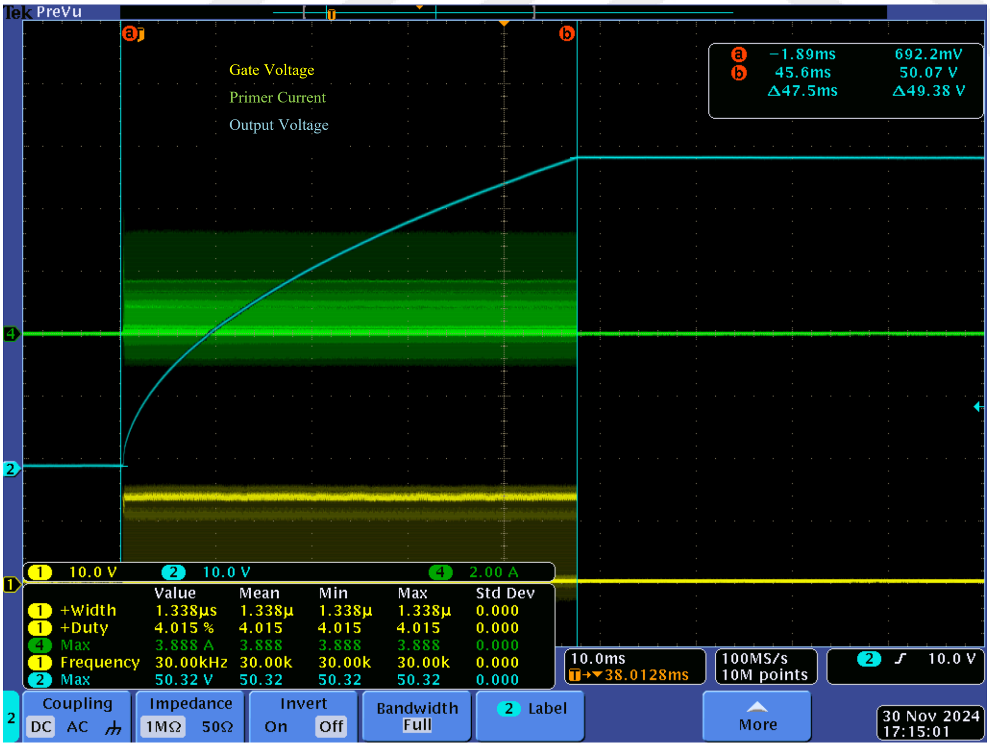

Image 5.20. Charging graphs with 4% duty cycle

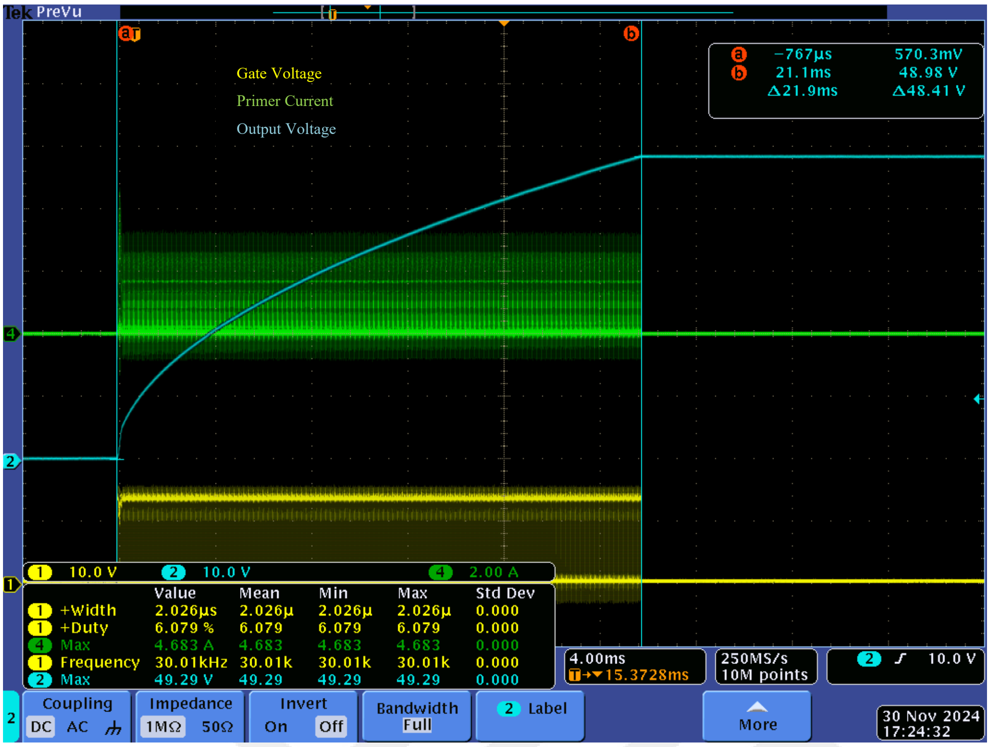

Image 5.21. Charging graphs with 6% duty cycle

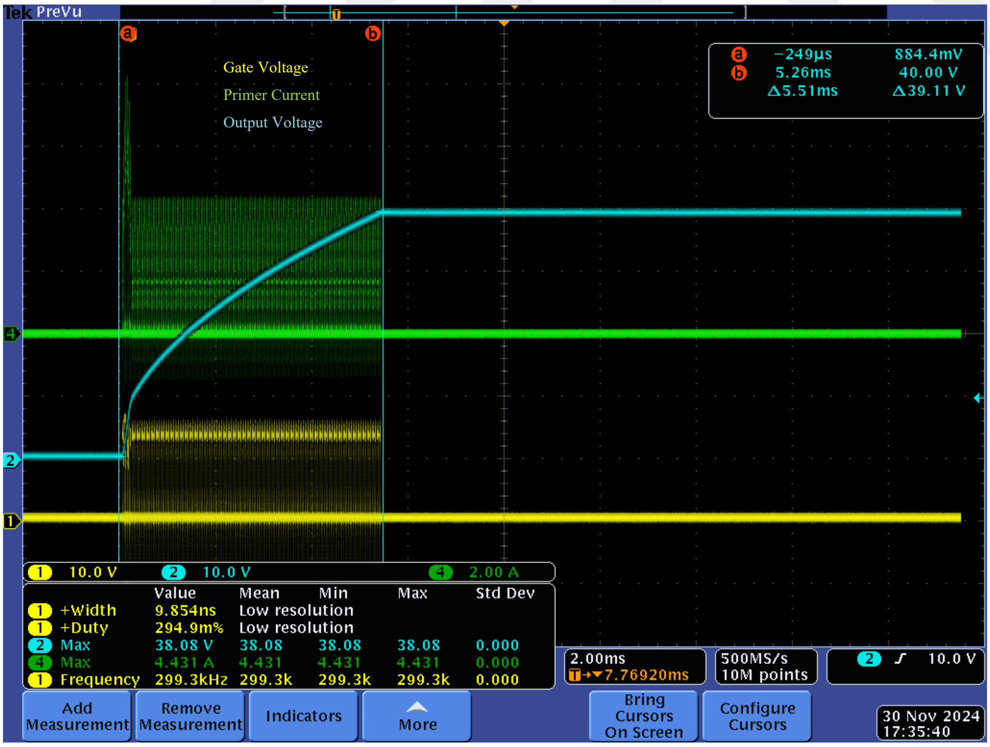

Image 5.22. Charging graphs with 10% duty cycle

5.4.3. Effects of switching frequency

Working in CCM mode affects the reliability of the system. However, working in DCM mode affects the efficiency of the system. Low switching frequency will increase the idle time. Therefore, the charging process will be longer. In order to show the effect of switching frequency on charging time, charging was performed at 30kHz, 36kHz, 48kHz and 72kHz. However, the PWM peripheral is not used when changing the switching frequency. The duty cycle must be specified in the PWM method. Even if 1% duty cycle is selected, it may cause undesirable levels of primary current at high switching frequencies. At the same time, since the effect of switching frequency is analyzed, the primary current must remain constant. Therefore, analyses were performed with constant duty cycle by using timer interrupt.

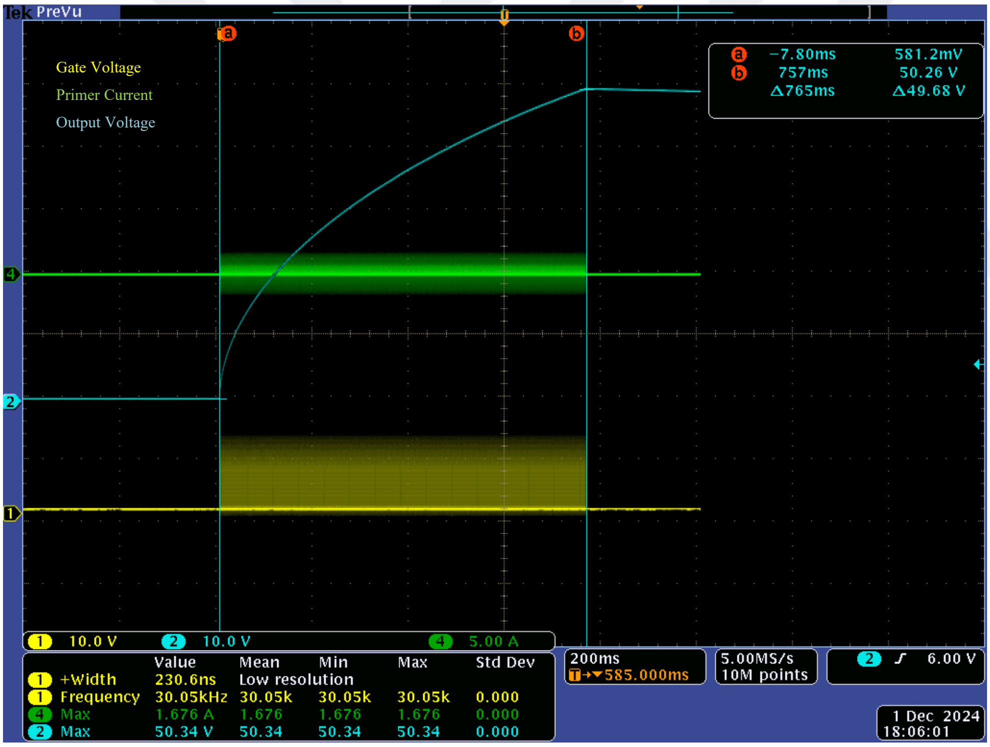

Image 5.23. Charging graphs with 30kHz

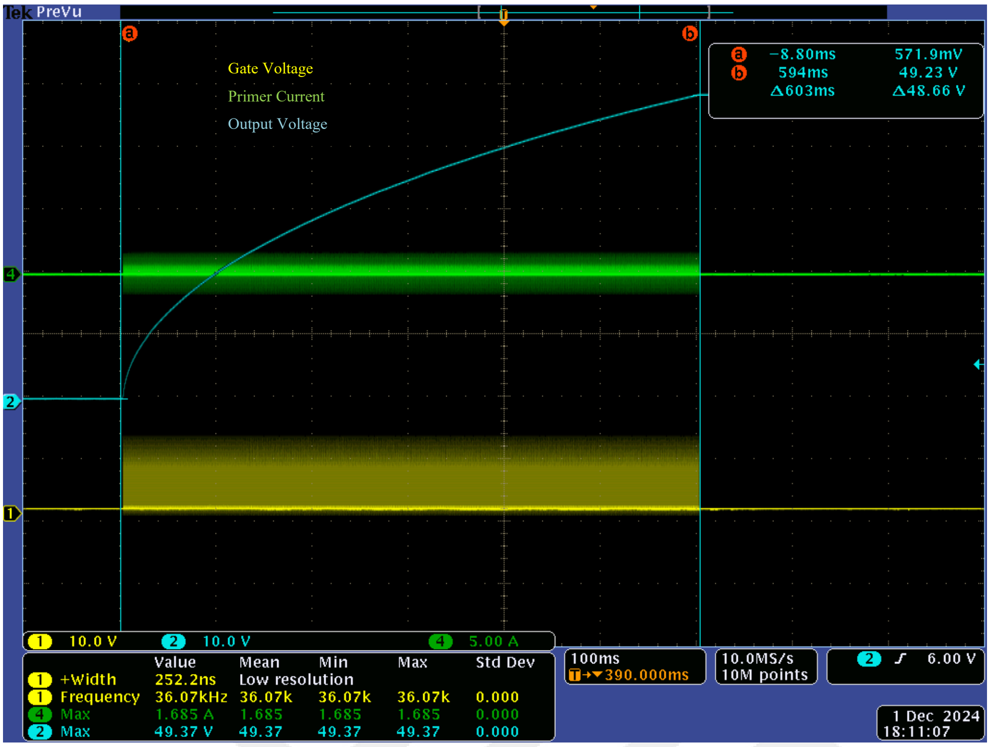

Image 5.24. Charging graphs with 36kHz

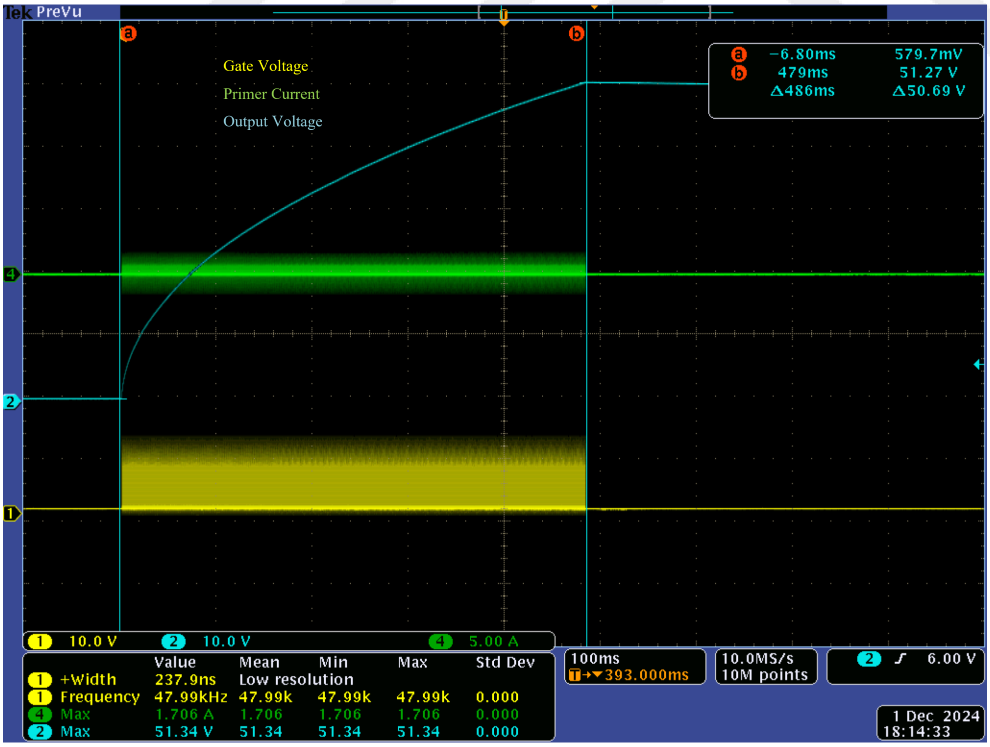

Image 5.25. Charging graphs with 48kHz

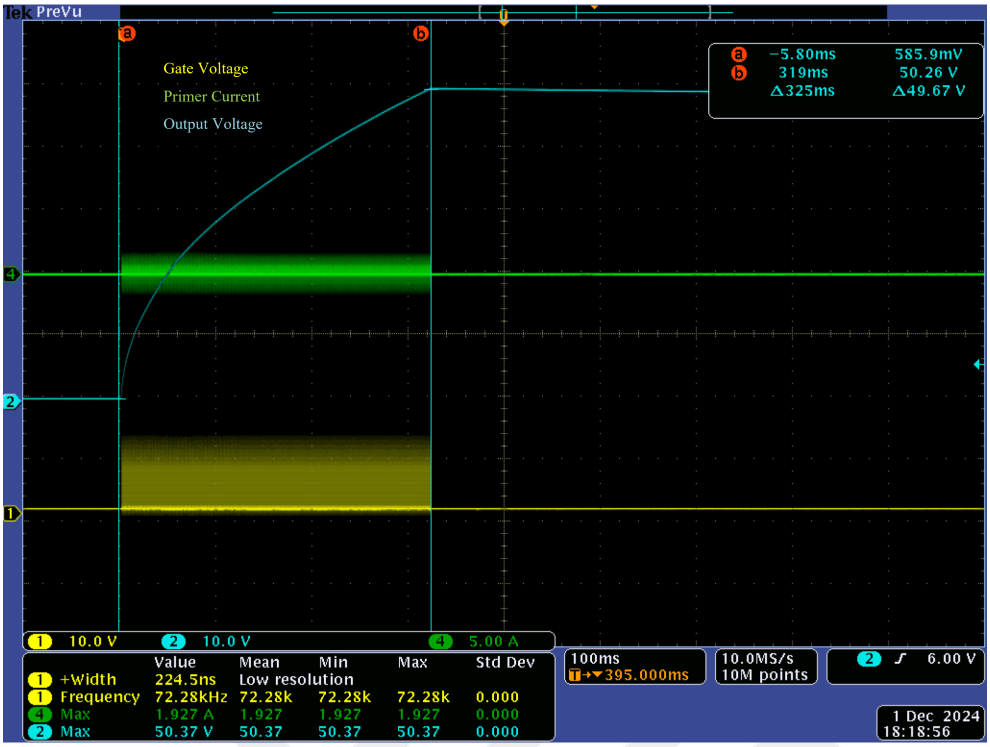

Image 5.26. Charging graphs with 72kHz

As a result of the analyses, it was observed that the charging time decreased as the switching frequency increased. However, although the conduction time of the MOSFET is kept constant, an increase in the primary current is observed. The reason for this is that as the switching frequency increases, the system switches to CCM and current spikes occur. The initial and final current graphs of the study with 72kHz were analyzed. It was observed that the current was high at the beginning of the charging process and decreased to a stable value at the end of the charging process. It is inferred from this that the increase in the primary current is due to the operation in CCM at the beginning of the charging process.

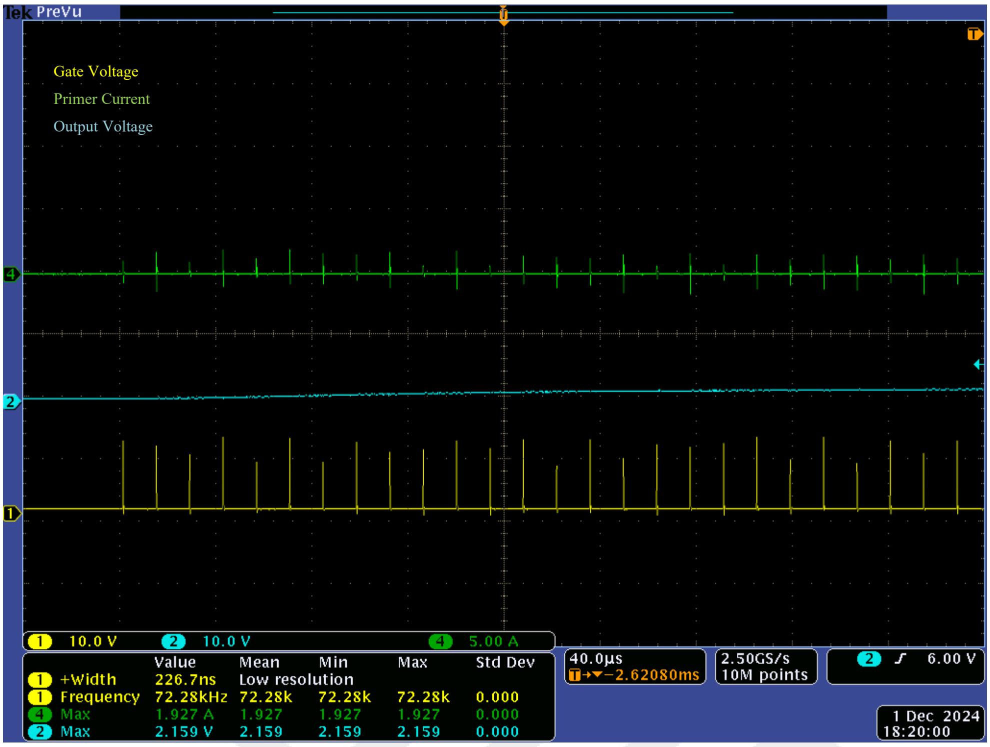

Image 5.27. Initial charging graphs of 72kHz

Image 5.28. End of charging graphs of 72kHz

In order to understand the effect of CCM in more detail, the tests were continued by increasing the conduction time of the MOSFET with 72kHz. The peak primary current is expected to increase with increasing duty cycle. However, increasing the primary current at high switching frequencies causes a high current spike at the beginning of the charging process. The reason why current spikes are seen only at the beginning of the charging process is that the rate of decrease in the secondary current accelerates as the capacitance voltage increases.

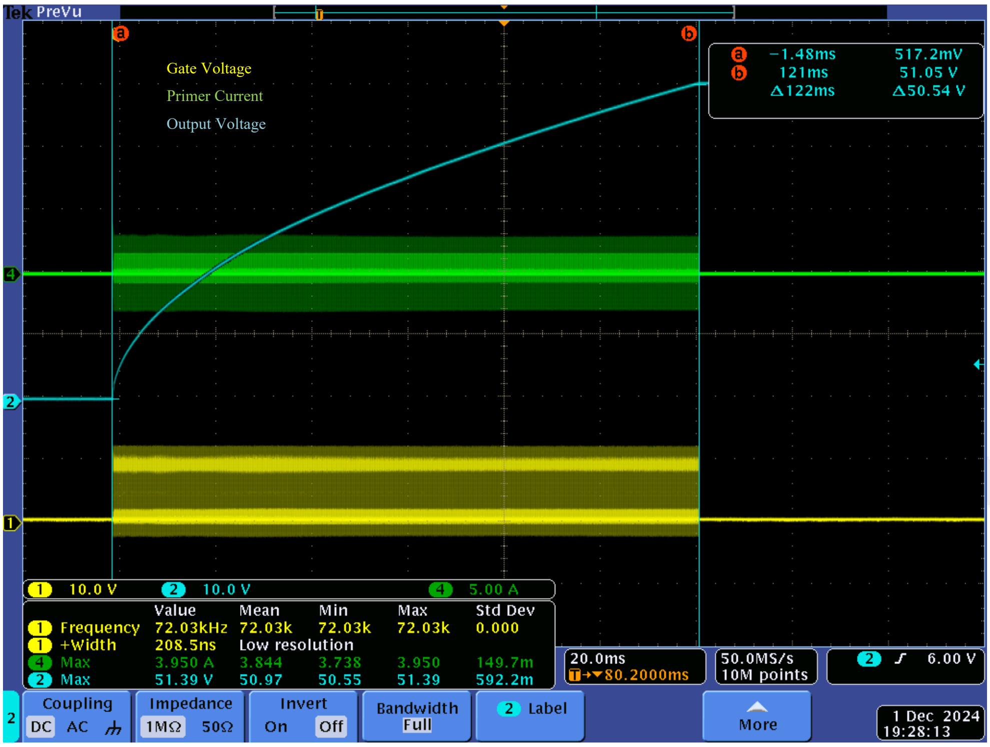

Image 5.29. Charging graphs with 208ns on-time

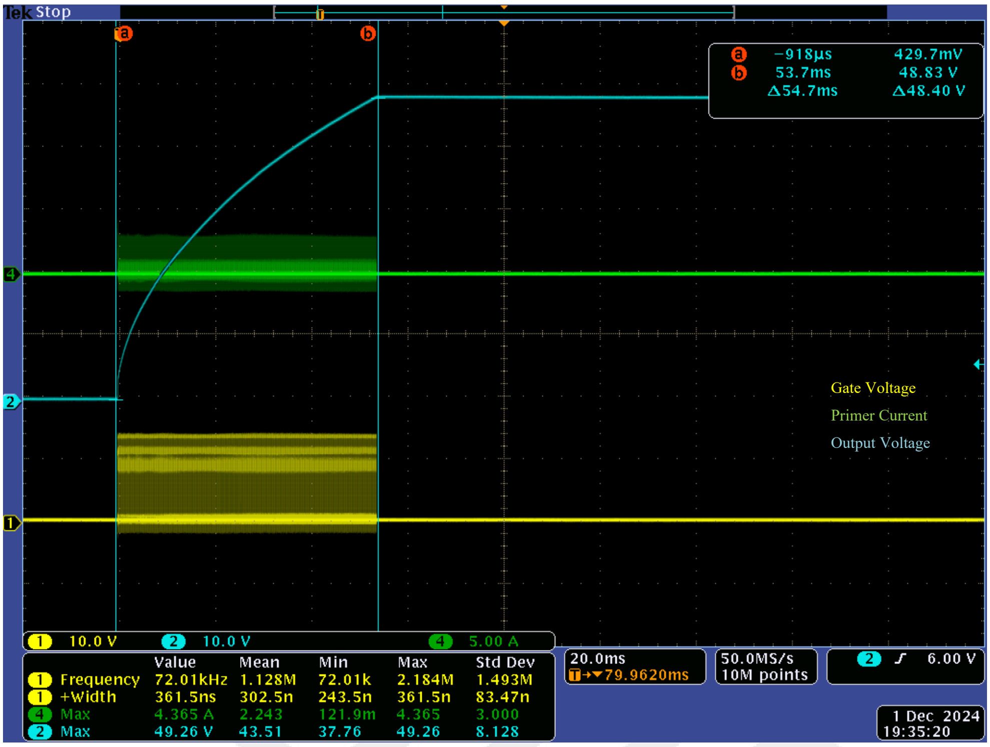

Image 5.30. Charging graphs with 360ns on-time

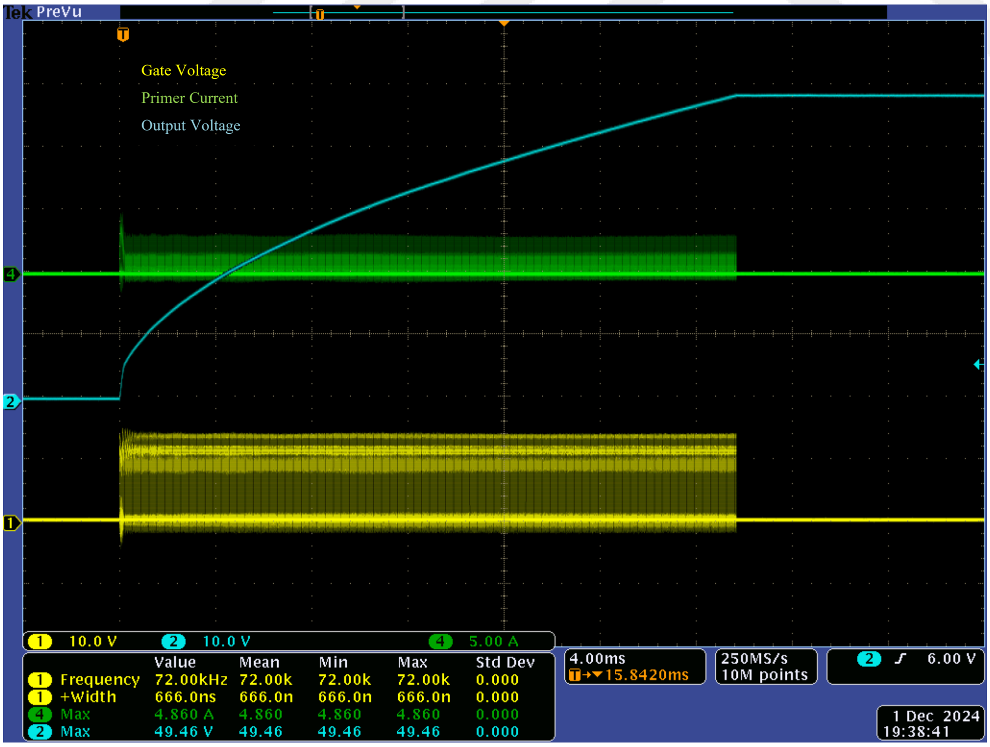

Image 5.31. Charging graphs with 666ns on-time

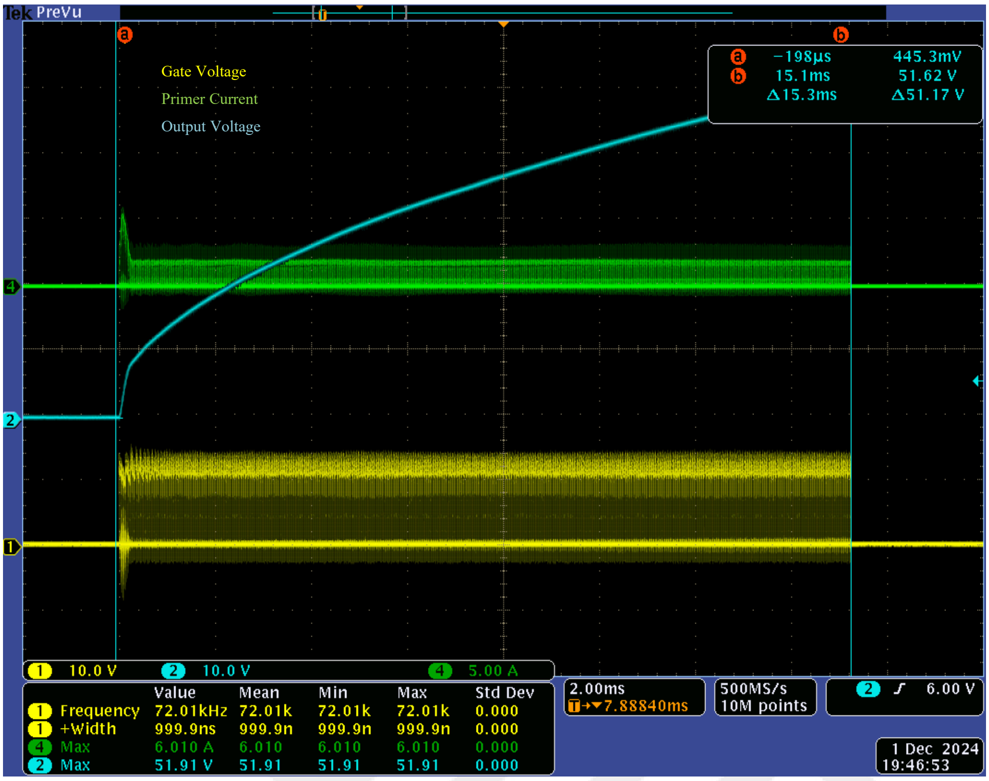

Image 5.32. Charging graphs with 999ns on-time

Image 5.33. Charging graphs with 999ns on-time zoom x1

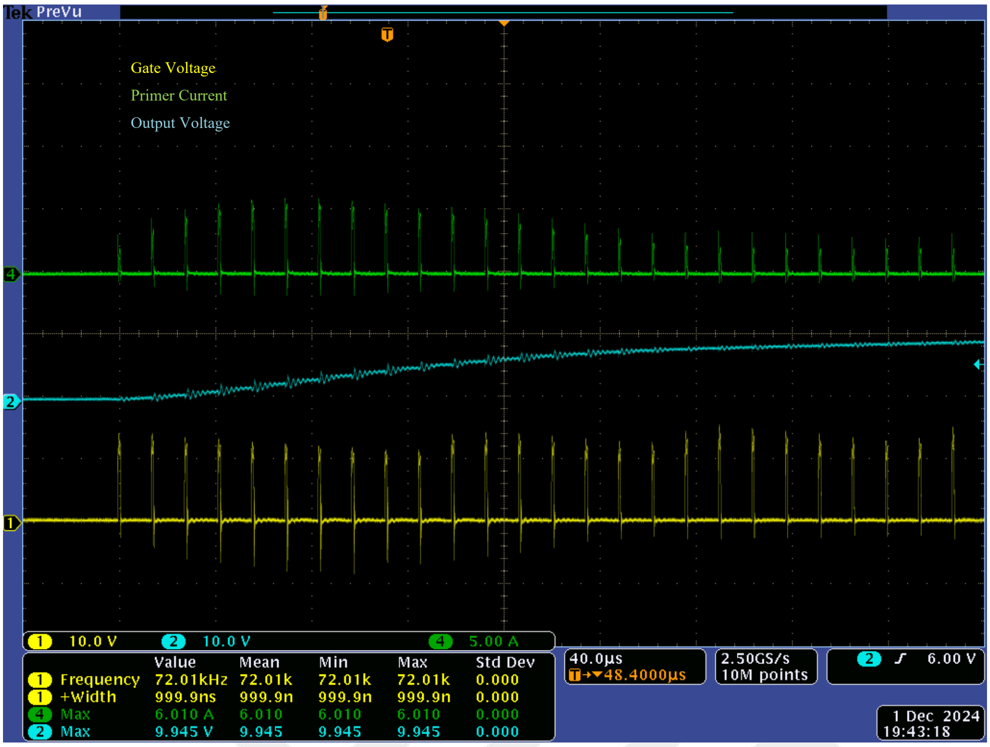

Image 5.34. Charging graphs with 999ns on-time zoom x2

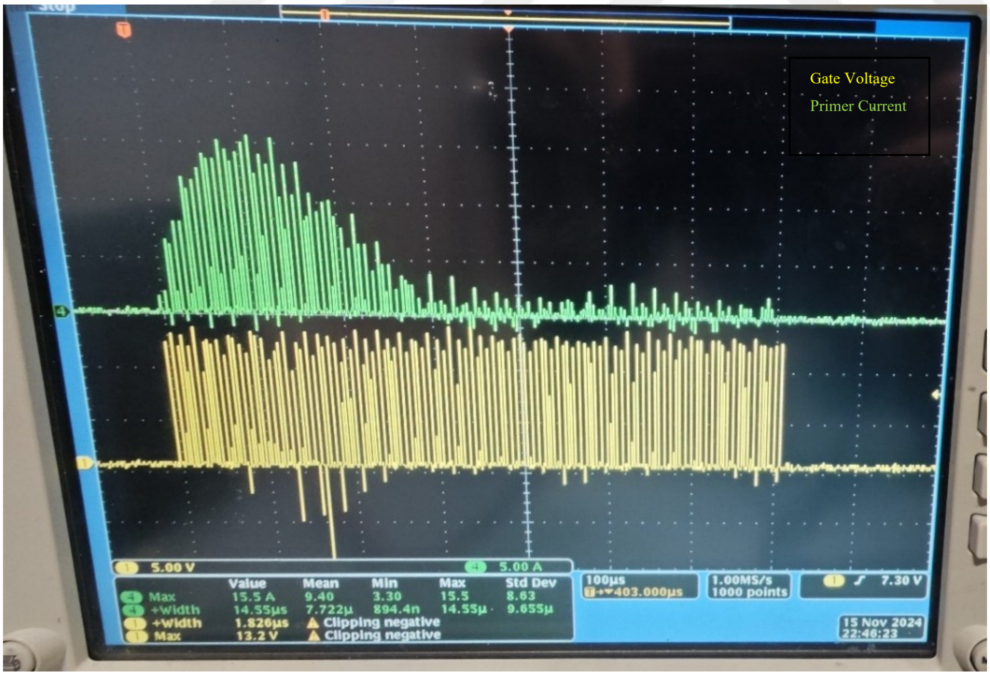

Image 5.35. Primer current spikes in CCM

5.4.4. Changing switching frequency

Low switching frequency prolongs the charging time as it increases the idle time towards the end of the charging process. However, high switching frequency causes current spikes at the beginning of the charging process. For this reason, it was decided to add the start-up mode. In start-up mode, charging is started with low frequency. After the capacitor voltage reaches a certain level, the switching frequency is increased.

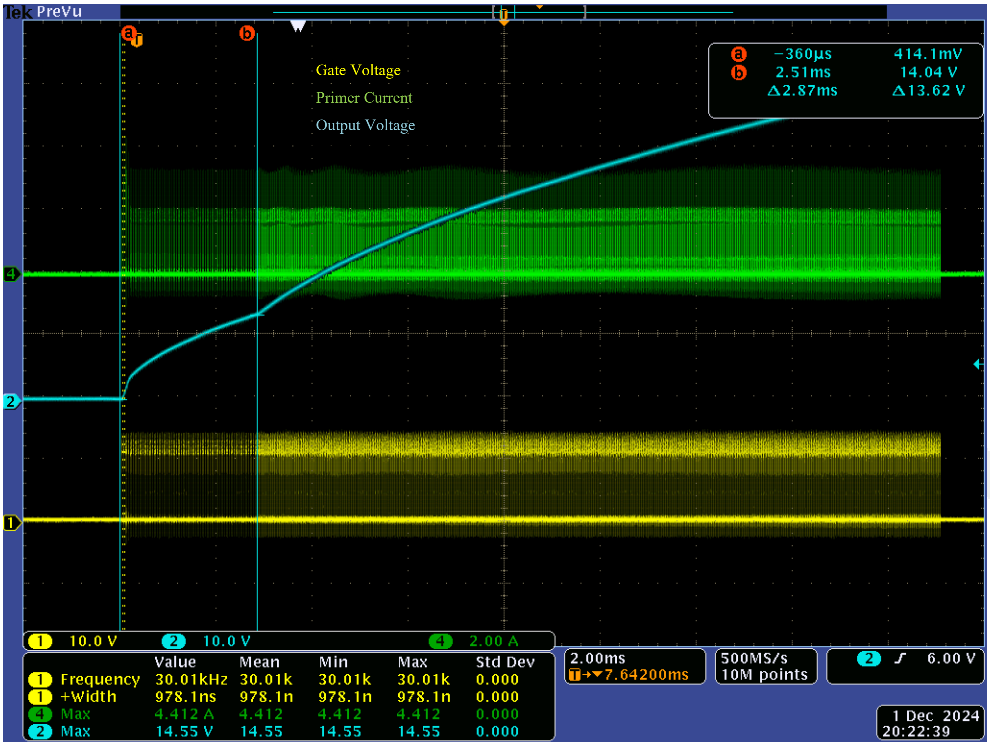

Image 5.36. Start-up frequency

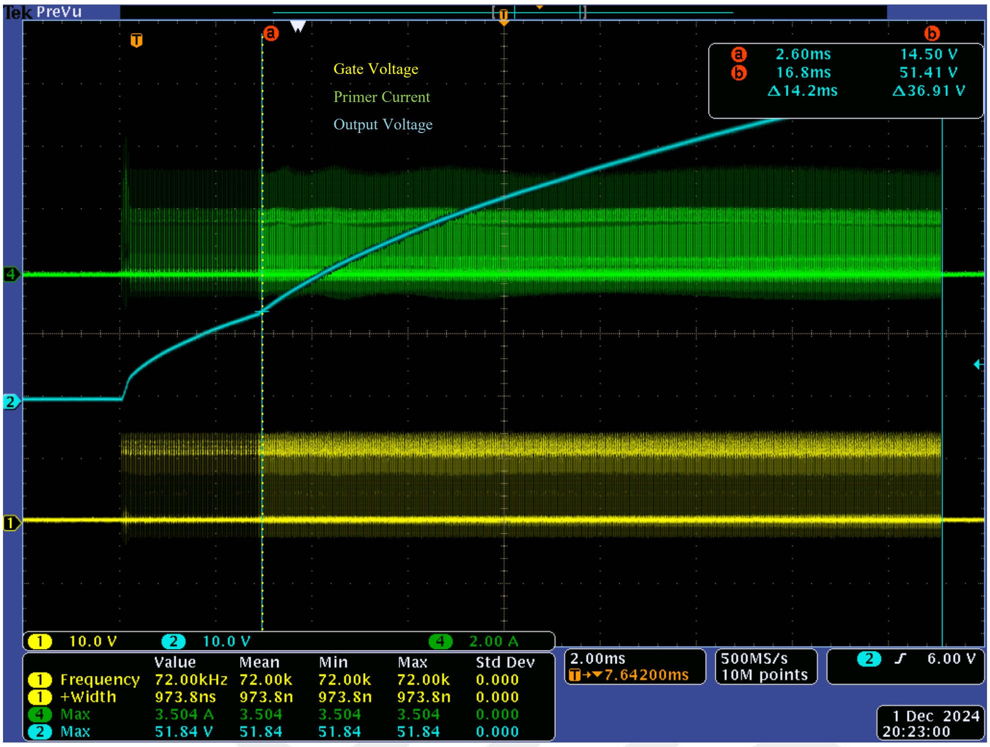

Image 5.37. After start-up frequency

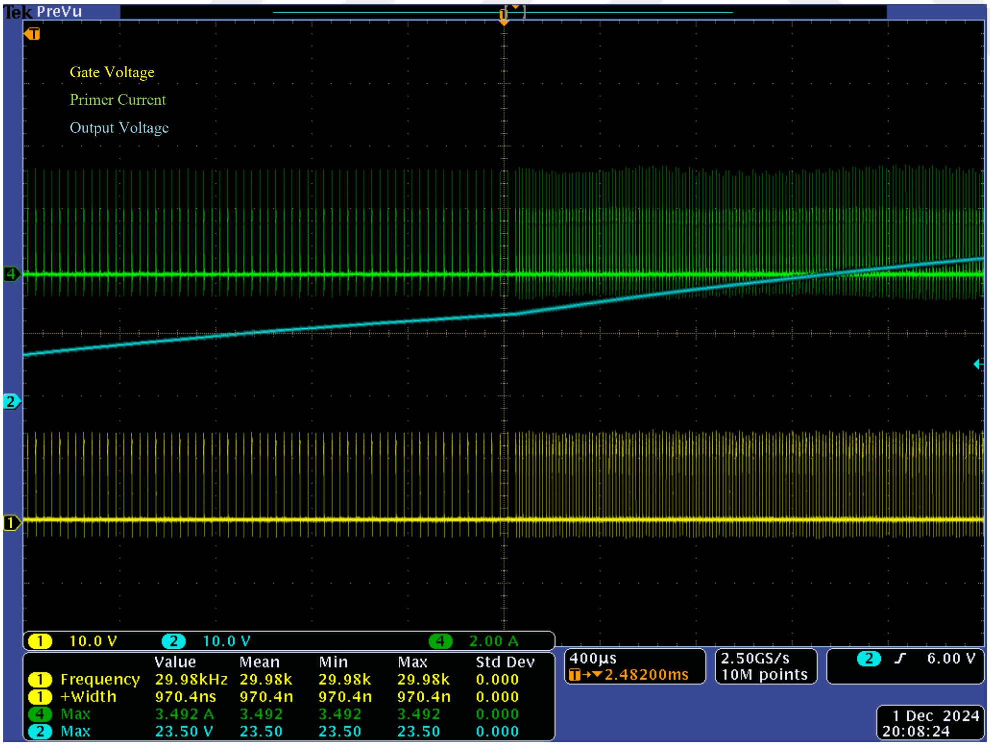

Image 5.38. Changing the frequency

Changing the switching frequency reduced the spikes of the current. At the same time, the target in charging time is also achieved by increasing the frequency. For more stable operation, the switching frequency can be changed in more than two ranges. In this way, the initial current spikes can be further minimized.

Changing the switching frequency is to approach the concept of variable frequency operation. Boundaries should be determined by sensing the primary and secondary current. However, in capacitor charging applications, the boundaries of the secondary current are frequently changing. Therefore, operating with boundary conduction mode emphasizes the necessity of operating at variable frequency.

6. CONCLUSION AND RECOMMENDATIONS

In the study, the parameters affecting the charging time were investigated. The charging time depends on input voltage, peak current and switching frequency. Increasing of these parameters decreases the charging time. However, there is always a balance between benefits and drawbacks. The current effects the conduction losses. Also, in many applications there was a limit to peak current that the CCPS draw. Experimental studies have shown that CCM and DCM modes are not suitable for CCPS applications. CCM reduces the reliability of the system by causing spikes in the primary current. In applications where charging time is not critical, the system can be operated in DCM mode. Nevertheless, the use of a fixed switching frequency in DCM mode may result in suboptimal efficiency. This results in energy loss and consequently prolongs the charging time. In order to circumvent this issue, it is imperative that CCPS be operated in boundary condition mode. As the capacitor voltage increases, the boundary conditions are shifted. A change in the boundary conditions results in a variable switching frequency.

The performances of the proposed control methods are analyzed and the optimizations are mentioned for the CCPS. The choice of control method depends on the specific requirements of the capacitor charging power supply, such as efficiency, input current limit, charging time, voltage regulation, complexity of control and cost. Each control method has its advantages and disadvantages. The selection of the control methods should be based on the application's needs. However, the system’s reliability is crucial. The simulation results obtained under LTspice environment. According to the simulations, it has been observed that measuring the output voltage and input current increases the reliability of the control structure. Thus, the sensing of the primer current with peak current commanding control is more preferential.

The Feed-Forward-Control could be implemented to the peak current commanding control. In the peak current control method, the peak current limit is defined for all conditions. Nevertheless, an increase in the input voltage will result in the charging process being completed in a shorter time than is necessary. The peak current limit can be calculated depending on the input voltage. Thus, allowing for a more efficient charging process.

In the constant on-time control method, the reliability of the controller is of paramount importance. Given that any malfunction in the controller has the potential to damage the transistor, it is of paramount importance to ensure the controller is functioning correctly. Accordingly, the input voltage must be employed as a continuous input in the calculation of the on time.

An increase in the α brings the secondary current closer to a flat-topped profile and decreased the charging time. When using the hysteretic current-mode control, it is more appropriate to use ultrafast or silicon carbide diodes to reduce the reverse recovery current.

In contrast to charge mode, regulation mode is a low power mode in which the CCPS waits for the capacitor to discharge. Therefore, small energy packets are enough to compensate the losses. To decrease the overshoot and ripple of the capacitor voltage especially in low voltages, sensing of the capacitor voltage is necessary. To respond to load changes, it may be useful to calculate the current limit with the PI controller in regulation mode.

The microcontroller must be able to detect the boundaries for the variable frequency and the PI controller. The sampling rate of the ADC is very important for high speed applications. The operating speed of the ADC must be fast enough to sample the signals to be read. According to "Nyquist criterion", the sample frequency should be at least twice of the sampled signal frequency. However, in BCM operation, the rate of change in current should be considered rather than the switching frequency. Generally, transformers designed for CCPS have low primary inductance values. This causes the primary current to rise rapidly. In this thesis, a microcontroller with a base operating speed of 168MHz and an ADC operating speed of 36MHz was selected. Although a high-speed microcontroller was selected, the control inputs required for variable frequency could not be sampled. With the optimization, it was found that ADC conversion speed can be accelerated with register-based instructions. However, the analysis only shows the duration of a single conversion. Considering the operations that need to be performed after the conversion, the speed of the chosen microcontroller was not sufficient. Faster microcontrollers would be a disadvantage in terms of both cost and size requirements.

The design can be performed with existing microcontrollers by slowing down the speed of the primary current. The rate of change in current can be slowed down by adding an inductor on the primary side. However, this will prolong the charging time and is not an efficient solution.

Start-up mode is used in many controllers. Especially, The LT3751 controller, developed for CCPS, starts charging with a low switching speed to avoid initial current spikes. Therefore, choosing different switching frequencies during the charging process would be a more optimal solution for microcontrollers with low clock frequencies. The rate of change of capacitor voltage is more sensible than currents. Therefore, the points of change of the switching frequency can be decided by measuring the voltage of the capacitor. Adding more points will bring the control structure closer to the principle of variable frequency operation.

Future studies will focus on implementing the input voltage as an input of the variable frequency operations. Also, the addition of the PI controller in CCPS applications will be studied to make the regulation mode more effective.

REFERENCES

Caldeira, P., Liu, R., Dalal, D., and Gu, W. J. (1993). *Comparison Of EMI Performance of PWM And Resonant Power Converters.* Proceedings of IEEE Power Electronics Specialist Conference - PESC '93*,* Seattle, 134-140.

Candan, M. Y., Kavak, H., and Ankaralı, M. M. (2019). *28VDC Askeri Baradan Beslenen Yüksek Kazançlı 700VDC Çıkışlı ve Çıkışı Endüktörsüz Tam Köprü Kondansatör Şarjörünün Modellenmesi ve Benzetimi.* OSMOS. Ankara: ODTÜ.

Chang, C.-W., Lin, Y.-T., and Tzou, Y.-Y. (2009). *Digital Primary-Side Sensing Control for Flyback Converters*. International Conference on Power Electronics and Drive Systems (PEDS), Taipei, 689-694.

Chen, K.-H., and Liang, T.-J. (2014). *Design of Quasi-resonant flyback converter control IC with DCM and CCM operation.* International Power Electronics Conference (IPEC-Hiroshima 2014 - ECCE ASIA), Hiroshima, 2750-2753.

Cravero, J. M., Maestri, S., Retegui, R. G., Benedetti, M., and Uicich, G. (2014 December). *Comparison of topologies suitable for capacitor charging systems.* CERN.

Einbinder, H. M. (1975). *US4070699A,* United States of America Patent.

Elmes, J., Jourdan, C., and Abdel-Rahman, O. (2009). *High-Voltage, High-Power-Density DC-DC Converter for Capacitor Charging Applications.* Twenty-Fourth Annual IEEE Applied Power Electronics Conference and Exposition, Washington, 433-439.

Fang, J., Lu, Z., Li, Z., and Li, Z. (2002). *A new flyback converter with primary side detection and peak current mode control.* International Conference on Communications, Circuits and Systems and West Sino Expositions, Chengdu, 1707-1710.

Furukawa, Y., Shibata, Y., Suetsugu, T., Colak, I., and Kurokawa, F. (2022). *Digital Peak Current Mode Control DC-DC Converter for Renewable Energy System.* 11th International Conference on Renewable Energy Research and Application (ICRERA), Istanbul, 485-489.

Ginsberg, H. S. (1983). *US4489369A,* United States of America Patent.

Internet: onsemi. (August 2021). LM317 Datasheet, Web: https://www.onsemi.com/pdf/datasheet/lm317-d.pdf, Last access date: 04.12.2024.

Internet: Linear Technology. (2003). LT3468 Datasheet, Web: https://www.analog.com/media/en/technicaldocumentation/datasheets/346812fa.pdf, Last access date: 04.12.2024.

Internet: Linear Technology. (2005). LT3750 Datasheet, Web: https://www.analog.com/media/en/technical-documentation/data-sheets/3750fa.pdf, Last access date: 04.12.2024.

Internet: Linear Technology. (2017). LT3751 Datasheet, Web: https://www.analog.com/media/en/technical-documentation/data-sheets/lt3751.pdf, Last access date: 04.12.2024.

Internet: Linear Technology. (2022). LT3420 Datasheet, Web: https://www.analog.com/media/en/technical-documentation/datasheets/3420fb.pdf, Last access date: 04.12.2024.

Internet: Falco, E. (August 2023). ANP113 Feedback loop compensation of a current-mode Flyback converter with optocoupler. Web: https://www.we online.com/components/media/o760916v410%20ANP113a%20EN.pdf, Last access date: 04.12.2024.

Internet: Monolithicpower. (n.d.). An Introduction to Flyback Converters: Parameters, Topology, and Controllers. Web: https://www.monolithicpower.com/en/learning/resources/an-introduction-to-flyback-converters-parameters-topology-and-controllers, Last access date : 04.12.2024.

Internet: Matsuada. (December 2021). Capacitor Charging Web: https://www.matsusada.com/application/ps/capacitor_charging/#:~:text=Capacitor%20charging%20stores%20electrical%20energy,or%20high%20voltage%20power%20supply.), Last access date: 04.12.2024.

Internet: Redhair, J. (n.d.). AN-2583: Comparing the Boundary and Discontinuous Conduction Modes in Flyback Converters, Web: https://www.analog.com/en/resources/app-notes/an-2583.html, Last access date: 04.12.2024.

Internet: st. (n.d.). STM3214 Analog Adc, Web: https://www.st.com/resource/en/product_training/stm32l4_analog_adc.pdf, Last access date: 04.12.2024.

Internet: st. (December, 2020). Stm32f4discovery, Web: https://www.st.com/en/evaluation-tools/stm32f4discovery.html, Last access date: 04.12.2024.

Internet: TOSHIBA. (January 2023). Power MOSFETElectrical Characteristics, Web: https://www.scribd.com/document/684095385/Application-Note-en-20230209-AKX00063, Last access date: 04.12.2024.

Islas, M. (2009). *Efficiency Improvement Techniques For High Voltage Capacitor.* Master's Thesis, University of Central Florida, Department of Electrical Engineering and Computer Science, Orlando, Florida, USA.

Kavak, H. (2020). *Kondansatör şarjı için yüksek kazançlı da-da dönüştürücü tasarımı ve uygulaması.* Master's thesis, Gazi University, Department of Electrical and Electronics Engineering, Ankara.

Kavak, H., Candan, M. Y., and Aydemir, M. T. (2020). Experimental Verification of Output Inductor-less Phase-Shifted Full-Bridge. *Gazi University Journal of Science Part A,* 7(2), 59-68.

Negrete, M. G. (2004, January 16). *Design and Control of Photoflash Capacitor.* Master's Thesis. Massachusetts Institute of Technology, Department of Electrical Engineering and Computer Science, Massachusetts Ave, Cambridge, USA.

Oh, J. S., Jang, S. D., Son, Y. G., Cho, M. H., and Namkung, W. (2001). *Development Of a Capacitor-Charging Power Supply for A Smart Modulator.* Second Asian Particle Accelerator Conference (APAC), Beijing, 719-721.

Pehlivan, Ö. (2019). *Design and analysis of an exploding foil initiator (EFI) based ignition safety device for missile system.* Master's Thesis, Hacettepe University, Department of Electrical and Electronics Engineering. Ankara.

Pokryvailo, A., Carp, C., and Scapellati, C. (2010 October). *High-power high-performance low-cost capacitor charger concept and implementation.* IEEE Transactions on Plasma Science, 38, 2734-2745.

Rotman, E., and Ben-Yaakov, S. (2013). *Rapid push pull resonant charger for high power, high voltage applications using low input voltage.* IEEE Energy Conversion Congress and Exposition, Denver, 2325-2332.

Schenkel, J., Wu, A. M., Dobkin, R. C., and Pietkiewicz, S. M. (2001). *US6518733B1,* United States of America Patent.

Sheng, H., Shen, W., Wang, H., Fu, D., Pei, Y., Yang, X., Tipton, C. W. (2007 May). *Design And Implementation of High Power Density Three-Level Parallel Resonant Converter for capacitor charger.* APEC 07 - Twenty-Second Annual IEEE Applied Power Electronics Conference and Exposition, Anaheim, 745-749.

Smith, R. H., and Laws, P. G. (1977). *US4104714A,* United States of America Patent.

Sokal, N. O. (1995). *US5485361A,* United States of America Patent.

Sokal, N. O., and Redl, R. (1997). *Control algorithms and circuit designs for optimal flyback-charging of an energy-storage capacitor (e.g., for flash lamp or defibrillator).* IEEE Transactions on Power Electronics. 12(5), 885-894.

Song, I. H., Shin, H. S., and Choi, C. H. (2001). *A Capacitor-Charging Power Supply Using a Series-Resonant Three-Level Inverter Topology.* PPPS-2001 Pulsed Power Plasma Science 2001, Las Vegas 2, 1583-1586.

Suru, C. V., Linca, M., Preda, A., and Subtirelu, E. (2016). *Design And Analysis of The Compensating Capacitor Charging Algorithm for Active Filtering Systems.* IEEE International Power Electronics and Motion Control Conference (PEMC), Varna, 889-896.

Wang, C., Sun, D., Zhang, X., Hu, J., Gu, W., and Gui, S. (2020). *A Constant Current Digital Control Method for Primary-Side Regulation Active-Clamp Flyback Converter.* IEEE Energy Conversion Congress and Exposition (ECCE), Detroit, 36(6), 2934-2938.

Gazili olmak ayrıcalıktır